1984

Progress Report No. 20

Biomedical Computer Laboratory

PROGRESS REPORT

No. 20

1 July 1983 – 30 June 1984

Biomedical Computer Laboratory

Washington University School of Medicine

700 South Euclid Ave.

St. Louis, Missouri 63110

BIOMEDICAL COMPUTER LABORATORY

WASHINGTON UNIVERSITY SCHOOL OF MEDICINE

PROGRESS REPORT NO. 20

JULY 1, 1983 - JUNE 30, 1984

TABLE OF CONTENTS

I. INTRODUCTION

This progress report from the Biomedical Computer Laboratory (BCL) summarizes activities during the period from July 1, 1983 through June 30, 1984. The Biomedical Computer Laboratory collaborates with research investigators throughout the Washington University School of Medicine and its affiliated hospitals in the application of advanced computer techniques to problems in biology and medicine. This often requires work in areas stretching from basic physiology through mathematical models to equipment design. Our orientation is interdisciplinary with the recognition that effective communication for workers with differing backgrounds comes only through extended collaboration and mutual respect.

The vigorous development and evolution of specialized computer systems for use in the solution of research and clinical problems has continued to be the central focus of BCL activities. Several systems now in clinical use have seen a progression from exploratory pilot studies, to major developmental project, to local clinical trial, to clinical trials in multiple locations, to public availability through commercial manufacture. Perseverance in this sometimes tedious chain of development has found reward in the effective fielding of specialized computer systems to the medical community.

One class of computer applications requires strong coupling of the computer to its environment for digital signal processing. These applications typically involve the use of commercially available minicomputers and microprocessors in conjunction with specialized hardware designed and built locally. We have pursued many such applications by bringing signals from hospital wards and research laboratories to BCL by means of either analog or digital tape recordings or telephone lines and, more frequently, by taking the computers to the investigator's laboratory or the patient's bedside. In this context, of particular importance to current and future BCL projects is the development, in a closely related sister lab (Computer Systems Laboratory, or CSL), of a capability for the design and fabrication of custom very-large-scale integrated (VLSI) circuits. The realization of such circuits through collaboration with CSL is already opening up new opportunities for solving problems intractable with conventional computing devices.

For those classes of applications dominated by information processing requirements, provisions have matured from telephone lines linking our minicomputers to the IBM System/370 at the Washington University Computing Facilities, through development and support of a minicomputer based MUMPS system, to the establishment of independent groups such as the Medical Computing Facility and the Medical Computing Service Group which serve the local medical complex. Diverse needs continue to be met by these various options while collaborative work continues on more advanced information-processing developments.

Still another class of applications requires extensive use of large-scale computational services. Many investigators are assisted in their research through the use of generalized numerical, non-numerical, and

statistical routines. This work is carried out in part by staff members of BCL, but primarily by members of the Division of Biostatistics and under direction of Dr. Dabeeru C. Rao, and the University Computing Facilities whose director is Robert J. Benson.

The BCL enjoys collaboration with most departmental divisions within the medical school but also finds support and enrichment through close ties with other facilities throughout the University. These arrangements are of benefit both to the BCL and to graduate students who find projects and employment among the activities in the laboratory. The Department of Computer Science is under the direction of Dr. Jerome R. Cox, Jr., past Director of the BCL. Close collaboration with the department has emphasized the area of information systems. Strong ties with the Department of Electrical Engineering are sustained through the Engineering School's Biomedical Engineering Program and common interest in digital signal processing techniques. The Department of Electrical Engineering is chaired by Dr. Donald L. Snyder, past Associate Director of BCL.

A major development completed during the past year has been the establishment at Washington University of an interschool Institute for Biomedical Computing. The new Institute encompasses the Biomedical Computer Laboratory and the Computer Systems Laboratory in an organizational setting designed to recognize and foster the joint interests in biomedical computing of the School of Medicine and the School of Engineering and Applied Science. The purpose of the reorganization is to recognize that the development and application of advanced computing and engineering technology to problems in biomedical science are essential components of the research and teaching activities of Washington University. Accordingly, attention has been given to the development of a stable organizational structure that will 1) provide a means by which the primary academic affiliations of its faculty can be in an organizational setting with an adequately broad commitment to research and teaching in biomedical computing; 2) establish a formal administrative connection to the School of Engineering and Applied Science that will facilitate the involvement of its students and faculty in research and instructional activities in biomedical computing; 3) establish mechanisms for adminstration, funding, and review of appointments, promotion, and tenure for the academic staff of this activity; 4) foster organizational and procedural coherence between the Biomedical Computer Laboratory and the Computer Systems Laboratory by placing them within a common administrative structure; 5) create a focal point for interdisciplinary teaching and student research, both in the School of Medicine and the School of Engineering and Applied Science, in areas that do not fit comfortably into existing departments; and 6) encourage a scholarly environment for the activities of the two computer laboratories that will promote and encourage teaching, research, and publication as vehicles for personal development and academic contribution.

In addition to current BCL and CSL space on the Medical School campus, space for part of the activities of the Institute has been provided on the Engineering School campus by completion of a fifth-floor addition to Lopata Hall in December of 1983. This new space (about 6000 square feet),

called the Edward L. Bowles Laboratory, is immediately adjacent to the Departments of Computer Science and Electrical Engineering.

The Institute for Biomedical Computing (IBC) now replaces the former Washington University Computer Laboratories (WUCL) which was a less formal federation of BCL and CSL plus working groups within the Departments of Computer Science and Electrical Engineering. Dr. Charles E. Molnar, Director of the Computer Systems Laboratory, and Dr. Lewis J. Thomas, Jr., Director of the Biomedical Computer Laboratory, have been appointed as respective Director and Associate Director of the Institute. Both BCL and CSL continue to retain their identities and internal organizations. Accordingly, this Progress Report addresses activities centered primarily within BCL.

Planning and policy development of the Institute are overseen by a Governing Board, the membership of which is drawn from both Schools. The present composition of the Governing Board is:

J. R. Cox, Jr., Chairman, Department of Computer Science
R. G. Evens, Head, Department of Radiology
M. K. King, Dean, School of Medicine
D. M. Kipnis, Chairman, Department of Internal Medicine
E. L. MacCordy, Associate Vice-Chancellor for Research
J. M. McKelvey, Dean, School of Engineering and Applied Science
C. E. Molnar, Director, Computer Systems Laboratory
P. Needleman, Head, Department of Pharmacology
D. L. Snyder, Chairman, Department of Electrical Engineering
L. J. Thomas, Jr., Director, Biomedical Computer Laboratory

To aid in long-range planning of the health-related activities of the Institute, a National Advisory Panel is convened periodically. Particular attention is given to the confluence of important needs in biology and medicine with the technical advances capable of meeting these needs. Successful development may suggest implementation on a larger, perhaps national scale. The present composition of the National Advisory Panel is:

P. H. Abbrecht, Professor of Physiology and Internal Medicine, Uniform Services University of the Health Sciences, Bethesda, Maryland
H. L. Bleich, Associate Professor of Medicine, Harvard University
W. A. Clark, Consultant and former Director of CSL, New York, New York
J. N. Gray, Tandem Computer Company, Cupertino, California
F. E. Heart, Bolt, Beranek & Newman, Cambridge, Massachusetts
D. M. Kipnis, Professor and Chairman, Department of Internal Medicine, Washington University
B. W. Matthews, Professor of Physics and Director of the Institute of Molecular Biology, University of Oregon

J. M. Smith, Computer Corporation of America, Cambridge, Massachusetts
E. A. Stead, Jr., Professor of Medicine, Duke University
C. Vallbona, Professor and Chairman, Department of Community Medicine, Baylor College of Medicine

II. SOURCES OF SUPPORT

During the period covered by this report the primary source of support for the Biomedical Computer Laboratory was from two grants from the National Institutes of Health, Division of Research Resources.

RR 01380	A Resource for Biomedical Computing.
RR 01362	Tissue Characterization via Ultrasonic Imaging.

NHLBI contract NO1 HV 72941 continues to fund a Holter Monitoring Core Laboratory to support a Multicenter Investigation of Limitation of Infarct Size.

NCHSR grant HS 03792, to develop a medical information systems design methodology, continues to support the research in the Computer Science Department and this Laboratory.

Collaboration with other investigators often involved work already supported by other grants.

Public Health Services Grant.

AM 07296	Cell Biological Approaches to Diabetes Research,
AM 20579	Diabetes Research and Training Center,
EY 03703	Chromatic Static Perimetry in the Diagnosis of Glaucoma,
GM 07564	Analytical and Computational Methods in Physiology,
GM 27889	Yeast TRNA Genes,
GM 28232	Physical Mapping of Yeast Chromosomal DNA,
HL 12839	Erythrocyte Deformability and Vascular Pathophysiology,
HL 13851	Cyclotron Produced Isotopes in Biology and Medicine,
HL 17646	Study of Ischemic Heart Disease,
HL 25430	Characterization of Left Ventricular Diastolic Function,
HL 25944	Time-of-Flight Positron Tomography for Cardiac Imaging,
HL 28995	Adrenergic Factors and Arrhythmogenic Metabolites,
HL 28998	Tissue Characterization with Ultrasound,
HL 29229	Familial Hypercholesterolemia in Cultured Cells,

NS 06833 An Interdisciplinary Stroke Program,

NS 14834 Mechanisms of Seizures and Anticonvulsant Drugs,

NS 15070 Regeneration and Functional Recovery in Cerebral Cortex,

RR 01379 Research in VLSI Systems for Biomedical Applications,

RR 01828 A New Approach to Fast Gamma-Radiation Detection.

National Science Foundation Grant.

ECS-82-15181 Study of Time-of-Flight Tomography.

Research support was also received from the following industrial collaborators.

Biosensor Corporation, Brooklyn Center, Minnesota,
Computer Services Corporation (CSK), Tokyo, Japan,
Mead Johnson, Evansville, Indiana.

III. PERSONNEL

EMPLOYEES

Personnel employed by the Biomedical Computer Laboratory during the period covered by this report were:

Director

Lewis J. Thomas, Jr., M.D., and Associate Director of Institute for Biomedical Computing, and Associate Professor of Anesthesiology, Physiology and Biophysics, Biomedical Engineering, and Electrical Engineering

Associate Director

G. James Blaine III, D.Sc., and Affiliate Associate Professor of Electrical Engineering and Computer Science, and Senior Research Associate, Computer Systems Laboratory

Senior Research Associates

Jerome R. Cox, Jr., Sc.D., and Chairman and Professor of Computer Science, and Professor of Electrical Engineering, and Senior Research Associate, Computer Systems Laboratory
Harold W. Shipton, C.Eng., and Chairman and Professor of Biomedical Engineering
Donald L. Snyder, Ph.D., and Chairman and Professor of Electrical Engineering, and Senior Research Associate, Computer Systems Laboratory

Business Manager

Virginia M. Bixon, B.S.

Research Associates

Robert J. Arnzen, Ph.D., and Computer Systems Laboratory
R. Martin Arthur, Ph.D., and Associate Professor of Electrical Engineering
Kenneth W. Clark, M.S.
James G. Dunham, Ph.D., and Associate Professor of Electrical Engineering
Robert O. Gregory, D.Sc., and Professor of Electrical Engineering
Kenneth B. Larson, Ph.D.
James G. Miller, Ph.D., and Professor of Physics, and Associate Director for Biomedical Physics, Laboratory for Ultrasonics, and Research Associate Professor of Medicine
Michael I. Miller, Ph.D., Assistant Professor of Electrical Engineering
Frederick U. Rosenberger, D.Sc., and Associate Director, Computer Systems Laboratory, and Assistant Professor of Electrical Engineering

Research Assistants

David E. Beecher, M.S., Lecturer in Computer Science
Steven R. Broadstone, B.A., B.S.
John C. Chabut, B.S., B.A.
John D. Gorman, B.S.
Russell E. Hermes, M.S.
Timothy J. Holmes, M.S.
Patrick H. Johnston, M.A.
Joanne Markham, M.S., Research Instructor in Medicine
Charles N. Mead, M.D.
J. Philip Miller, A.B., and Associate Professor of Biostatistics in Preventive Medicine
Stephen M. Moore, M.S.
Jack G. Mottley, M.A.
John M. Ollinger, M.S.
David G. Politte, M.S.
Kenneth B. Schechtman, Ph.D., Instructor in Biostatistics in Preventive Medicine, and Research Instructor in Medicine
Chung-Dak Shum, M.S.

Engineering Assistant

Stanley R. Phillips, A.A.S.

Technical Assistants

Kristin K. Foss, B.S.
Kathleen A. Madden, B.A.
Melissa Marlo McLear, A.B.
Alexander W. Stangl
Donald W. Stein, Jr.

Electronic Technicians

Michael J. Rainey
Deborah A. Schwab

Librarian

Monica W. Shieh, M.L.S.

Secretaries

Rebecca J. Bozesky
Shirley A. Gonzalez-Rubio
Polly E. Raith

The following members from other departments and divisions have joint appointments with the Biomedical Computer Laboratory to facilitate collaboration and enhance interdisciplinary research:

H. Dieter Ambos, Research Assistant Professor of Medicine (Cardiology)
A. Maynard Engebretson, D.Sc., Assistant Director of Research in Engineering, Central Institute for the Deaf, and Affiliate Associate Professor of Computer Science
William M. Hart, Jr., M.D., Ph.D., Associate Professor of Ophthalmology
Rexford L. Hill, III, M.S., Associate Professor of Computer Applications in Radiology
J. Stevadson Massey, M.S., Research Assistant in Neurological Surgery
John W. Wong, Ph.D., Assistant Professor of Radiation Physics in Radiology

In addition, the following people worked at the laboratory for brief periods:

George L. Engel, B.A., B.S.
Abdelkader Gacem
Sudjiwo Husodo
Rosalie J. Paisley, M.S.
David F. Sandel, B.S.

RESEARCH COLLABORATORS

During the period covered by this report the following investigators from other laboratories, departments, or institutions, collaborated with BCL staff members on problems of joint interest.

D. R. Abendschein, Ph.D., Medicine
J. Achtenberg, A.B., Medical Computing Service
G. G. Ahumada, M.D., Medicine
H. D. Ambos, Medicine
T. R. Baird, Medicine
W. E. Ball, D.Sc., Computer Science
B. Becker, M.D., Ophthalmology
R. J. Benson, J.D., Computing Facilities
S. R. Bergmann, Ph.D., Medicine
D. R. Biello, M.D. Radiology
W. R. Bosch, M.S., Computer Systems Laboratory
S. R. Broadstone, B.A., B.S., Electrical Engineering
T. L. Buettner, Medicine
M. E. Cain, M.D., Medicine
T. J. Chaney, M.S., Computer Systems Laboratory
K. C. Chang, Ph.D., Pathology
P. A. Cole, B.S., Pathology
J. D. Collins, B.S., Computer Systems Laboratory
P. B. Corr, Ph.D., Medicine and Pharmacology
M. R. Courtois, M.A., Medicine

R. D. Edelman, B.S., Computer Systems Laboratory
J. O. Eichling, Ph.D., Radiology
J. D. Eisenberg, M.D., Medicine
P. R. Eisenberg, M.D., Medicine
S. E. Elnahas, M.S., Electrical Engineering
B. Emami, M.D., Radiology
R. G. Evens, M.D., Radiology
D. C. Ficke, B.S., Radiology
L. Fields, M.D. Medicine
K. A. A. Fox, M.B., Ch.,B., Medicine
P. T. Fox, M.D., Neurology and Radiology
M. S. Frank, M.D., Genetics
M. H. Gado, M.D. Radiology
E. D. Galie, R.N., Medicine
R. A. Gardner, Ph.D., Mechanical Engineering
E. M. Geltman, M.D., Medicine
W. D. Gillette, Ph.D., Computer Sciences
R. M. Glueck, M.D., Medicine
S. Goldring, M.D., Neurological Surgery
M. E. Gordon, Ph.D., Ophthalmology
A. M. Grace, Medicine
E. M. Gregorie, M.D., Neurological Surgery
R. L. Grubb, Jr., M.D., Neurological Surgery
W. M. Hart, Jr., M.D., Ph.D., Ophthalmology
K. H. Haserodt, M.S., Computer Science
H. Hashimoto, M.D., Medicine
P. Herscovitch, M.D., Neurology and Radiology
G. R. Hoffman, B.A., Radiology
J. T. Hood, B.S., Radiology
B. Hughes, Ph.D., Medicine
S. Igielnik, Ph.D., Medical Computing Facilities
A. S. Jaffe, M.D., Medicine
G. C. Johns, B.S., Computer Systems Laboratory
E. G. Jones, M.D., Ph.D., Anatomy
R. G. Jost, M.D., Radiology
M. A. Kass, M.D., Ophthalmology
E. W. Kiebler, M.S., Computer Systems Laboratory
R. M. Knabbe, Ph.D., Medicine
S. J. Kovacks, Jr., M.D., Ph.D., Medicine
J. B. Kramer, M.D., Medicine and Surgery
A. Kumar, B. Tech., Radiology
P. B. Kurnik, M.D., Medicine
J. L. Lauter, Ph.D., Central Institute for the Deaf
F. Lifshits, Medicine
B. D. Lindsay, M.D., Medicine
P. Lombardo, B.A., Neurological Surgery
P. A. Ludbrook, M.D., Medicine
E. T. Macke, M.S., Computer Systems Laboratory
J. S. Marvel, B.S., Pathology
J. W. Matthews, D.Sc., Computer Systems Laboratory
J. M. McAninch, Medicine
T. R. Miller, Radiology
M. A. Mintun, M.D., Neurology

C. E. Molnar, Sc.D., Computer Systems Laboratory
R. A. Moses, M.D., Ophthalmology
S. R. Mumm, Medicine
H. Nomura, M.D., Medicine
M. V. Olson, Ph.D., Genetics
R. E. Ostlund, Jr., M.D., Medicine
D. S. Payne, Medicine
C. A. Perez, M.D., Radiology
J. E. Perez, M.D., Medicine
D. G. Politte, M.S., Radiology
W. J. Powers, M.D., Neurology and Radiology
J. L. Price, Ph.D., Anatomy
J. A. Purdy, Ph.D., Radiology
M. E. Raichle, M.D., Neurology and Radiology
D. C. Rao, Ph.D., Biostatistics
C. S. Ritter, Medicine
A. P. Rueter, B.S., Radiology
J. E. Saffitz, M.D., Pathology
M. L. Sieger, B.S., Electrical Engineering
B. A. Siegel, M.D., Radiology
B. E. Sobel, M.D., Medicine
J. J. Spadero, Jr., M.D., Medicine
A. W. Strauss, M.D., Biochemistry
S. P. Sutera, Ph.D., Mechanical Engineering
A. G. Swift, B.A., Radiology
M. M. Ter-Pogossian, Ph.D., Radiology
W. J. Thomas, M.S., Electrical Engineering
A. J. Tiefenbrunn, M.D., Medicine
R. G. Tilton, Ph.D., Pathology
A. W. Toga, Ph.D., Neurology
D. F. Wann, D.Sc., Electrical Engineering
M. R. Weber, Electrical Engineering
M. J. Welch, Ph.D., Radiology
R. A. Wettach, Medicine
J. R. Williamson, M.D., Pathology
F. X. Witkowski, M.D., Medicine
K. F. Wong, M.S., Computer Science
J. W. Wong, Ph.D., Radiology
A. L. Ysaguirre, Medicine
J. D. Zions, Pathology

Columbia University, New York, New York

J. T. Bigger, Jr., M.D.

Creighton University, Omaha, Nebraska

F. M. Nolle, D.Sc.
Z. Zencka, M.D.

Hahnemann Medical College, Philadelphia, Pennsylvania

R. A. Levy, M.D.

Indiana University School of Medicine, Indianapolis, Indiana

C. Fisch, M.D.
S. B. Knoebel, M.D.

Jewish Hospital, St. Louis, Missouri

B. R. Hieb, M.D.
R. E. Kleiger, M.D.
R. J. Krone, M.D.
R. Ruffy, M.D.

Massachusetts General Hospital, Boston, Massachusetts

H. K. Gold, M.D.
H. W. Strauss, M.D.

Pennsylvania State University, University Park, Pennsylvania

D. B. Geselowitz, Ph.D.

Peter Bent Brigham Hospital, Boston, Massachusetts

E. Braunwald, M.D.

Research Triangle Institute, Research Triangle Park, North Carolina

W. K. Poole, Ph.D.

Roosevelt Hospital, New York, New York

H. M. Greenberg, M.D.

St. Louis University, St. Louis, Missouri

E. D. Slessinger, B.S.

University of Illinois at Chicago Circle, Chicago, Illinois

R. Langendorf, M.D.

University of Iowa, Iowa City, Iowa

R. C. Arzbaecher, Ph.D.

University of Kentucky College of Medicine, Lexington, Kentucky

B. Surawicz, M.D.

University of Louisville School of Medicine, Louisville, Kentucky

N. C. Flowers, M.D.

University of Texas Health Science Center, Dallas, Texas

J. T. Willerson, M.D.

University of Vermont College of Medicine, Burlington, Vermont

D. S. Raabe, M.D.

As in the past, collaborative efforts with various commercial firms continue (see Section VI). This year projects of joint interest have involved:

Biosensor Corporation, Brooklyn Center, Minnesota,
Computer Services Corporation (CSK), Tokyo, Japan,
International Business Machines (IBM) Biomedical Systems,
Hopewell Junction, New York,
Mead Johnson, Pharmaceutical Division, Evansville, Indiana,
Medicomp, Inc., Melbourne, Florida,
Mennen-Medical, Inc., Clarence, New York.

IV. PHYSICAL RESOURCES

The Biomedical Computer Laboratory (BCL) was formed on April 15, 1964 and the original staff moved into 3,800 square feet (net) of laboratory space at 700 South Euclid Avenue in St. Louis. While remaining at this location, adjacent to the Washington University School of Medicine's main building complex, the floor space has been increased to the present 12,000 square feet (net). As a result of the establishment of an interschool Institute for Biomedical Computing at Washington University, space for part of the activities of the Institute (which encompasses both the BCL and the Computer Systems Laboratory (CSL) has been created on the Engineering School campus by completion of a fifth-floor addition to Lopata Hall. This new space (about 6000 square feet), called the Edward L. Bowles Laboratory, is immediately adjacent to the Departments of Computer Science and Electrical Engineering. It became available in December, 1983. In addition to the 700 South Euclid and Bowles Laboratory space, BCL staff members and systems frequently occupy other areas within the Washington University Medical Center at the sites of collaborative project activities.

During the past twenty years BCL has addressed diverse biomedical problems for which digital computing techniques seemed promising and appropriate. A single Laboratory Instrument Computer (LINC) provided the original staff with an opportunity to apply digital computing to a few interesting problems in medicine and biology. Currently BCL has interest and involvement in several specialized instrumentation and computing systems which provide access to diverse image-data sources (modalities) and offer opportunities for collaborative research in biological modeling and algorithm development. BCL has primary responsibility for a complement of computing hardware and software from a variety of system manufacturers. These resources include: PDP-11's and LSI-11's from Digital Equipment Corporation, TI-980's from Texas Instruments Incorporated, 135's from California Data Processors and Versamodule M68000's from Motorola, Inc. An MMS-X stroke graphics display system developed by the Computer Systems Laboratory, a Lexidata raster-graphic display system and a MASSCOMP raster-graphic workstation are available for biomedical imaging studies.

A local computer network, TERRANET, provides remote terminal-to-computer and inter-computer data communications at rates up to 9600 bps among thirty stations including terminals and processor ports located throughout the laboratories. Personal-class microcomputer systems have been incorporated into the design of biomedical research systems and numerous special-purpose devices have been developed using microprocessor chip-sets and microcomputer board-level assemblies.

A machine shop and reference room are located on the 700 S. Euclid premises and shared with CSL. Other physical resources include a well-stocked electronics shop, a large inventory of electronic and computer test equipment, a variety of digital system modules and both analog and digital recording instruments. Systems for use in developing eight-bit, sixteen-bit and bit-slice microprocessor applications are available.

V. RESEARCH PROJECTS

Introduction

The research program of the Biomedical Computer Laboratory (BCL) is organized into several major project areas with the staff grouped into teams whose interests are focused correspondingly. For this Progress Report, the following paragraphs offer a brief orientation to the headings under which research activities are discussed. For each category, a summary is provided on the first page of the corresponding section.

Ischemic heart disease and ECG analysis (Section A) continues to be a major category of research activity, but the development of new algorithms for ECG processing has become less prominent than in the past as a result of a shift in emphasis to exportation of the latest version of our "Argus" algorithm. More prominent than before are modeling, signal processing, and data analysis work in collaboration with the division of Cardiovascular Medicine as part of their broad program addressed to ischemic heart disease.

Information extraction from quantitative biomedical images continues to increase in prominence within the BCL program. Accordingly, last year's organization of such activities into three categories (by imaging modality) is continued this year. The work in ultrasonic tissue characterization (Section B) now emphasizes the interpretation of backscatter to achieve quantitative estimates of tissue properties, including anisotropy and the state of contraction of cardiac and skeletal muscle, while parallel efforts are directed toward design of a system to employ adaptive beamforming for backscatter measurements.

Work in radiation treatment planning (Section C) has moved ahead with enhancements and evaluations of our "delta volume" algorithm for three-dimensional absorbed-dose calculations, display experiments employing high-performance stroke graphics (MMS-X system), and the recent submission for fabrication of two VLSI circuits for expeditious achievement of a demanding kernel of the computations (3-D ray tracing).

For positron-emission tomography (Section D) work in support of applications and system improvements have continued on several fronts, but the main thrust of BCL activities has been in research on algorithms. Emphasis has been on application of the maximum-likelihood method for improving image quality and for achieving better estimates of physiological parameters through studies of dynamic distributions of tracers.

Systems for Specialized Biomedical Studies (Section E) embraces a variety of projects that are less broad in scope either because they are in an earlier stage of development or because the nature of the work is necessarily more specialized. The biomedical-imaging theme is well represented in this section as well.

Projects reported under Resource Development Activities (Section F) are directed toward improving the Laboratory's capabilities for addressing the needs of more than one project area. Again, the biomedical-imaging theme is manifest in work to upgrade BCL's resources for communicating and processing image data from a variety sources and in a variety of contexts.

Individual Projects

A. Ischemic Heart Disease and ECG Analysis

The projects reported in this section continue longstanding work in real-time and high-speed ECG analysis. Many of the clinical studies reported here are natural outgrowths of the ECG-analysis work, as are the strong interests in the evaluation of automated arrhythmia detectors. Modeling and signal-processing endeavors in the field of cardiology have supported collaborations which address other aspects of ischemic heart disease, such as myocardial metabolism and blood flow, the electrophysiologic characterization of abnormal myocardial depolarization, various antidysrhythmic drug studies, infarct-size modification, and the study of ventricular diastolic mechanics.

A real-time computer-based arrhythmia monitoring system, called Argus, in operation in the Barnes Hospital Coronary Care Unit from 1969-1975, was replaced in 1975 by "Argus/Sentinel," a commercially available version developed through collaboration with the Mennen-Greatbatch Company. The experience garnered with Argus led directly to the development of a system, called Argus/H, for the high-speed (60 times real time) processing of long-term ECG recordings. Argus/H has since processed several thousand recordings for a study of ventricular arrhythmias in survivors of myocardial infarction and several hundred recordings for a host of other studies. Extensive evaluations have verified the integrity of the analysis algorithms, proven the value of the quantified results as compared to conventional manual-scanning techniques, and confirmed the consistency of results on reprocessing. The importance of such issues stimulated the more recent development of a stochastic model for the performance evaluation of event detectors.

By the mid-1970's, it was apparent that Argus/H could not support rigorous algorithm development, could not efficiently process the now more-popular dual-channel recordings, and could not meet the demand for the system from the growing volume of recordings resulting from interests in therapeutic trials of antiarrhythmic agents and interventions designed to protect the ischemic myocardium. A newer system, called Argus/2H, emerged in 1977 and was duplicated in 1978. The two Argus/2H systems have processed long-term ECGs for national multicenter clinical studies of interventions to limit infarct size and of post-infarction risk stratification. The systems also provide the power and flexibility necessary for work on algorithm revision and on new signal-processing strategies and they have further served the analysis and documentation needs of other work to generate an annotated digital ECG database for the evaluation of automated arrhythmia detectors. Newer signal-processing strategies employing frequency-domain analysis of the ECG are now bearing fruit and have led to a continuing industrial collaboration to implement the algorithms in a CMOS processor for real-time dysrhythmia analysis in the ambulatory setting.

A-1. Argus Algorithm Development

Personnel: K. W. Clark, BCL
K. B. Larson, BCL
C. N. Mead, BCL
D. W. Stein, Jr., BCL
L. J. Thomas, Jr., BCL

Support: RR 01380
Biosensor Corporation
Washington University

For more than 15 years, this laboratory has been developing algorithms for efficient analysis of the surface ECG signal (PR 19, A-1). These efforts have culminated in the implementation of a device designed and marketed by Biosensor Corporation (see VI. Industrial Collaboration). The device is a portable "real-time analyzer" which continuously monitors a patient's ECG, records clinically significant data (heart-rate trends, ectopic depolarizations, waveform examples), and transmits stored information to a central station. The central station prints a summary for the patient's physician. Much of the past year was expended assisting Biosensor with their implementation and debugging.

Concurrently, additional efforts have focused on improvements in several areas of the time-domain-based QRS detector/delineator algorithm. First, logic was added for inclusion of small septal vectors at the leading edge of QRS complexes. Second, the logic for detecting low-amplitude events was completely redone; the prior version performed well for isolated events but not so well for consecutive and interpolated low-amplitude events. Third, the noise rejection logic was completely redone and is still undergoing evaluation and tuning.

There have been several enhancements in the area of QRS classification. First, the QRS centroid replaces the point of maximum sample difference as a fiducial point for aligning QRS complexes to be correlated in the frequency domain. The correlation is performed when the algorithm updates the ideal "time-local" normal against which suspicious beats are compared. For purposes of speed, the centroid computation uses Aztec data rather than raw data. Second, the frequency-domain logic, invoked when time-domain analysis has flagged a QRS as non-normal (PR 19, A-2), is being translated from FORTRAN in a time-shared environment (where it was developed) to assembly language in a (faster than) real-time environment. Third, plans have been laid for a Sequence processor to follow QRS classification. Sequence may re-label one or more QRS complexes after examining those complexes in their larger neighborhood of several or many QRSs. Ideally, Sequence mimics the cardiologist who looks at beats in context and their relationships to one another rather than judging isolated complexes.

In the next several months, when these enhancements have been put in place, we plan to evaluate the full system against the American Heart Association database of ventricular arrhythmias (PR 19, A-4).

A-2. Processing of Long-term ECG Recordings

Personnel: K. W. Clark, BCL
K. A. Madden, BCL
M. A. Marlo, BCL
C. N. Mead, BCL
A. W. Stangl, BCL

Support: RR 01380
Biosensor Corporation
Jewish Hospital
Mead-Johnson Pharmaceuticals

After many years of analyzing long-term ECG recordings for a variety of local studies and multicenter trials, these activities have been greatly reduced. A few recordings (10-20 per month) are still analyzed for Jewish Hospital patients who are being studied with a variety of antiarrhythmic agents. A few recordings are analyzed for Mead-Johnson Pharmaceuticals in a multicenter, placebo-controlled study of an antidepressant agent, trazadone (see VI, Industrial Collaboration).

Biosensor Corporation, which recently implemented and now markets a portable device for analyzing ECG signals in real time (see VI, Industrial Collaboration), has enlisted our help in providing them with a variety of ECG arrhythmias in digital form against which they might test their product(s). After Biosensor analyzes those digital signals and sends to us their beat-by-beat results, we plot waveforms and labels in condensed fashion for rapid review and analysis. The arrangement has allowed Biosensor access to a wealth of diverse waveforms and precluded the investment of duplicating proven or investing in new support software.

A-3. Assessment of Vascular Integrity of the Myocardium Following Ischemic Injury

Personnel: R. G. Tilton, Ph.D., Pathology
K. C. Chang, Ph.D., Pathology
P. A. Cole, B.S., Pathology
R. A. Gardner, Ph.D., Mechanical Engineering
K. B. Larson, BCL
J. S. Marvel, B.S., Pathology
B. E. Sobel, M.D., Medicine
S. P. Sutera, Ph.D., Mechanical Engineering
J. R. Williamson, M.D., Pathology
J. D. Zions, Pathology

Support: RR 01380
AM 07296
HL 12839
HL 17646
The Kilo Diabetes and Vascular Research Foundation

We have continued our previously reported studies (PR 15, A-10; PR 16, A-10, PR 17, A-7; PR 18, A-7; PR 19, A-7) of the pathophysiology of ischemic injury to the heart. In these studies, we employed bolus-injection, external-detection radiotracer techniques to quantify albumin transport across the coronary vasculature under physiological conditions, and during reperfusion after selected intervals of global, no-flow ischemia in isolated-perfused rabbit hearts. The resulting residue-detection data, analyzed on the basis of a two-compartment model of tracer transport, were used to estimate parameters indicative of microvascular integrity such as permeability and ultrafiltration conductance of the endothelium. Our continuing goal has been to understand the role of endothelium in the pathogenesis of the vascular hemodynamic and permeability changes associated with ischemia and reperfusion.

We have studied the effects of diltiazem on coronary vascular hemodynamics and permeability changes during reperfusion after ischemia. Four-μM diltiazem significantly increased total water content (8.5%) and decreased perfusion pressure (11%), left ventricular developed pressure (22%), and +dP/dt (24%) in nonischemic control experiments, but did not affect estimates of vascular volume, interstitial fluid volume, mean-transit time, or albumin permeation. Four-μM diltiazem blocked ischemia- and reperfusion-induced increases in water content, interstitial fluid volume, vascular resistance, vascular volume, and vascular permeability to ^{125}I-BSA, without reducing left ventricular developed pressure or +dP/dt relative to nonischemic diltiazem controls. These data suggest that production of ischemic myocardium by diltiazem is mediated, at least in part, by preservation of vascular functional integrity.

To study the effect of selective phospholipase A_2 damage to endothelium, we have developed techniques for covalently linking proteolytic and lipolytic enzymes to uniformly sized 0.2-μm spherical

carboxylate-modified, polystyrene particles. In preliminary experiments, we have assessed vascular permeability and myocardial contractility changes in isolated, buffer-perfused rabbit hearts exposed to phospholipase A_2 bound to 0.2 μm microspheres during 30 minutes of no flow. During reperfusion following the no-flow period, increases in vascular resistance were of equal magnitude in untreated and phospholipase-A_2-treated hearts. Our interpretation of this observation is that the resistance increases are probably caused by ischemic injury to arterial smooth muscle which would be expected to be similar in both groups. On the other hand, albumin leakage in the phospholipase-A_2-treated hearts was about twice that of untreated ischemic hearts during reflow, and was about six times that of nonischemic control hearts at comparable time intervals.

We have carried out additional experiments to optimize conditions of bead concentration and duration of contact with the vasculature in which the duration of no flow is decreased by 50%. Changes in vascular tone and myocardial contractility are reversible after this brief interval of ischemia and vascular permeability is unaffected during reperfusion of control hearts. Experiments currently in progress are extending these initial findings and are evaluating effects of trypsin and phospholipase C on endothelium as well.

To determine whether hypercholesterolemia renders vascular endothelium more susceptible to ischemia-reperfusion injury, we have utilized our external detection technique to characterize permeation of the coronary vasculature by ^{125}I-BSA in hearts of rabbits fed a 2% cholesterol diet for 2-3 weeks. In these experiments, isolated rabbit hearts were perfused at constant flow for 1 hour prior to 30 minutes of global, no-flow ischemia, then reperfused for 3.5 hours. In continuously perfused controls and in ischemic hearts of animals on a normal cholesterol diet, indices of vascular and myocardial function were identical to the values reported in our previous studies with this model. Albumin permeation across the coronary vasculature was twice that of control values prior to ischemia in hearts from hypercholesterolemic rabbits and, during reflow, was two to three times the values in ischemic hearts of animals on a normal diet. During reperfusion of hypercholesterolemic hearts, vascular resistance increased 85%, while vascular volume increased about eight times over baseline (compared to 58% and 37% increases, respectively, in hearts from normal cholesterolemic animals). We have attributed the dramatic increase in vascular volume to a breakdown of the endothelial cell barrier to albumin.

In these studies, we have shown for the first time that after rabbits have been kept on a high cholesterol diet for only 3 weeks, coronary vascular permeability is significantly increased even before ischemia, and the damaging effects of ischemia on vascular integrity are far greater than in control animals. These changes are independent of the presence or absence of atherosclerotic occlusive disease of the coronary vasculature and therefore suggest an important, independent mechanism whereby hypercholesterolemia may render an individual at increased risk for ischemic heart disease. In studies currently in progress we are assessing the effect of still shorter durations of hypercholesterolemia (7-10 days), and preliminary results are consistent with the findings reported above.

In our previous isolated-heart experiments, flow rate was held constant; if perfusion pressure has been held constant, presumably the flow rate would have declined and left-ventricular contractile function would not have recovered during reperfusion. In future experiments, we shall test this hypothesis and examine the impact of these vascular changes on myocardial contractile performance during reperfusion following ischemia. Alternate hearts will be perfused under conditions of constant pressure or constant flow. We anticipate that when hearts are perfused under conditions of constant flow, myocardial contractile function will be preserved but that increases in perfusion pressure during reflow after ischemia may further damage vessels, contributing to increased vascular leakage and myocardial edema as we have observed previously. On the other hand, during reperfusion under conditions of constant pressure, we anticipate that vascular leakage and interstitial myocardial edema may be somewhat reduced, but that flow rate also will be reduced causing deterioration of myocardial contractile function. If these predictions are confirmed, the experiments would demonstrate the potential importance of compromised vascular integrity, induced by ischemic injury, in the pathogenesis of ischemic heart disease caused by transient vasospasm or vascular narrowing.

In additional experiments planned for the future, we shall evaluate vascular permeability changes in hearts from alloxan-diabetic rabbits to assess the effects of diabetes on the susceptibility of the vasculature to ischemic injury. We shall investigate these problems in rabbits with experimental diabetes of two to three months duration using both constant-flow and constant-pressure perfusion protocols.

A-4. Modification of Infarct Size

Personnel: A. S. Jaffe, M.D., Medicine
H. D. Ambos, BCL
J. D. Eisenberg, M.D., Medicine
P. R. Eisenberg, M.D., Medicine
E. M. Geltman, M.D., Medicine
R. M. Glueck, M.D., Medicine
S. J. Kovacs, Jr., M.D., Ph.D., Medicine
P. B. Kurnik, M.D., Medicine
B. D. Lindsay, M.D., Medicine
P. A. Ludbrook, M.D., Medicine
J. Markham, BCL
B. E. Sobel, M.D., Medicine
J. J. Spadaro, Jr., M.D., Medicine
A. J. Tiefenbrunn, M.D., Medicine

Support: RR 01380
HL 17646

Studies were performed in the Cardiac Care Unit at Barnes Hospital to assess the effects of pharmacological therapy on infarct size. Infarct size was estimated from serial plasma creatine kinase changes and with the use of serial positron emission transaxial tomographs. Results in control were compared to those observed in the treated groups. During the past year our efforts have focused on the evaluation of thrombolytic therapy, treatment of extension of infarction, an important contributor to the overall infarct size in patients with non-transmural infarction, and defining the relationship of extension and the complications of infarction to abnormalities in platelet function as assessed by platelet factor 4 and beta thromboglobulin.

To evaluate the effects of thrombolytic therapy directly on the heart, we studied 19 patients with first transmural myocardial infarction immediately upon admission and again 48 to 72 hours after the intracoronary administration of either tissue plasminogen activator or streptokinase. In all patients who received streptokinase, there was marked depression in fibrinogen, elevations of fibrin degradation products to a dilution of > 1:16, abnormal thrombin times, prothrombin times, and partial thromboplastin times. Patients treated with tissue plasminogen activator did not manifest reductions in fibrinogen nor coagulation parameters. In nine patients, lysis was achieved with streptokinase and in two with tissue plasminogen activator. In eight patients, lysis was not achieved. The mean time to the onset of symptoms to the initiation of the infusion with streptokinase was 5.4 ±1.3 (SE) hours in the group that achieved lysis and 9.9 ±2.8 hours in patients who did not achieve lysis. The two patients treated with tissue plasminogen activator received therapy in 3.8 to 7.5 hours after the onset of symptoms. In all patients in whom lysis occurred, there was a prompt rise in creatine kinase which reached peak levels rapidly. This was not observed in patients who did not achieve thrombolysis. After thrombolytic therapy, patients were maintained on heparin to keep the partial thromboplastin time at approximately two times

the normal level. Patients in whom thrombolysis was achieved, manifested a 29% reduction in PET infarct size (areas manifesting < 50% of maximal ventricular counts). Improvement was 27% in patients with anterior infarction and 30% in those with inferior infarction. This was significantly different than the results in the patients in whom lysis could not be achieved. Only two patients in the latter group improved, and the mean change was an increase of 4 PETT gm-eq. An example of myocardial salvage documented by positron tomography is shown in Figure 1. Although myocardial salvage was documented by positron-emission tomography, overall the left ventricular ejection fraction did not change significantly (50.9 ±3.6% before to 51.4 ±4.1% after thrombolysis) although the trend was favorable in these patients.[1]

Encouraged by the beneficial effects indicated by positron-emission tomography in patients utilizing streptokinase, and aware of data reported in project D-1 that tissue plasminogen activator (t-PA) had comparable benefit, we proceeded with a pilot project to evaluate the efficacy of t-PA. Tissue plasminogen activator is a naturally occurring clot-selective activator of fibrinolysis similar if not identical to the activator found in uterus. Recent experiments by Dr. Desire Collen in Belgium indicated that it does not bind avidly to circulating plasminogen (K_m = 65 μM) but has a high affinity for fibrin (K_d = .16 μM). Circulating plasminogen binds avidly to the tissue plasminogen activator fibrin c/mplex through the plasminogen lysine binding sites (K_m = .14 μM). Thus, plasminogen is not converted to plasmin in the plasma but is converted at the fibrin surface of the clot, making t-PA a very selective fibrin active agent with little effect on fibrinogen. Any plasmin that does escape into the circulation is rapidly inactivated by alpha-2 anti-plasmin. We utilized a t-PA product extracted from a melanoma cell culture line which we previously utilized to lyse clots in animals. We showed that prompt thrombolysis could be induced without effects on circulating fibrinogen or plasminogen or consumption of circulating alpha-2 anti-plasmin in seven patients studied with our Belgian colleagues. Coronary thrombolysis was induced in 19 to 50 minutes with either intravenous or intracoronary utilization of the agent. Circulating fibrinogen and alpha-2 anti-plasmin were not depleted in these patients except for the two patients who necessitated some degree of streptokinase therapy because the large amount of the clot exceeded the doses allowed for administration of tissue plasminogen activator (see Figure 2). In association with these findings, there was a prompt reduction in chest pain, resolution of ST segment abnormalities and improved ventricular performance. We have followed those studies with a pilot trial looking at the efficacy of tissue plasminogen activator made in a different manner which would allow more extensive utilization. Positron-emission tomographs also have been obtained in such patients, however the experience to date is not ripe for analysis. The lack of changes in coagulation parameters or bleeding is encouraging and suggests that t-PA will be an important agent in thrombolytic therapy in the future.[2]

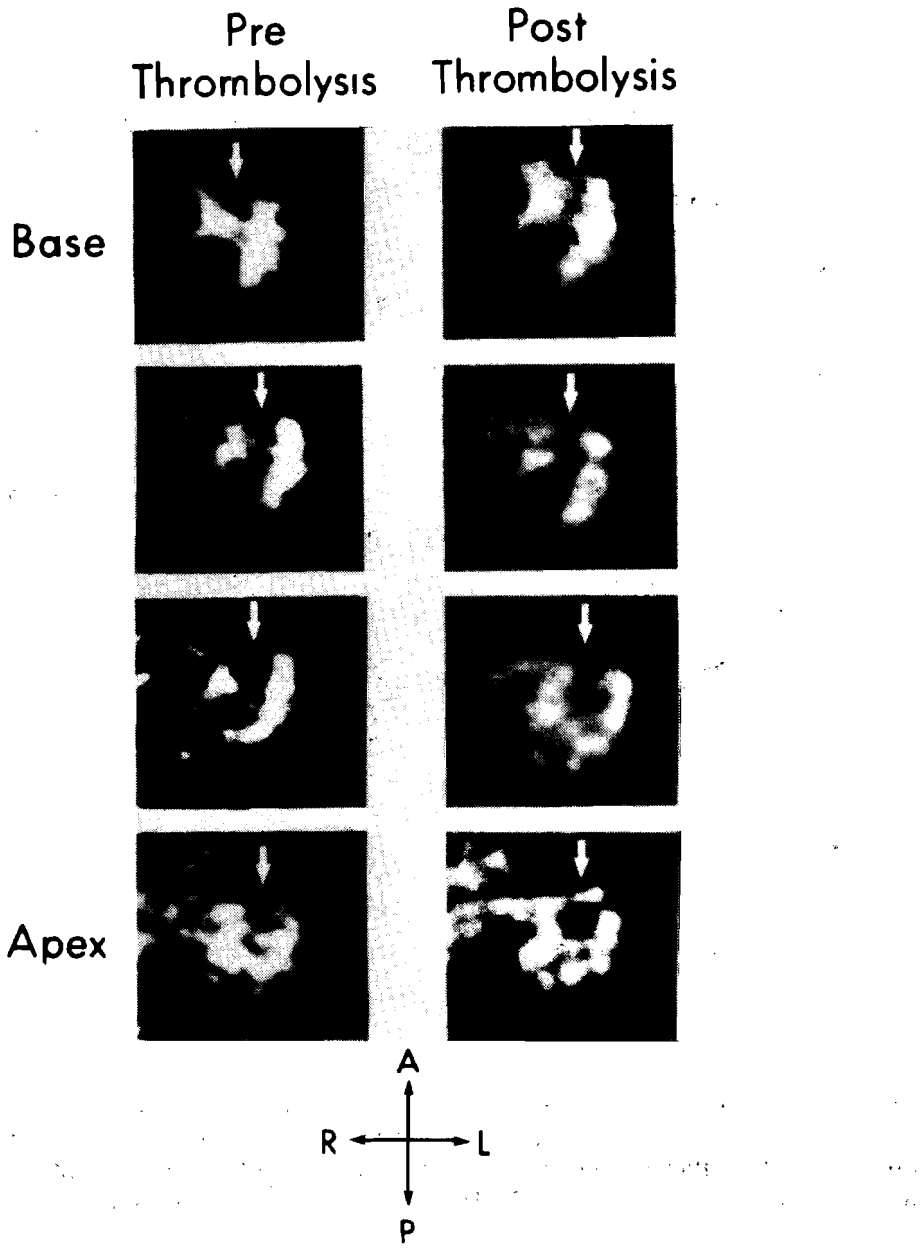

Figure 1. Positron emission tomograms reflecting uptake of ^{11}C-palmitate in four 1.5 cm thick transverse sections from the base, high ventricle, midventricle, and apex of the heart before (left) and after thrombolysis (right) induced with t-PA. Compromise of myocardial metabolism in the anterior left ventricular wall is visualized as a confluent, diminution of accumulation of ^{11}C-palmitate before thrombolysis (arrow). The anterior left ventricular regions indicated by arrows in the tomograms after thrombolysis show increased accumulation of ^{11}C-palmitate in jeopardized zones (arrows) in several sections.

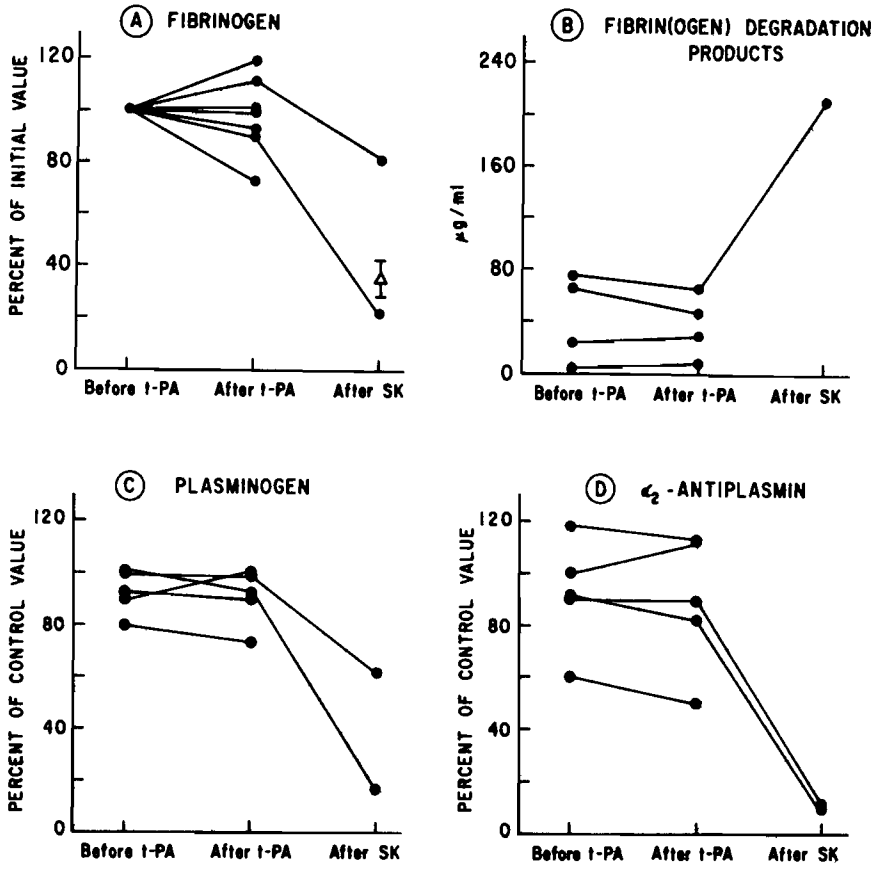

Figure 2. Effect of Tissue-Type Plasminogen Activator (t-PA) and Streptokinase (SK) on the Fibrinolytic Systems of the Patients. The triangle (Panel A) denotes the mean $\pm$S.E. of results in 17 other patients treated with intracoronary streptokinase alone.

An additional interest of ours for many years has been in the impact of recurrent injury on overall infarct size and our ability to reduce its incidence. We recently completed a 50-patient trial to assess the contribution of coronary vasospasm to the pathogenesis of chest pain in patients with non-transmural infarction. We hypothesized that the mechanism of recurrent injury, which in many studies occurs in as many as 40% of the patients, is likely similar to that which induces recurrent chest discomfort. Since many feel that ST-segment depression at the time of presentation of acute infarction is indicative of subtotal coronary occlusion and a propensity to a high incidence of recurrent infarction, coronary vasospasm has been suggested as a possible mechanism. Such a hypothesis has been bolstered by the suggestion that ST segment elevation occurs in some of these patients. In our randomized study, 50 patients with non-transmural infarction were randomized and received nifedipine or placebo in a double-blinded randomized manner. Chest pain occurred in 52% of the treated patients; 38 episodes on 33 days compared to 49% of control patients; 42 episodes on 35 days. Concurrent therapy with beta blockers was utilized in 11 patients in the control group and 11 in the treated group, and with nitrates in 12 patients in the control group and 11 in the treated group. There was no relationship between concurrent therapy and the incidence of chest discomfort. Recurrent infarction occurred in 12% and was comparable between the groups. The incidence of recurrent infarction was identical to that of all patients with non-transmural infarction followed prospectively (12%). In an attempt to improve the sensitivity for the diagnosis of recurrent injury, we also evaluated MB creatine kinase data to select patients in whom a 50% change in the level of MB CK occurred regardless of whether or not the absolute value reached the abnormal range. In patients stratified in this manner, 48% of the treated group and 44% of the control group had evidence of recurrent ischemia/infarction by this measure. Accordingly, it seems unlikely that the lack of a higher incidence of recurrent injury was related to a lack of sensitivity of the MB creatine kinase criteria. Ejection fraction, which was also monitored sequentially throughout the study, was identical between the groups. It increased in six control patients, decreased in nine, and did not change in six. In treated patients, ejection fraction increased in seven, did not change in seven, and decreased in six. Logistic regression failed to identify predictors for the recurrent chest discomfort or extension. Accordingly, we felt that remediable coronary vasospasm is not a likely cause of post infarction ischemia in these patients and therefore attempts to preclude increases in infarct size by precluding extension will likely have to focus on other interventions such as thrombosis, impaired myocardial function, or fixed obstructive disease.

In an attempt to further understand the pathophysiology of acute infarction and its complications, we utilized serial determinations of platelet factor 4 and beta thromboglobulin to assess the possible role of platelet aggregation in the pathophysiology of these phenomena. Platelet factor 4 and beta thromboglobulin are protein constituents of platelet granules. Their elevation in plasma is a sensitive marker of platelet degranulation. We utilized both platelet factor 4 and beta thromboglobulin since the clearance of platelet factor 4 is quite rapid, allowing for more precise timing of events, whereas beta thromboglobulin has a longer half-life, allowing one to delineate whether elevations are spurious due to

rough handling of the sample or due to in vivo degranulation. Previous data had suggested that platelet factor 4 was elevated in patients with acute infarction and therefore was a reflection of coronary thrombosis. We evaluated 52 patients with acute myocardial infarction under rigorous conditions verified to minimize platelet degranulation in vitro and performed correlative studies to detect left ventricular mural thrombus as well as other clinical complications of acute infarction. In a subset, coronary thrombosis was evaluated with indium-labeled platelets. Platelet factor four was normal at the time of admission in patients with infarction averaging 6.3 ±3.3 ng/ml (SD), similar to values in 44 other patients with chest pain without subsequent infarction (5.7 ±2.7) and in 25 normal subjects (4.3 ±1.6). Platelet factor four generally did not increase throughout the hospitalization in patients with infarction, recurrent chest pain, development of left ventricular thrombus, or documented recurrent infarction. The mean level of platelet factor 4 over time did not correlate with transmural versus non-transmural infarction, the presence of diabetes, the location of infarction (i.e., inferior or anterior), the incidence of prior infarction, the use of anti-platelet drugs, the presence of prior bypass surgery, or clinical congestive heart failure. Platelet factor 4 was, however, increased consistently after invasive procedures. Elevations after invasive procedures accounted for 104 of the total of 110 elevations that were seen. Such elevations were confirmed to be real by concomitant and sustained elevations (in the next sampling period) of beta thromboglobulin. An additional 86 elevations were thought to be due to in vitro granulation since beta thromboglobulin returned promptly to normal in the next sampling period. In only six other samples, platelet factor 4 was found to be elevated in vivo as confirmed by persistent elevation in beta thromboglobulin. These six samples came from one young woman with acute anterior myocardial infarction who was receiving oral contraceptive agents, and subsequently appeared to have a recanalized left anterior descending coronary artery. In this patient massive thrombosis was likely the etiology of her infarction. In patients studied with indium-labeled platelets, we were unable to delineate patients with positive or negative indium images on the basis of platelet factor 4. Thus, we found that platelet factor 4 values generally remained normal despite myocardial infarction. The rare elevations that we found were due to sampling artifacts in vitro which could be corrected with the use of beta thromboglobulin due to invasive procedures. Thus, platelet factor 4 does not provide a definitive basis for the assessment of abnormalities either acutely or during the evolution of acute myocardial infarction.

1. B. E. Sobel, E. M. Geltman, A. J. Tiefenbrunn, A. S. Jaffe, J. J. Spadaro, M. M. Ter-Pogossian, D. Collen, and P. A. Ludbrook, "Improved Regional Myocardial Metabolism after Coronary Thrombolysis with Tissue-Type Plasminogen Activator (t-PA) or Streptokinase," Circulation, vol. 69, pp. 983-989, 1984.

2. F. Van de Werf, P. A. Ludbrook, S. R. Bergmann, A. J. Tiefenbrunn, K. A. A. Fox, H. de Geest, M. Verstraete, D. Collen, and B. E. Sobel, "Coronary Thrombolysis with Tissue-Type Plasminogen Activator in Patients with Evolving Myocardial Infarction," New England Journal of Medicine, vol. 310, pp. 609-613, 1984.

3. A. S. Jaffe, R. Lee, J. Perez, E. M. Geltman, G. Wilner, and B. E. Sobel, "Factors Responsible for Elevated Platelet Factor Four in Plasma from Patients with Myocardial Infarction," Journal of the American College of Cardiology, in press.

A-5. Electrophysiological and Biochemical Factors Underlying the Genesis of Dysrhythmias Due to Myocardial Ischemia and Infarction

Personnel: P. B. Corr, Ph.D., Medicine and Pharmacology
J. B. Kramer, M.D., Medicine and Surgery
S. M. Moore, BCL
B. E. Sobel, M.D., Medicine
F. X. Witkowski, M.D., Medicine

Support: AHA 81-108
HL 17646
HL 28995

The overall purpose of these studies is the correlation of electrophysiological derangements with biochemical and adrenergic neural factors underlying malignant arrhythmias associated with ischemia as well as evolving myocardial infarction. The overall concept of the research is that potential arrhythmogenic metabolites accumulate in ischemic tissue and exert deleterious effects on membranes and that their effects may be exacerbated by the concomitant influences of the adrenergic nervous system. Over the past several years studies have been completed demonstrating a major electrophysiological role of α-adrenergic stimulation during myocardial ischemia as well as reperfusion. In addition, it has been demonstrated using radioligand binding procedures that there is a reversible increase in α_1-adrenergic binding sites in ischemic and reperfused myocardium. More recently, we have demonstrated that α-adrenergic blockade specifically attenuates the increase in intracellular calcium associated with reperfusion in reversibly injured tissue.[1] Studies performed in our laboratory have also indicated that lysophosphatides, including lysophophatidyl choline (LPC) and ethanolamine (LPE) accumulate in ischemic myocardium in situ and have been implicated as potential mediators of arrhythmogenesis in the ischemic heart.[2]

During the past year, studies have been completed assessing the influence of α-adrenergic blockade on the functional abnormalities associated with reperfusion of ischemic tissue. These studies were performed to assess whether α-adrenergic blockade could attenuate the depression in mitochondrial function associated with 35 minutes of ischemia followed by 10 minutes of reperfusion in vivo. After the ischemic and reperfusion interval, hearts were excised, rinsed in saline (4°) and anterior ischemic and posterior normal zones were removed and placed in sucrose (4°). Mitochondria were isolated by differential centrifugation and their function was assayed polarographically. State III oxygen

consumption (QO_2) was significantly depressed in the untreated group, n = 8 (195 ±11 natoms O_2/min/mg in the normal zone versus 138 ±5 natoms/min/mg in the ischemic zone, $p < 0.01$). Treatment with phentolamine (1 mg/kg), 2 to 4 min prior to reperfusion (n = 7), prevented the depression of mitochondrial function in the ischemic zone (185 ±18 natom/min/mg) as compared to the nonischemic zone (194 ±12 natoms/min/mg). Thus, blockade of α-adrenergic receptors during reperfusion in reversibly injured tissue enhances mitochondrial functional recovery independent of changes occurring during the antecedent ischemic interval. Currently, studies are underway to assess whether long-term ischemia (2 to 3 hours) with subsequent reperfusion can be influenced by α-adrenergic blockade just prior to the reperfusion interval.

Since delayed after-depolarizations (DADs) and triggered activity (TA) have been implicated in arrhythmogenesis in the ischemic heart, a series of studies have been completed recently to determine whether lysophosphatides, which accumulate within minutes in ischemic tissue, could induce DADs and TA in normoxic canine Purkinje fibers superfused with Krebs buffer studied with standard microelectrode procedures (n = 10). When maximum diastolic potential (MDP) was modestly depressed by -11.5 ±4 mV and amplitude by -18.8 ±5 mV, $p < .01$, 8 of 10 fibers exhibited DADs with a mean amplitude of 7.8 ±1.2 mV. Triggered activity was seen in 4 of 10 fibers, even at an extracellular calcium concentration of 3.0 mM. Treatment with epinephrine (10^{-6} M) in the presence of LPC, increased the DAD amplitude nearly 2-fold to 13 ±2.9 mV ($p < .05$). Five of 6 fibers exhibited TA. Increases in extracellular calcium increased DAD amplitude as well without increasing the incidence of TA. Thus, LPC-induced DADs and TA may contribute to initiation of arrhythmias in the ischemic heart and these effects appear to be enhanced by catecholamines. This lends further support to the contention that lysophosphatides accumulate in the ischemic heart and may contribute substantially to arrhythmogenesis and that inhibition of their accumulation is likely to influence the generation of malignant arrhythmias during myocardial ischemia.

Previously, transmural isochronic and isovoltaic mapping from multiple simultaneous sites has been limited by the need for analysis of stable repetitive rhythms. In a new system recently developed in our laboratory, electrograms from epicardial and transmural electrodes can be simultaneously recorded from up to 240 sites.[3] Likewise, this system is now operational in the cardiothoracic operating room for detailed transmural mapping for use in the surgical interruption of refractory atrial and ventricular arrhythmias. With the aid of this unique three-dimensional mapping system, we have recently identified a specific mechanism responsible for inducible ventricular tachycardia in 11 dogs 3 to 7 days after transient coronary occlusion. Analysis of data recorded simultaneously from 232 bipolar sites at 4 intramural levels showed that VT in each dog was due to intramural reentry comprising endocardial bi-directional conduction block, a fast alternate limb of endocardial conduction (1.1 ±0.1 M/sec during sustained VT), slow intra-myocardial conduction (0.4 ±0.1 M/sec), with return to the endocardium initiating the next beat. The slow limb of the reentry was subepicardial in each dog with sustained VT (n = 5), and greater epicardial delay was evident in this group compared to dogs with nonsustained VT both in sinus rhythm

(epicardial activation time = 46 ±5 versus 24 ±1 ms; $p < .01$) and with pacing (68 ±3 versus 54 ±3 ms; $p < .02$). Animals with only nonsustained ventricular tachycardia exhibited reentry confined to subendocardial zones. These findings demonstrate, for the first time, intramural reentry in vivo and delineate the critical factors important for development and assessment of therapeutic interventions.

Invasion of inflammatory cells during evolving myocardial infarction occurs in association with maximal arrhythmogenesis and we have recently shown that this is reflected by increased capacity for synthesis of thromboxane A_2 (TxA_2), a putative arrhythmogenic metabolite.[4] Using programmed electrical stimulation in conscious dogs, we demonstrated no limitation of ventricular tachycardia (VT) by thromboxane synthetase blockade despite verified inhibition within the infarct. With the three-dimensional cardiac mapping system, we assessed simultaneous regional activation information at 232 sites from 4 intramural layers in 5 anesthetized dogs 3 to 7 days after transient coronary artery occlusion. Infusion of OKY-1581 (100 μg/kg/min) a thromboxane synthetase inhibitor, did not alter ventricular refractory periods during pacing at 300 ms (ERP = 156 ±12 to 172 ±31 ms, NS) or 250 ms (ERP = 145 ±8 to 146 ±12 ms, NS). OKY-1581 did not affect epicardial activation time in sinus rhythm (34 ±8 to 33 ±8 ms, NS) or with pacing 60 ±6 to 61 ±5 ms). It also did not alter transmural activation time in normal or peri-infarct zones with sinus rhythm (peri-infarct transmural activation time = 11.1 ±1 to 11.1 ±1 ms) or pacing (9 ±2 to 9 ±1 ms). Thus, inhibition of thromboxane synthesis during infarction fails to protect against arrhythmogenesis and exerts negligible electrophysiological effects.

1. A. D. Sharma, J. E. Saffitz, B. I. Lee, B. E. Sobel, and P. B. Corr, "Alpha-adrenergic Mediated Accumulation of Calcium in Reperfused Myocardium," Journal of Clinical Investigation, vol. 72, pp. 802-818, 1983.

2. P. B. Corr, R. W. Gross, and B. E. Sobel, "Arrhythmogenic Amphiphilic Lipids and the Myocardial Cell Membrane," invited editorial for Journal for Molecular and Cellular Cardiology, vol. 14, p. 619, 1982.

3. F. X. Witkowski, and P. B. Corr, "Simultaneous Multiple Electrode Cardiac Mapping System," American Journal of Physiology, in press.

4. E. R. McClusky, P. B. Corr, B. I. Lee, J. E. Saffitz, and P. Needleman, "The Arachidonic Acid Metabolic Capacity of Canine Myocardium is Increased During Healing of Acute Myocardial Infarction," Circulation Research, vol. 51, p. 743, 1982.

A-6. Research Projects Utilizing the Isolated-Probe Data-Acquisition System

Personnel: H. D. Ambos, BCL
D. E. Beecher, BCL
S. R. Bergmann, Ph.D., Medicine
L. Fields, M.D., Medicine
K. A. A. Fox, M.B., Ch.B., Medicine
B. Hughes, Ph.D., Medicine
R. M. Knabb, Ph.D., Medicine
B. E. Sobel, M.D., Medicine

Support: RR 01380
AM 20579
HL 13851
HL 17646

The research in this project is designed to define the kinetics of positron-emitting tracers that are potentially useful for the noninvasive characterization of myocardial perfusion and metabolism and for the determination of adrenergic-receptor occupancy. Studies are conducted in isolated rabbit hearts perfused with washed sheep erythrocytes suspended in a modified Krebs-Henseleit buffer. The methodology permits control of factors that can modify myocardial perfusion and metabolism. Studies are also conducted in anesthetized, open-chest dogs prior to the implementation of approaches of proven value in studies using positron-emission tomography.

The development of accurate, quantitative, noninvasive measurements of myocardial metabolism and perfusion is dependent on the thorough characterization of the factors that can influence tracer kinetics. Since fatty acid is the major fuel for the myocardium under normal circumstances, we currently utilize ^{11}C-palmitate to estimate myocardial metabolism. In addition to the external detection of myocardial time-activity curves via coincidence detection of emitted gamma photons in isolated hearts and via a B-probe in open-chest dogs (with data fed to the isolated-probe data-acquisition system) we measure a number of myocardial and metabolic functions such as left-ventricular pressure and arteriovenous differences of substrate simultaneously. Washout curves of ^{11}C-palmitate are analyzed and correlated with myocardial work and substrate utilization. Assessments of myocardial metabolism based on external detection of accumulation of radiolabeled substrates may be influenced as a result of alterations in flow, by altered substrate delivery as well as altered work (with concomitant changes in metabolic requirements).

To determine whether reduced delivery limits substrate utilization under defined conditions of reduced perfusion, an isolated rabbit heart preparation was employed in which flow was reduced but myocardial oxygen consumption (MVO_2) and work were kept constant by adjustment of left ventricular end-diastolic pressure and heart rate. During the past year we completed a study in 27 isolated perfused rabbit hearts to determine whether substrate extractions (palmitate, glucose, oxygen) were limited

under conditions of low flow.[1] Myocardial work was kept constant by adjustment of left ventricular end-diastolic pressure and heart rate while flow was reduced from 1.5 to 0.5 mg/min. Consumption of ^{11}C-palmitate remained constant (48.8 ±11.6 in low work hearts and 68.8 ±23.3 nmols/g/min in high work hearts) because the proportion of palmitate extracted increased (8.8 ±4 to 29.1 ±7.2% and 10.3 ±3.4 to 21 ±6.1% in high work hearts). The results of the study indicate that despite reduction of flow, hearts at constant work loads can extract increasing proportions of delivered substrates such that net utilization remains constant until flow is reduced below the level required to maintain cellular function. They suggest that under conditions of low flow, impaired extraction of substrates reflects either primarily or secondarily depressed myocardial metabolism rather than simply decreased delivery of substrate. The study has implications on the interpretation of remote detection of radiolabeled fatty acid clearance from hearts either with isolated-probe data-acquisition systems or with positron-emission tomography. The question addressed is whether altered extraction of substrate reflects reduced metabolic demand or decreased substrate availability per se. The results suggest that decreased net extraction of radiolabeled palmitate in zones of transient ischemia in vivo (detectable by positron-emission tomography) is not attributable simply to decreased substrate delivery. They suggest that impaired net extraction of substrates reflects either transiently or persistently depressed regional metabolism.[1]

In the past year we have extended and completed a series of studies for the measurement of myocardial blood flow with $H_2{}^{15}O$.[2,3] Noninvasive quantification of regional myocardial blood flow is necessary for the assessment of dynamic and fixed coronary vascular obstruction and for objective assessment of therapy designed to augment nutritional perfusion. The current approach for the measurement of blood flow with diffusible tracers derives from the work of Kety and Schmidt.

Using $H_2{}^{15}O$ ($t_{1/2}$ = 2.1 min), we demonstrated that a modification of the tissue autoradiographic approach permitted quantification of myocardial blood flow (MBF) in open-chest dogs with direct myocardial tissue assay and that noninvasive estimation with positron-emission tomography (PET) delineated relative MBF in intact dogs. In open-chest anesthetized dogs, the single-pass extraction fraction of $H_2{}^{15}O$ averaged 96 ±5% at flows of 80 to 100 ml/100 g/min. This high extraction fraction did not differ significantly over the range of 12 to 238 ml/100 g/min. MBF calculated after a 60 sec i.v. infusion with $H_2{}^{15}O$ and direct tissue analysis correlated well with results obtained with results obtained with microspheres ($r = .94$, $n = 9$ dogs). Subsequently the approach was adapted for preliminary use with PET. Estimation of myocardial content of radiolabeled $H_2{}^{15}O$ after i.v. infusion of 20 to 30 mCi of $H_2{}^{15}O$ was corrected for vascular-pool radioactivity with the use of tomographic data obtained after separate administration of $C^{15}O$ (to label red blood cells). Tomograms obtained in vivo in six dogs with either normal or reduced regional blood flow correlated closely with the tomographically detectable distribution of ^{68}Ga-labeled microspheres ($r = .93$) and with microsphere distribution determined post-mortem ($r = .95$). The technique accurately reflects myocardial blood flow. Using PET, rapid sequential noninvasive estimation of relative regional MBF has been demonstrated and should

ultimately permit improved objective assessment of nutritional blood flow in patients in response to medical and surgical interventions designed to augment perfusion.[2,3]

We have previously shown that myocardial washout of extracted ^{11}C-palmitate is quantitatively diminished with ischemia or hypoxia. To define the quantitative influence of back diffusion of non-metabolized tracer, ^{11}C-palmitate was injected intracoronarily in 15 open-chest dogs with the LAD perfused extra-corporeally.[4] Myocardial blood flow (MBF) was measured with $H_2{}^{15}O$. Arterial and coronary-venous total fatty acids, $^{11}CO_2$, ^{11}C-palmitate, lactate, and O_2 were measured directly. Under baseline conditions or under conditions with no intervention (control), 60.0 ±13% (mean ±SD) of initially extracted ^{11}C-palmitate was oxidized to $^{11}CO_2$, and 10.1 ±6.2% was liberated unaltered as from 1 to 20 min after injection of tracer. With ischemia (arterial flow <20% of control, n=6), or hypoxia (perfusion of venous blood at normal flow, n=6), <25% of initially extracted ^{11}C-palmitate was oxidized to $^{11}CO_2$ but >17% appeared as unchanged ^{11}C-palmitate. Quantitative analysis of efflux from 1-20 min revealed that with ischemia and hypoxia ^{11}C-palmitate back-diffusion comprised 40.3 ±11.2% and 48.9 ±17.3% of total efflux compared with 10.5 ±3.6% in controls. The fraction of extracted ^{11}C-palmitate liberated as $^{11}CO_2$ (in 1-10 min) correlated closely with MVO_2 (r=.82, n=27). Thus, with hypoxia or ischemia, assessment of oxidation of fatty acid based on analysis of residue time-activity curves must be corrected for back-diffusion of initially extracted but non-metabolized fatty acid.[4]

To evaluate the extent of early recovery of ^{11}C-palmitate (^{11}Cp) metabolism after 20 minutes of myocardial ischemia followed by reperfusion, 16 open-chested anesthetized dogs were perfused extracorporeally through the LAD or LCX.[5] Arterial and local coronary venous fatty acids, $^{11}CO_2$, ^{11}Cp, lactate, glucose, and oxygen were measured directly and regional residue time-activity curves assessed with a B-probe after intracoronary injection of ^{11}Cp. Under baseline conditions or those with no intervention, 66.1 ±11.5% of initially extracted ^{11}Cp was oxidized to $^{11}CO_2$ and 10.5 ±5.9% liberated from myocardium as unaltered ^{11}Cp from 1 to 20 min after injection of tracer. With ischemia (flow < 30% of baseline, n=6), 25.5 ±13.8% of initially extracted ^{11}Cp was oxidized to $^{11}CO_2$ and 17.2 ±9.3% released as ^{11}Cp. After 30 min of reperfusion (n=7), 42 ±19% of ^{11}Cp was oxidized to $^{11}CO_2$ and 8.6 ±3.9% released as ^{11}Cp while the monoexponential clearance of residual ^{11}Cp ($t_{1/2}$) increased from 5.3 ±0.9 min to 9.5 ±3.2 min. MVO_2decreased from 16.9 ±5.0 (baseline) to 9.8 ±4.4 (reperfusion) ml/100 g/min. Thus, despite brief (20 min) myocardial ischemia, myocardial metabolism of fatty acid remains depressed when accessed early after reperfusion.[5]

It has been established that adrenoreceptor number and binding affinities may change in a number of cardiac disease states such as ischemia and congestive heart failure. To assess the feasibility of characterizing cardiac B-receptors noninvasively, a study was completed in the past year in isolated, isovolumically beating rabbit hearts to extend our earlier observations. ^{125}I-hydroxybenzylpindolol was added to the recirculating perfusate for 40 minutes. Uptake and release were monitored

externally with a single gamma probe and the isolated-probe data-acquisition system. Specificity of binding was assessed by measuring the clearance of the ligand from the heart during perfusion with D- or L-isomers of adrenoreceptor agonists and antagonists. The L-isomers of epinephrine, norepinephrine and isoproterenol cause significant dissociation of the ligand from its binding sites, while no effect was seen with D-isomers or perfusate. Thus specific binding of ^{125}I-hydroxybenzylpindolol to cardiac B-receptors can be detected externally.[6] These earlier studies demonstrated that hearts from animals treated with thyroid hormone exhibited increased uptake of the ligand (^{125}I-hydroxybenzylpindolol) which was detectable externally and was confirmed by an increase in receptor number by means of Scatchard analysis of ventricular membrane preparations. In the past year these studies were extended to determine the feasibility of distinguishing specific and non-specific binding. We conducted studies in vitro and in vivo with ^{131}I-labeled d- and l-pindolol (^{131}I-d-P, ^{131}I-l-P). Each isomer was iodinated with chloramine T and purified by high-pressure liquid chromatography. In rabbit left-ventricular-membrane preparations, binding of ^{131}I-l-P (Kd=0.37 ±0.18 (SD) nM) was saturable and stereospecific. In contrast ^{131}I-d-P did not exhibit specific binding over the concentration range of 0.05 - 10 nM. To determine whether specific binding could be assessed in vivo, we injected New Zealand white rabbits with 500 μCi (0.3 nmols) ^{131}I-l-P (n=4) or ^{131}I-d-P (n=4) and sequential one-minute scintigrams were obtained for eight minutes. ^{131}I-l-P exhibited marked uptake in the lung and heart, which was blocked by pretreatment with 0.2 mg/kg propranolol. Binding of ^{131}I-d-P was diffuse and not affected by propranolol. Thus, with the use of labeled isomers and ligands, the l-isomer for detection of specific and non-specific sites, and the d-isomer for detection of non-specific sites, noninvasive visualization and quantification of specific receptor binding is possible in vivo under conditions devoid of disruption of the normal receptor environment.[7]

Cardiac dysfunction seen in hearts from diabetic animals has been attributed to vascular atherosclerotic lesions even though specific cellular metabolic defects have been observed as well. To characterize the relationship between MVO_2, substrate utilization, and myocardial work we evaluated hearts isolated from normal (n=13) and alloxan-induced diabetic rabbits (n=8). The paced, isovolumically beating hearts were retrogradely perfused with RBC-enriched buffer. Hearts from diabetic rabbits exhibited diminished peak LV systolic pressure (55 ±8 (SE) versus 88 ±5 mm Hg in hearts from normal rabbits). Similarly dP/dt was reduced (670 ±122 versus 1091 ±88 mm Hg/sec) and LV pressure-time index was also reduced in diabetic hearts (LVPTI, 2024 ±298 versus 3198 ±210 mm Hg.sec/min) ($p < .01$ for each). Levels of LVEDP and coronary flow were equivalent. Despite diminution of levels of work of >35% compared to hearts from normals, MVO_2 in hearts from diabetic rabbits diminished only 16%. MVO_2/LVPTI, an index of O_2 utilization/unit work, was higher in hearts from diabetics (1.88 ±0.17 versus 1.41 ±0.12, $p < .05$). Exogenous palmitate utilization was not different between the two groups, but hearts from diabetics produced lactate (613 ±337 nmols/g/min) compared with net extraction of lactate in normals (-253 ±114, $p < .01$). The results are consistent with a partial uncoupling of MVO_2 from myocardial work and suggest that a metabolic defect independent from vascular damage may contribute to the dysfunction of hearts from diabetic animals.[8]

The studies performed in the past year with ^{11}C-palmitate have permitted a better understanding of factors that influence the uptake and efflux of this tracer in intact animals and specifically have looked at the influence of back diffusion of nonmetabolized ^{11}C-palmitate. Studies planned for the next year include further characterization of the kinetics of ^{11}C-palmitate handling in association with direct kinetics of ^{11}C-palmitate handling in association with direct determinations of efflux. In addition, preliminary investigations will be undertaken to evaluate the handling of fatty-acid analogs, including beta-methyl-heptadecanoic acid, under conditions of normoxia and ischemia. The studies performed in the past year have confirmed and validated the $H_2{}^{15}O$ diffusible tracer technique for the measurement of myocardial perfusion. The studies of $H_2{}^{15}O$ have been extended to intact animals and patients and tissue perfusion has been characterized based upon the clearance of $H_2{}^{15}O$ with the use of positron-emission tomography. The results of studies with beta-adrenoreceptor ligands have been encouraging and raise the possibility that receptor occupancy may be detectable by positron-emission tomography in vivo. Finally, the studies in diabetic hearts have suggested partial uncoupling of myocardial oxygen consumption from myocardial work in this model, and will lead to further investigation of mitochondrial function in diabetic hearts in the next year.

1. K. A. A. Fox, H. Nomura, B. E. Sobel, and S. R. Bergmann, "Consistent Substrate Utilization Despite Reduced Flow in Hearts with Maintained Work," American Journal of Physiology, vol. 244, pp. H799-H806, 1983.

2. S. R. Bergmann, K. A. A. Fox, A. L. Rand, J. Markham, and B. E. Sobel, "Quantitation of Myocardial Perfusion with Radiolabeled Water," Journal of the American College of Cardiology, vol. 1, p. 577, 1983 (abstract).

3. S. R. Bergmann, K. A. A. Fox, A. L. Rand, K. D. McElvany, M. J. Welch, J. Markham, and B. E. Sobel, "Quantification of Regional Myocardial Blood Flow In Vivo with $H_2{}^{15}O$, Circulation, in press.

4. K. A. A. Fox, H. D. Ambos, H. Nomura, S. R. Bergmann, and B. E. Sobel, "The Importance of Back-Diffusion on Myocardial Kinetics of ^{11}C-Palmitate," Journal of the American College of Cardiology, vol. 3, p. 200, 1984.

5. K. A. A. Fox, D. R. Abendschein, B. E. Sobel, and S. R. Bergmann, "Detection of Persistent Metabolic Impairment Despite Reperfusion After Transient (20 Min) Myocardial Ischemia," Federation Proceedings, vol. 43, p. 902, 1984.

6. B. Hughes, S. R. Bergmann, and B. E. Sobel, "External Detection of Beta-adrenoreceptor Occupancy in Isolated Perfused Hearts," Circulation, vol. 66, p. II-206, 1982 (abstract).

7. B. Hughes, D. R. Marshall, J. E. Bakke, B. E. Sobel, and S. R. Bergmann, "In Vivo Characterization of Beta-adrenoceptors with ^{131}I-Pindolol," Federation Proceedings, vol. 43, p. 1097, 1984.

8. L. E. Fields, A. Dautherty, B. E. Sobel, and S. R. Bergmann, "Dissociation of Oxygen Utilization from Work in Diabetic Rabbit Hearts," Federation Proceedings, vol. 43, p. 374, 1984.

A-7. Analysis of Plasma CK Isoforms

Personnel: B. E. Sobel, M.D., Medicine
D. R. Abendschein, Ph.D., Medicine
A. M. Grace, Medicine
H. Hashimoto, M.D., Medicine
J. Markham, BCL
A. W. Strauss, M.D., Biochemistry

Support: RR 01380
HL 17646

Subforms of individual CK isoenzymes were delineated with a non-denaturing procedure developed to permit quantification. Analysis of 2-ml plasma samples precipitated with ETOH to remove globulins was accomplished with 2- to 10-µl aliquots subjected first to agarose electrophoresis. Each aliquot contained between 1 and 10 mIU of MM CK activity. Separated subforms of the MM isoenzyme (isoforms) were transferred to nitrocellulose, treated with anti-MM CK and ^{125}I-anti-IgG. The resulting native blot was exposed to film, isoforms localized autoradiographically, and isoforms quantified by well counting. Reproducibility was consistently within 11%. Intrapreparative conversion of one isoform to another did not occur. Values were linear from 1 to 10 mIU for each isoform (MM_A, MM_B, and MM_C) with correlation coefficients of .93 to .96 (n = 225 determinations). Results correlated closely with those obtained by chromatofocusing, a more laborious procedure developed and validated previously (average difference = 0.3 ±1.4 (SE) %, n = 74). The blot procedure was 100-fold more sensitive, permitted assay of as many as 40 samples simultaneously, and provided quantitative assessment of isoform profiles in 2-ml plasma samples under conditions precluding intrapreparative conversion.

With the use of the isoform analysis procedures developed in this project, studies were performed to evaluate the potential of isoform assays for early detection of myocardial infarction. Eight conscious dogs were subjected to coronary occlusion. Plasma samples were obtained before occlusion and serially thereafter for analysis of MM_A, MM_B, and MM_C. In control samples values averaged 12 ±5 (SD), 22 ±6, and 66 ±10% of total MM CK respectively. The fraction of MM_C, the isoform formed slowly in plasma from MM_A via MM_B, decreased within 1 hr ($p < .01$), reached a minimum of 14 ±4% of MM in 5 ±1 hr, and returned to baseline in 13 ±3 hr. Thus, even though total CK activity did not become significantly elevated for 4 hr after coronary occlusion, early significant changes in plasma isoform proportions permitted detection of infarction within 1 hr after coronary

occlusion. Changes in isoform proportions were consistent, independent of peak total CK activity or cumulative CK release over a 10-fold range, and antecedent to elevated total CK regardless of infarct size.

Ongoing activities in this project include mathematical modeling of processes involved in isoform release, clearance, and interconversion with correlative experiments designed to assess the applicability of assumptions in models undergoing development and the utility of models in delineating precisely the time of occurrence of initial myocardial irreversible injury on the one hand and reperfusion with accelerated washout of the tissue isoform on the other. Appropriate application of validated models should permit differentiation between reperfusion with accelerated washout of already liberated tissue enzyme from liberation of enzyme associated with reperfusion injury.

A-8. Multicenter Investigation of Limitation of Infarct Size (MILIS)

Personnel:
A. S. Jaffe, M.D., Medicine
G. G. Ahumada, M.D., Medicine
H. D. Ambos, BCL
D. R. Biello, M.D., Radiology
T. L. Buettner, Medicine
K. W. Clark, BCL
E. D. Galie, R.N., Medicine
E. M. Geltman, M.D., Medicine
F. Lifshits, Medicine
J. M. McAninch, Medicine
J. P. Miller, BCL
S. R. Mumm, Medicine
D. S. Payne, Medicine
J. E. Perez, M.D., Medicine
C. S. Ritter, Medicine
B. A. Siegel, M.D., Radiology
B. E. Sobel, M.D., Medicine
L. J. Thomas, Jr., BCL
A. J. Tiefenbrunn, M.D., Medicine
R. A. Wettach, Medicine
A. L. Ysaguirre, Medicine

Support:
RR 01380
HV 72941
Washington University

The MILIS protocol was initiated on August 1, 1978. The goals of the study were to evaluate the efficacy of the administration of hyaluronidase and of propranolol in limiting the extent of myocardial infarction. The primary end-point selected for analysis was MB-CK infarct size corrected for body surface area. Other end-points included ventricular function as assessed by radionuclide ventriculograms, the

incidence of positive pyrophosphate images, determinations of infarct size from the pyrophosphate imaging, total creatine-kinase infarct size, mortality and dysrhythmias at 10 days. Data were collected from five clinical centers including Washington University, the Massachusetts General Hospital, the Medical Center of Vermont, Parkland Hospital in Dallas, and the Peter Bent Brigham Hospital. All data were analyzed in core laboratory facilities in a blinded fashion. The Creatine Kinase Reference Laboratory and Holter Analysis Reference Laboratory were at Washington University. The Electrocardiographic Reference Laboratory was at the Peter Bent Brigham Hospital. The Infarct Scintigraphy Laboratory was at Parkland Memorial Hospital. The Radionuclide Ventricular Function Laboratory was at Duke University. Data from the clinical centers and core laboratories were centrally analyzed at the Data Coordinating Center at the Research Triangle Institute.

The Washington University components of this project included the Clinical Unit, directed by the Clinical Unit Director, Dr. Allan S. Jaffe, the Creatine Kinase (CK) Core Laboratory, directed by Dr. Burton E. Sobel, and the Holter Core Reference Laboratory, directed by Dr. Lewis Thomas, Jr. The Principal Investigator for this study at Washington University was Dr. Jaffe.

In February of 1983, the Policy Board mandated that propranolol administration be discontinued. All investigators were notified, reviewed the data and supported the recommendation of the Policy Board. Subsequently, an abstract of the propranolol data was presented at a session of the American Heart Association meeting in November of 1983. The data from that abstract are summarized in Table I. Two hundred sixty-nine patients were randomized to receive propranolol or beta blockers on the basis of at least 30 minutes of chest discomfort and ST-segment change, either elevation or depression of 1 mm or greater. Only patients who could receive therapy < 18 hours from the onset of their chest-pain syndrome were included. One hundred thirty-four patients were randomized to receive propranolol and 135 served as controls. Propranolol was given in a dose of .1 mg/kg intravenously over an initial three minute period, followed three hours thereafter by a second dose of half the initial dosage, and then oral therapy for the next nine days. In 18 patients who received propranolol and 14 patients in the control group, infarct size could not be calculated. Infarct size was not different between treated and control groups for the total group or for subsets stratified by time from the onset of symptoms to therapy into subsets treated 0 to 8 or 8 to 18 hours after onset. In addition, there were no significant differences between propranolol and control groups in the incidence of infarction, the amount or percentage of R-wave loss on the electrocardiogram, the change in left ventricular ejection fraction between 0 and 10 days, the incidence of positive pyrophosphate images, or mortality. The mean time to therapy was 8.9 ±0.2 hours. It is conceivable that the overall negative results were due to late administration of drug since other studies utilizing beta blockers have suggested salutary effects on infarct size when earlier administration of therapy is initiated.[1,2]

The hyaluronidase arm of the study was terminated on December 31, 1983. By that time 9,444 patients had been screened for eligibility and a

total of 985 had been randomized. Washington University contributed 244 patients (25%) of the overall recruitment. Analysis of the hyaluronidase data is ongoing and presently principal investigators who have been unblinded to the data are restricted from discussing the information until such time as the true nature of the data can be more completely defined.

During the last several years, several data bank studies from the MILIS investigation have reached fruition. Such investigations had involved a variety of different components of the MILIS effort at Washington University. Data from MILIS compared the clinical and electrocardiographic criteria for acute myocardial infarction. Diagnosis by MB creatine kinase was utilized as the reference standard. The presence of 30 minutes of chest discomfort and either new Q waves, 1 mm of ST elevation or depression in two of the three inferior leads, two of the six precordial leads, or in 1 or L, or left-bundle-branch block had an overall sensitivity of 81% for infarction. The overall infarct rate in this population, however, was 49%. The diagnostic specificity of these criteria was 69% and the predictive value 72%.[3] In addition, a computer algorithm was devised to estimate infarct size when the initial portions of the MB creatine kinase time-activity curves were missing. This investigation allowed for calculation of infarct size in an additional 20% of patients. The basis of the computer algorithm were complete time-activity curves from 120 patients. Estimates of CK infarct size based on data-inclusion intervals beginning at 24, 12, 8 and 4 hours before peak were 11, 14, 23, and 47% smaller than values based on complete curves but the correlations were good between complete and incomplete estimates with r values ranging from .91 to .98. When the correction factors which were derived from these relations were tested on a new population, the corrected estimates were within 7% of those based on the total curves. This correction was not different in relation to locus (transmural or nontransmural) or the location (anterior or inferior) of infarction.[4] The pathological correlates and significance of persistently positive pyrophosphate images were also described. The data suggested that MB-CK-determined infarct size was similar between patients with and without persistently positive images, 17.4 ±10.6 MB CK-gm-eq/m^2 for patients with persistently positive pyrophosphate scintigrams compared to 16.0 ±14.6 MB CK-gm-eq/m^2. Similarly, myocardial infarct areas by pyrophosphate images in patients who had well localized and intense uptake of tracer anteriorly were also not significantly different, 33.7 ±13.4 for patients with persistently positive images compared to 34.4 ±13.1 cm^2 for patients without persistently positive images. Nonetheless, patients with persistently positive images had lower ejection fractions (0.42 ±0.14 ejection fraction units compared to .49 ±0.14, $p < .01$) early after the onset of infarction as well as subsequently. Therefore as expected, there was a greater incidence of congestive heart failure in these patients (41 compared to 24%, $p < .01$). It was speculated that the presence of a persistently positive pyrophosphate image in patients with similar infarct size but greater impairment in left ventricular function might reflect ongoing intermittent necrosis or even perhaps "chronic ischemia,"[5] A large number of MILIS data bank studies are near completion at the present time and should be published in the near future. These include studies comparing the sensitivity of a variety of diagnostic measures for acute infarction, data evaluating the effects of infarction in patients with hypertension, an

analysis of the predictive value of ventricular ectopic depolarization and left ventricular function on the incidence of sudden death, data on the effects of abrupt beta blocker withdrawal and a manuscript defining the relationship between morphometric measures of infarct size obtained at pathology and creatine-kinase determined infarct size determined at the central laboratory. The latter manuscript confirms the excellent relationship between morphology and creatine kinase determined infarct size in 49 patients. The overall correlation coefficient (Spearman) was .87 for the 25 hearts where enzymatic estimates of infarct size were available.[6]

The MILIS study was a very successful endeavor, both overall and for Washington University. In addition to continued analysis of the hyaluronidase data, more than 40 ongoing data bank studies are now proceeding in an attempt to define a variety of important clinical relationships in patients with acute infarction. Continued involvement of the investigators has been assured and analysis of the data will extend for at least one and perhaps two more years.

1. J. Muller, R. Roberts, P. Stone, R. Rude, D. Raabe, H. Gold, A. S. Jaffe, W. Strauss, Z. Turi, K. Poole, E. Passamani, J. Willerson, B. E. Sobel, E. Braunwald, and the MILIS Study Group, "Failure of Propranolol Administration to Limit Infarct Size in Patients with Acute Myocardial Infarction," Circulation (Part II), vol. 68, p. 294, 1983.

2. R. Roberts, C. Croft, H. K. Gold, D. H. Tyler, A. S. Jaffe, J. E. Muller, S. M. Mullin, C. Parker, E. R. Passamani, W. K. Poole, D. S. Raabe, R. E. Rude, P. H. Stone, Z. G. Turi, B. E. Sobel, J. T. Willerson, E. Braunwald, and the MILIS Study Group, "Electrocardiographic and Clinical Criteria for Recognition of Acute Myocardial Infarction Based on Analysis of 3,697 Patients," American Journal of Cardiology, vol. 52, pp. 936-942, 1983.

4. J. L. Smith, H. D. Ambos, H. K. Gold, J. E. Muller, W. K. Poole, D. S. Raabe, R. E. Rude, E. Passamani, E. Braunwald, B. E. Sobel, R. Roberts, and the MILIS Study Group, "Enzymatic Estimation of Myocardial Infarct Size When Early Creatine Kinase Values Are Not Available," American Journal of Cardiology, vol. 51, pp. 1294-1300, 1983.

5. C. H. Croft, R. E. Rude, S. E. Lewis, R. W. Parkey, W. K. Poole, C. Parker, N. Fox, R. Roberts, H. W. Strauss, L. J. Thomas, D. S. Raabe, B. E. Sobel, H. K. Gold, P. H. Stone, E. Braunwald, J. T. Willerson, and the MILIS Study Group, "Comparison of Left Ventricular Function and Infarct Size in Patients With and Without Persistently Positive Technetium-99m Pyrophosphate Myocardial Scintigrams after Myocardial Infarction: Analysis of 357 Patients," American Journal of Cardiology, vol. 53, pp. 421-428, 1984.

6. D. B. Hackel, K. A. Reimer, R. E. Ideker, E. M. Mikat, T. D. Hartwell, C. B. Parker, E. B. Braunwald, H. K. Gold, A. S. Jaffe, D. S. Raabe, R. E. Rude, B. E. Sobel, P. H. Stone, M. Buja, J. E. Muller, R. Roberts, and the MILIS Study Group, "Comparison of Enzymatic and Anatomic Estimates of Myocardial Infarct Size in Man," submitted for publication.

Table 1
Infarct-Size Index and Peak Plasma MB Creatine Kinase

	Propranolol	Placebo	P Value
Infarct-size index (gram-equivalents of MB creatine kinase/m^2)			
Total population			
No. of patients	116	121	
Mean ±S.E.	13.3±1.2	13.6±1.1	0.87
Range	0.0-58.1	0.0-58.7	
Early-randomization subgroup (0-8 hr)			
No. of patients	67	57	
Mean ±S.E.	13.8±1.4	15.2±1.8	0.53
Range	0.0-50.0	0.0-58.7	
Late-randomization subgroup (8-18 hr)			
No. of patients	49	64	
Mean ±S.E.	12.7±2.0	12.2±1.4	0.83
Range	0.0-58.1	0.0-51.2	
Peak plasma MB creatine kinase (IU/liter)			
Total population			
No. of patients	133	134	
Mean ±S.E.	121.3±9.5	118.8±8.1	0.84
Range	0-540	0-507	
Early-randomization subgroup (0-8 hr)			
No. of patients	75	59	
Mean ±S.E.	121.4±11.2	140.4±13.9	0.29
Range	6-486	5-507	
Late-randomization subgroup (8-18 hr)			
No. of patients	58	75	
Mean ±S.E.	121.3±16.4	101.8±9.1	0.31
Range	0-540	0-336	

A-9. Model Development for Cardiac Diastolic Mechanics

Personnel: P. B. Kurnik, M.D., Medicine
M. R. Courtois, M.A., Medicine
P. A. Ludbrook, M.D., Medicine
J. Markham, BCL

Support: RR 01380
HL 17646
HL 25430
Barnes Hospital
Washington University

During the past year, our studies of cardiac diastolic mechanics (PR 19, A-15), i.e., the passive mechanical properties of the left ventricular (LV) muscle and chamber, have continued with emphasis on (1) refining our theoretical models of the stress-strain and pressure-volume relations and (2) evaluating these models in a number of physiologic and pathophysiologic situations in the animal and in the human catheterization laboratories.

Values for stress are computed from several variables including intra- and extra-cavitary pressures, measured in the cardiac catheterization lab using catheter-tip micromanometers, and the cavity radii calculated from the area and the longest chord of the ventricle as measured from single-plane angiographic silhouettes. To reduce the errors associated with the angiographic measurements, the area and the major chord were smoothed by fitting to a fourth-order polynomial. Stress can be derived as a function of strain, and strain as a function of radius to yield a stress-radius relationship for estimating elastic stiffness of the LV muscle. Our technique has a number of unique advantages over previous models, including (1) lack of explicit assumptions about the stress-radius relation, (2) avoidance of need for direct measurement of strain, and (3) performance of stress-strain analysis independently of pressure-volume calculation.

A dedicated Hewlett-Packard 5600 M computer system is used for all phases of this diastolic modeling. As described in PR 19, the angiographic data are digitized by sonic tablet and the raw areas, largest chords, and wall thicknesses are smoothed and utilized to derive volume and wall masses. In the last year, the system has been programmed to read hemodynamic information off-line from F-M magnetic tape and to detect and calculate a variety of pressure and dP/dt functions. The hemodynamic and dimensional data are now integrated automatically for calculation of a variety of stress-strain and pressure-volume curves and indexes. Improved access to and utilization of the SAS statistical system has also been implemented.

The analysis of early diastole, particularly as regards pressure and stress decay, is of fundamental importance and complements our previous investigation of filling-phase characterization. Our computer system has been programmed to digitize the pressure decay at 5 msec intervals and models of time-constant derivation are being tested.

Applications of our model to two important physiologic systems in man have been tested. Previous work by our group had demonstrated a reduction of LV end-diastolic pressure and volume by nifedipine, as well as a downward shift of the pressure-volume curve, without alteration of chamber stiffness. With our new model we have demonstrated that myocardial stiffness is also unchanged by nifedipine, indicating that constraints external to the LV mediate these effects of nifedipine. Additionally, this model was used to determine whether or not global myocardial stiffness differed between patients with normal LV function and those with LV function impaired by CAD. Despite differences in ejection fraction and end-diastolic pressure and volume, global myocardial stiffness was similar in the two groups.

Since May, 1984, research has been extended into a dog model, utilizing full-scale high-fidelity angiographic and hemodynamic monitoring. This will allow more extensive instrumentation and intervention than is available in the clinical setting, which will greatly add to refinement and expansion of our diastolic modeling. In particular, the effects of thrombolysis on diastolic mechanics is being investigated.

During the next year, efforts will be directed at developing models of regional stiffness which would greatly assist in characterization of segmental diseases such as CAD. We plan to expand our hemodynamic monitoring to allow assessment of transmural rather than just intracavitary pressure.

A-10. SCOR Patient Information Database

Personnel: K. B. Schechtman, BCL
H. D. Ambos, BCL
E. D. Galie, R.N., Medicine
E. M. Geltman, M.D., Medicine
A. S. Jaffe, M.D., Medicine
J. Markham, BCL
B. E. Sobel, M.D., Medicine

Support: RR 01380
HL 17646

The Specialized Center for Research (SCOR) database currently contains information pertinent to more than 1700 patients who suffered acute myocardial infarction. The variables contained in this database describe the patient's cardiovascular history, in-hospital course, and long term progress via follow-up examination. Until this year, the data have been entered into the Interdata 7/16 computer system in the coronary care unit and then transferred via magnetic tape to the IBM System/370 at the University's Computing Facilities. There, a permanent SAS database has been maintained in order to address a variety of clinical questions.

Currently, the data entry and storage system is being redesigned. When this process is completed, data will be entered through the use of interactive SAS under the Conversational Monitoring System (CMS) operating system. This will permit on-line retrieval and editing of all data and will provide on-line access to all SAS statistical procedures and data management capabilities. Through the use of CMS, all data will be stored on disk as SAS datasets. Backups will be maintained on tape.

Studies which have utilized the SCOR database include the use of positron-emission tomography to determine whether patients with myocardial infarction (MI) and apparent reciprocal ST-segment depression exhibit abnormal metabolism in zones distant from the primary zone of infarction; a consideration of the etiology of elevations in plasma MB creatine kinase in patients after cardiac catheterization; a study of the effect of clot lysis induced by intracoronary streptokinase on myocardial metabolic integrity and viability; a controlled trial employing prophylactic antivasospastic therapy to assess the contribution of coronary vasospasm to chest pain in patients with non-transmural MI; and a study utilizing positron emission tomography to assess the effects on the heart itself of coronary thrombolysis induced with either tissue-type plasminogen activator or streptokinase.

A-11. Lipoprotein Kinetics in Familial Hyperlipidemia

Personnel: R. E. Ostlund, Jr., M.D., Medicine
R. A. Levy, M.D., Hahnemann Medical College
J. Markham, BCL

Support: RR 01380
HL 29229

The objective of this project has been to determine parameters of apolipoprotein-B metabolism in subjects with familial hypercholesterolemia. Two unrelated patients with familial hypercholesterolemia but with divergent clinical features were chosen. One had classic disease with half of the expected cell-surface low-density lipoprotein apoB receptors and the other had only a mild deficiency of low-density lipoprotein receptors but overproduction of cholesterol was present. ApoB in low density lipoprotein was labeled with 125-iodine and apoB in very-low-density lipoprotein was labeled with 131-iodine.

The data were analyzed using various multicompartment models. Low-density lipoprotein apoB turnover was found to fit a two-pool model consisting of a vascular space and a small extravascular space with irreversible removal of lipoprotein from the blood. The fractional rate of the exit of low-density lipoprotein apoB from the vascular compartment was

0.09/hr. in the classic patient and 0.15/hr. in the patient with atypically high skin-fibroblast apoB receptor activity. These results support the physiologic relevance of the in vitro skin-fibroblast assay.

Over the next year we expect to start studies of cholesterol turnover and high-density apolipoprotein turnover in humans. Data from the studies will be analyzed by multicompartment models.

B. Quantitative Imaging: Ultrasonic Tissue Characterization

Although ultrasound has proven to be a useful source of diagnostic information, results of examinations based on current ultrasonic methods are primarily qualitative and pictorial. In a collaborative effort with Cardiology and the Department of Physics work has continued on methods of tissue characterization via ultrasound. Our overall goal is to use ultrasound for the noninvasive identification of tissue pathologies within two-dimensional images of tissue properties. Specific objectives of this effort are: 1) to investigate the magnitude and character of anisotropy in tissue, 2) to systematize the representation of the ultrasonic field and to reduce the data needed to describe that field by determining the moments of the spatial distribution of energy over the receiver aperture, 3) to seek improvement in measurement capability of imaging systems via interactive, adaptive beamforming for both linear and variable-aperture transducer arrays, 4) to test the hypothesis that quantitative images based on intrinsic tissue properties can be produced with reflected ultrasound, and 5) to construct a digital multiprocessor system to perform post-echo ultrasonic estimation of attenuation, phase velocity and backscatter in two dimensions.

Quantitative images based on ultrasonic tissue properties have been made at the BCL for several years using transmitted ultrasound with a multiple-frequency tomographic reconstruction system. In the past year we have extended that processing environment (B-7), so that it now supports acquisition, storage, and processing of reflected ultrasound from arrays, as well as transmitted ultrasound using single-element transducers.

The cyclic variation in backscatter from canine myocardium that we reported previously was found to diminish during ischemia, but returned following reperfusion (B-2). This study required development of extensive software to analyze time-varying ultrasonic parameters (B-1). In order to elucidate causes for the variation of attenuation and backscatter with state of contraction in cardiac muscle, these parameters were measured in skeletal muscle as the state of contraction was changed (B-3).

The other three studies we performed showed some of the limitations of the transducer on quantitative imaging. A two-dimensional receiving array was simulated by scanning a small-aperture, broadband piezoelectric transducer (B-4). The first three spatial moments of the acoustic field at this simulated receiver gave a good description of the ultrasonic field after transmission through a polyethylene slab. We measured the pressure patterns generated by single-elements of linear-array transducers and the signal scattered from a slotted tube to develop a phenomenological model for the acousto-electric transfer function of transducer elements (B-5). The diffraction-limited performance of linear phased arrays in pulse-echo mode was simulated to provide estimates of the size of tissue regions which could be characterized at locations throughout the field of view of the array (B-6).

B-1. Software Development for Analysis of Time-Varying Ultrasonic Parameters

Personnel: J. G. Mottley, BCL
J. G. Miller, BCL

Support: RR 01362
HL 17646
HL 28998

Analysis of the data reported in Section B-2 required the development of an extensive system of computer programs. The data consisted of simultaneously digitized recordings of the outputs of a spectrum analyzer and the time derivative of the left ventricular pressure. Backscatter data were recorded from separate sites in the apical region of the left ventricle under several conditions, i.e., normal (before arterial occlusion), during ischemia, and at several intervals after reperfusion.

In order to properly synchronize the values of the ultrasonic parameters to the left ventricular pressure, the following processes were carried out. Data from the spectrum analyzer at each frequency were referenced to measurements from a planar reflector and expressed logarithmically. A typical example of the backscatter recorded at a single frequency (in this case 4 MHz) and from a single site in the apex is presented in Figure 1 along with the simultaneous recording of the time derivative of left ventricular pressure.

In order to permit averaging of the data to enhance components of the backscattered signal which are synchronous with the heart cycle, and to deal with the variation in heart rate among animals and the changing fraction of the heart cycle occupied by systole as the heart rate changed, the data acquired during each cardiac cycle were time-renormalized by dividing systole into one set of 16 uniform time windows and diastole into another set of 16 uniform time windows.

Renormalization was accomplished by first finding the onset of systole, defined as the start of the upstroke of the derivative of left ventricular pressure, and the onset of diastole, defined as the nadir of the pressure derivative. The data recorded during each phase of the heart cycle were then distributed among 16 uniform time windows assigned to that phase. Data assigned to each window were then averaged. The measurements of the derivative of left ventricular pressure were time-renormalized in an analogous fashion.

After time-renormalization had been accomplished, the frequency-averaged (integrated) backscatter was calculated at each site. Within each time window, the integrated backscatter values from similarly defined regions of all animals were averaged. The average integrated backscatter value was thus available as a function of occurrence throughout the cardiac cycle.

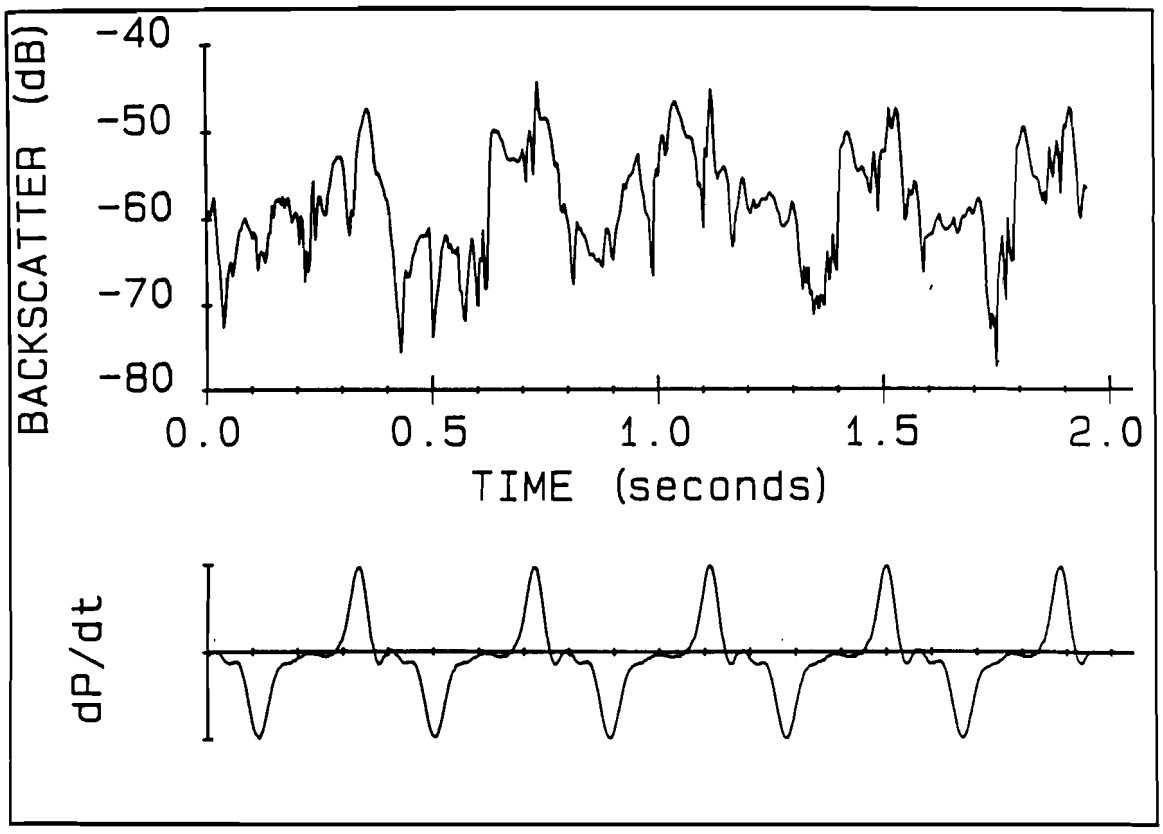

Figure 1. An example of the backscatter at 4 MHz from a single site in the apical region of a dog heart, recorded as a function of time. The backscatter is shown in units of decibels down from a planar, nearly-perfect reflector. The lower panel depicts the time derivative of the left ventricular pressure.

In order to more clearly identify changes in the integrated backscatter throughout the cardiac cycle, the relative integrated backscatter was calculated by offsetting the integrated backscatter from each region of the heart by the time-average of the backscatter from the same region. The relative integrated backscatter is therefore centered around zero dB and has equal positive and negative excursions.

For quantification of differences in amplitude of the cyclic variation of relative integrated backscatter for each condition of the heart, the relative integrated backscatter was Fourier transformed over the cardiac cycle, and the real and imaginary parts of the fundamental frequency (i.e., the frequency which would have one complete cycle over the cardiac period) were used to calculate the amplitude and phase of the cosine which would best fit the data. The cosine curve is mathematically identical to the curve which would be obtained by fitting the data with least-squared-error technique to a functional form $A\cos(\omega t+\phi)$ where A is the amplitude, ω is the frequency of the fundamental, given by $\omega = 2\pi/T$, if T is the duration of the normalized cycle, and ϕ is the phase offset. The amplitude of the fundamental was used as an index of the magnitude of the cyclic variation during each treatment.

B-2. Time Variation of Ultrasonic Backscatter from Canine Cardiac Muscle: Modification by Ischemia and Reperfusion

Personnel: J. G. Mottley, BCL
R. M. Glueck, M.D., Medicine
J. G. Miller, BCL
J. E. Perez, M.D., Medicine
B. E. Sobel, M.D., Medicine
L. J. Thomas, Jr., BCL

Support: RR 01362
HL 17646
HL 28998

The variation of the ultrasonic backscatter with contraction of canine myocardium (PR 19, B-1) was studied by dividing the cardiac cycle into 32 time windows and comparing the backscatter measured during each window (B-1). Backscatter of the muscle was measured over a range of frequencies (3-7 MHz in 1-MHz steps). Simultaneous measurements of the time derivative of the left ventricular pressure were recorded.

The apparent backscatter of the muscle increased significantly during diastole, relative to levels measured during systole (see Figure 1). Using the peak-to-peak amplitude of the time variation as an index, we observed in four canine preparations that transient ischemia of 5-10 minutes duration eliminated the cyclic pattern of variation. Following

reperfusion, the pattern of variation returned slowly, with the amplitude of variation returning to approximately 75% of pre-occlusion values in 2 hours (see Figure 2).

The cyclic pattern of variation of the ultrasonic backscatter appears to correlate with local mechanical performance, which is similarly attenuated by ischemia and recovers slowly with reperfusion following short periods of transient ischemia.

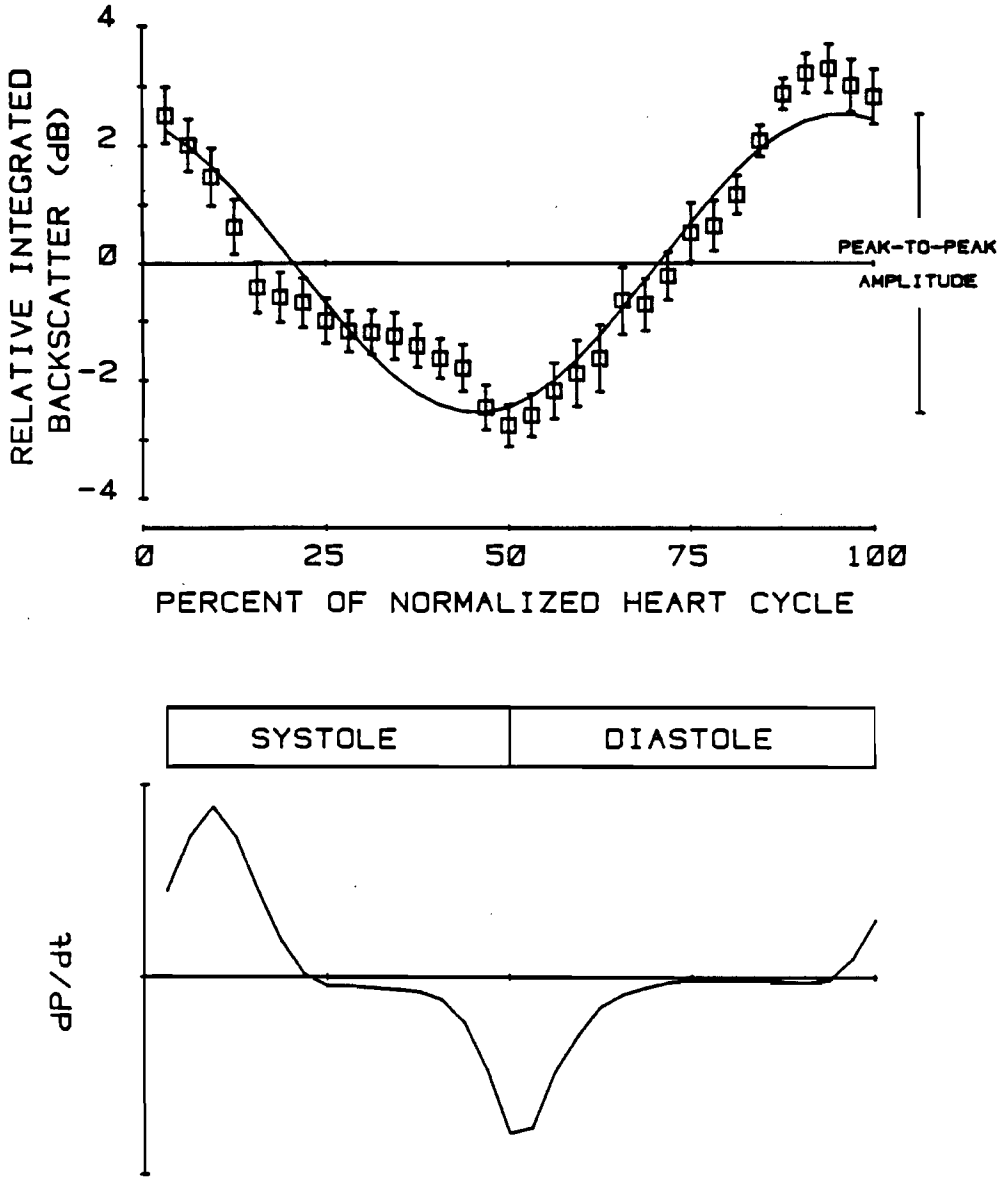

Figure 1. The relative integrated backscatter as a function of occurrence during the normalized cardiac cycle, shown with the time-renormalized time derivative of the left ventricular pressure. These data were acquired from the apical region of the hearts of 4 animals, prior to the induction of ischemia. The solid line is a cosine fit to the data, as described in the text.

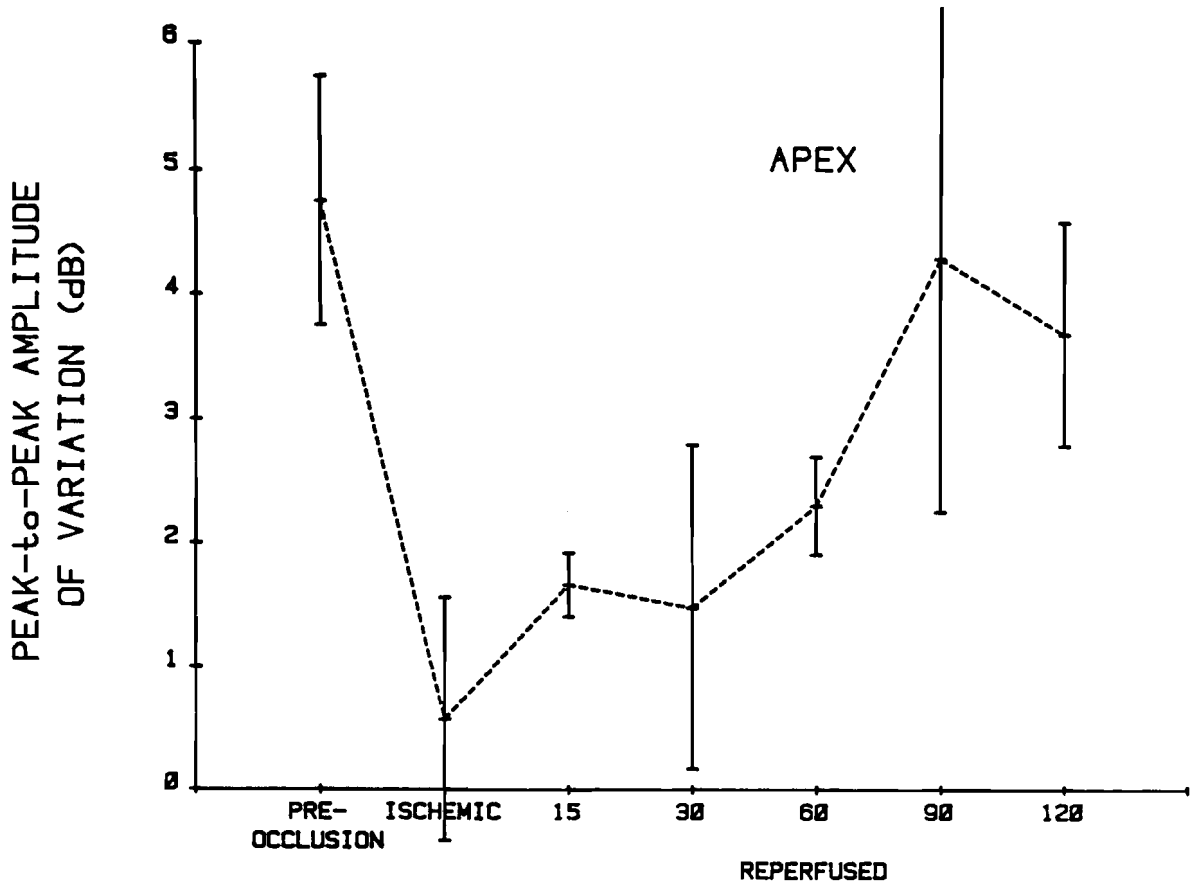

Figure 2. The peak-to-peak amplitude of the fundamental frequency of the integrated backscatter is shown for different conditions of canine myocardium. Error bars represent the standard error of the mean, indicating the extent of animal-to-animal variation (N=4). The numbers on the horizontal axis indicate the elapsed time since reperfusion has been accomplished.

B-3. Variation of Ultrasonic Attenuation and Backscatter of Amphibian Skeletal Muscle with State of Contraction

Personnel: J. G. Mottley, BCL
R. M. Glueck, M.D., Medicine
J. G. Miller, BCL
J. E. Perez, M.D., Medicine
B. E. Sobel, M.D., Medicine
L. J. Thomas, Jr., BCL

Support: RR 01362
HL 17646
HL 28998

The variation of the ultrasonic attenuation coefficient and the backscatter with contraction of skeletal muscle was studied in an isolated frog gastrocnemius muscle preparation, in which electrical stimulation induced tetany of the muscle. Both backscatter and attenuation of the muscle were measured over a range of frequencies (2-8 MHz in 1-MHz steps) prior to and during ten successive stimulations of the muscle, which was suspended in a bath of amphibian Ringer's solution. Simultaneous measurements of the displacement of the end of the muscle acting against a stiff spring were recorded.

Results of the measurements of the slope of the attenuation with frequency are illustrated in Figure 1, in which the average slope of attenuation from 12 muscles is plotted for successive stimulations. The slope of the attenuation increased significantly between rest and stimulation. The magnitude of the change between relaxation and tetany decreased with successive stimulations, presumably reflecting effects arising from fatigue. The apparent backscatter of the muscle (i.e., without compensation for the attenuation of intervening tissue and of the tissue within the electronic gate) did not increase significantly. After compensation of the backscatter for the attenuation, the intrinsic backscatter transfer function did increase significantly with contraction. The magnitude of increase was largest for the earlier stimulations and declined with successive stimulations, presumably indicating fatigue (see Figure 1).

Research to elucidate the possible relationships between the force of the contraction and the magnitude of the change in attenuation or backscatter is continuing.

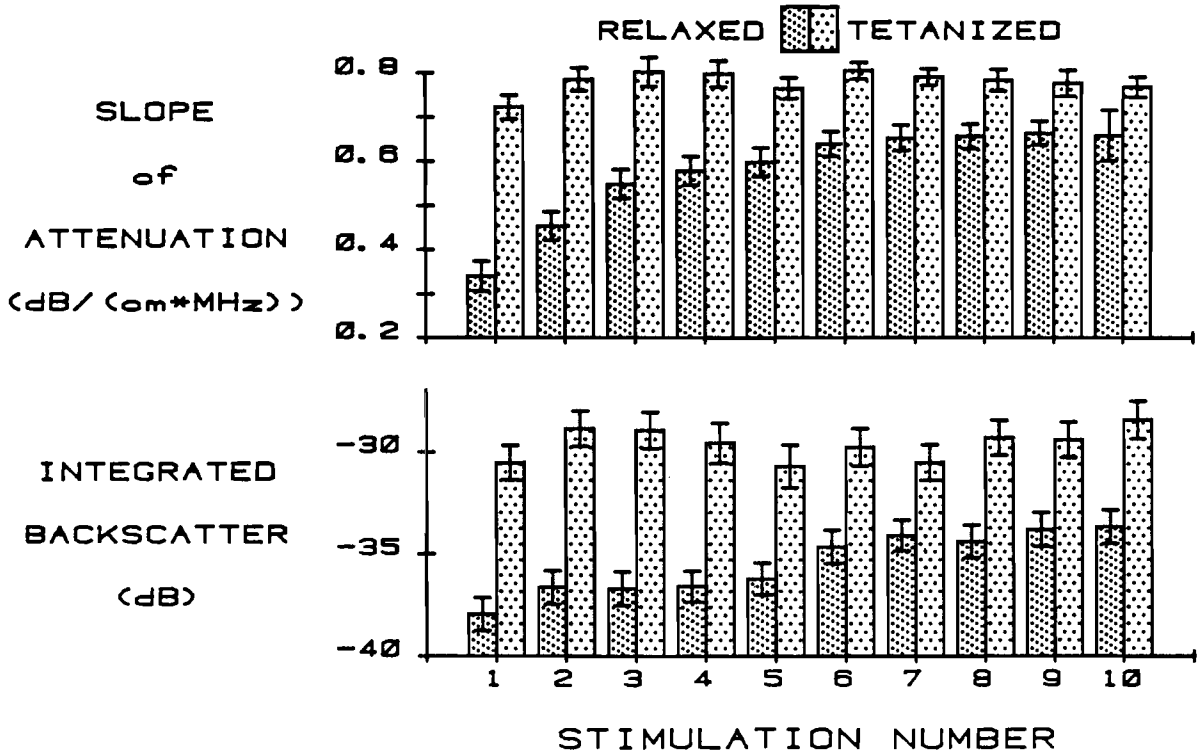

Figure 1. The changes in ultrasonic parameters of bullfrog gastrocnemius between rest and tetany are illustrated here. The upper panel shows the slope of the attenuation coefficient as a function of frequency for the two states, as successive tetanys are induced. The lower panel shows the integrated backscatter under the same conditions. Error bars indicate standard error of the means, obtained from 12 muscles from 7 frogs.

B-4. Determination of the Spatial Moments of Acoustic Fields

Personnel: P. H. Johnston, BCL
J. G. Miller, BCL

Support: RR 01362
HL 17646
HL 28998

We have proposed that the low-order spatial moments of the power in an acoustic field represent a limited variable set which contains most of the information that is meaningful for quantitative imaging in an inherently inhomogeneous medium such as soft tissue (PR 19, B-3). Specifically, the first three moments, M_0 through M_2, allow one to calculate the total incident power I_o (for "Intensity"), lateral deviation $\vec{c}$ (for "centroid"), and root-mean-squared beamwidth w (for "width") of the acoustic field according to

$$I_o = M_0,$$

$$\vec{c} = \vec{M}_1/M_0, \qquad (1)$$

$$w^2 = M_2/M_0 - |M_1|^2/M_0^2.$$

We have previously demonstrated (PR 19, B-3) the use of a two-dimensional array simulated by scanning a small phase-insensitive acoustoelectric receiver. In this report we show results from measurements made by scanning a small-aperture (1.4 mm) broadband piezoelectric receiver fabricated in our laboratory. This approach allowed the measurement of broadband rf signals using a spectrum analyzer, which facilitated the measurement of the spatial moments of the received field as a function of frequency. A block diagram of the experimental arrangement is presented in Figure 1. The transmitted beam from a fixed transmitting transducer (Panametrics V309, 0.5" diameter, 4" focal length, 5-MHz center frequency) was scanned in a plane perpendicular to the transmitter axis using the small-aperture receiver. The received signal was amplified, filtered, and gated into a spectrum analyzer (HP8551A). Under control of an LSI 11/23 computer, data from the spectrum analyzer was read via an IEEE-488 bus and stored on disc for subsequent processing. The computer also controlled the stepper-motor drives for the raster scanner. For this study, raster scans were made of either 11 x 11 elements with 1 mm spacing or 21 x 21 elements with 0.5 mm spacing to simulate a 1 cm by 1 cm sparsely sampled receiving array.

The spatial distribution of power at 5 MHz in the focal zone of the transmitting transducer in a homogeneous water-only path is presented in Figure 2. Each pixel represents the measurement from a single element of a simulated two-dimensional array of 21 x 21 elements with 0.5 mm spacing. The 32 gray levels correspond to quantitative relative amplitudes ranging from the maximum (black) to the minimum value (white) measured by the

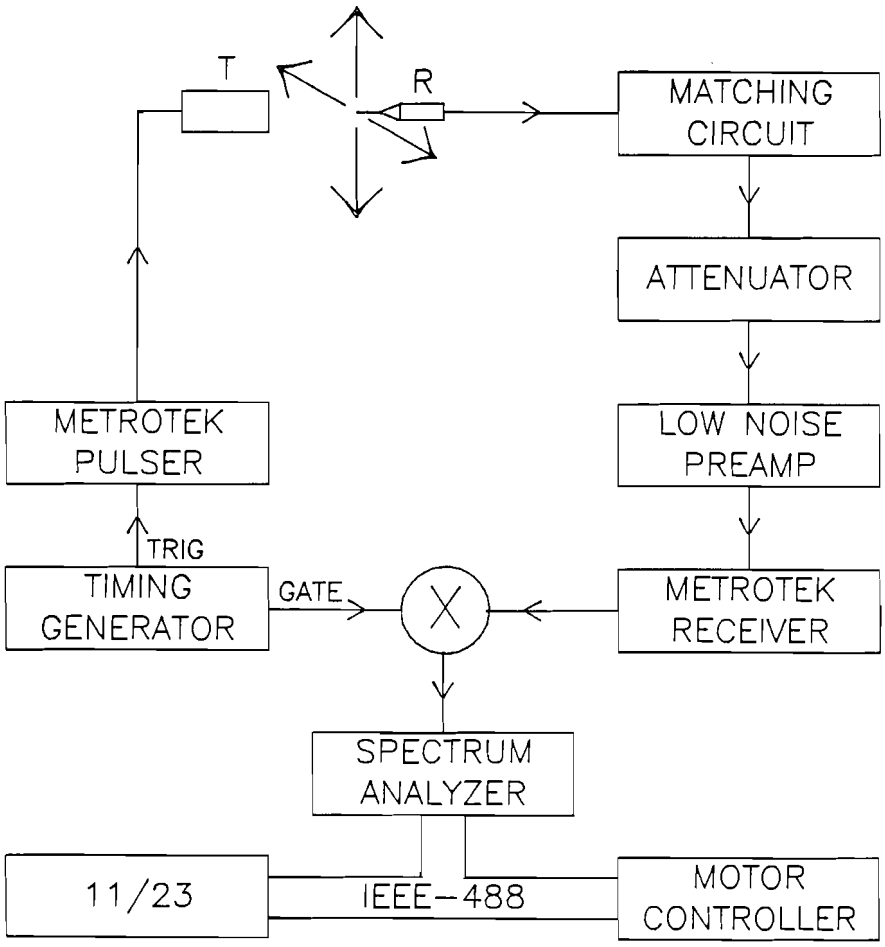

Figure 1. Block diagram of simulated array data-acquisition system.

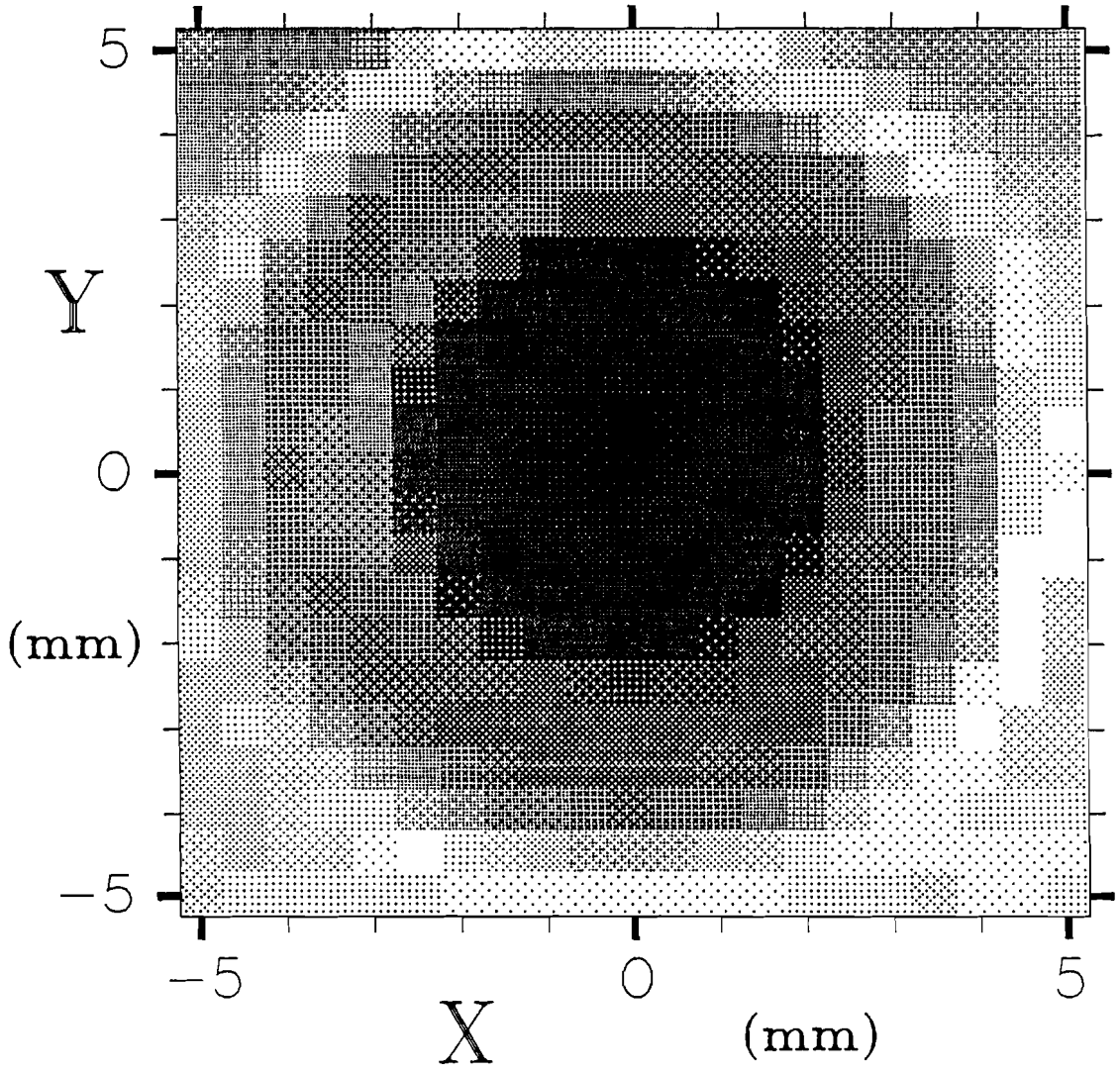

Figure 2. Gray scale representation of the spatial power distribution at 5 MHz in the focus of the transmitting transducer as measured by a 21 × 21 element simulated two-dimensional receiver array.

simulated array. One can clearly see the main lobe of the beam, as well as the first sidelobe and parts of the second sidelobe in the corners. This figure serves to define our coordinate system, with the center element defined as the origin, and X and Y directions defined as horizontal and vertical respectively.

A one-dimensional graph of the power at 5 MHz measured by the receiver elements lying along Y=0 is presented as a solid line in Figure 3. The line is similar to the $[2J_1(x)/x]^2$ form predicted for the power from a focused circular transducer as illustrated by the arrows which indicate predicted locations.

The distribution of power in the focal zone of the transmitting transducer in a water-only path is presented in Figure 4 for the frequencies 2, 5, and 8 MHz as measured by an 11 x 11 element simulated two-dimensional receiving array with 1.0 mm element spacing. These grayscale images demonstrate the variable width of the spatial distribution of acoustic power with frequency. The main lobe of power clearly decreases in spatial extent as the frequency increases. To the right of each grayscale image is a table of beam parameters based on the first three two-dimensional spatial moments calculated for that image. The quantity I_0 is the total relative power received by the array, and is expressed as dB relative to the power received at 5 MHz. The nominally 5-MHz center frequency transmitting transducer yields a maximum power which is down by approximately 10 dB at 2 MHz and at 8 MHz (i.e., by 9.9 dB and 11.6 dB respectively). The values of the x- and y-components of the measured centroid vector $\vec{c}$ are approximately zero (i.e., less than one half element spacing), indicating that the beam is aligned with the center of the receiving array. The width calculated from the spatial moments decreases with frequency in agreement with visual inspection of the grayscale images.

The moments calculations tabulated in Figure 4 were performed using only values obtained from those elements which yielded signals no more than 12 dB below the peak value measured. The significance of this truncation will be addressed below.

A measurement of the attenuation coefficient of a sample using the zeroth spatial moment is presented in Figure 5. The top curve in the upper panel is the zeroth moment M_0 measurement for the transmitted beam in a water-only path as a function of frequency over a 21 x 21 element simulated two-dimensional receiver array with 0.5 mm spacing. The lower curve in the upper panel corresponds to M_0 measured after insertion at perpendicular incidence of a 2 mm thick planar slab of polyethylene into the path of the beam. The attenuation coefficient is determined by comparing the two M_0 curves in the upper panel. The result is plotted in the lower panel as a solid curve. The dotted curve in the lower panel is a least squares line fit to the data, yielding a slope of 6.2 dB/cm-MHz. For purposes of comparison, a relatively large aperture (0.64 cm2) acoustoelectric receiver was also used to measure the attenuation of the polyethylene slab. The acoustoelectric measurement yielded a slope of 5.7 dB/cm-MHz. The reasonable agreement (~7% difference) between the slope values obtained suggests the viability of quantitative measurements based on the method of moments.

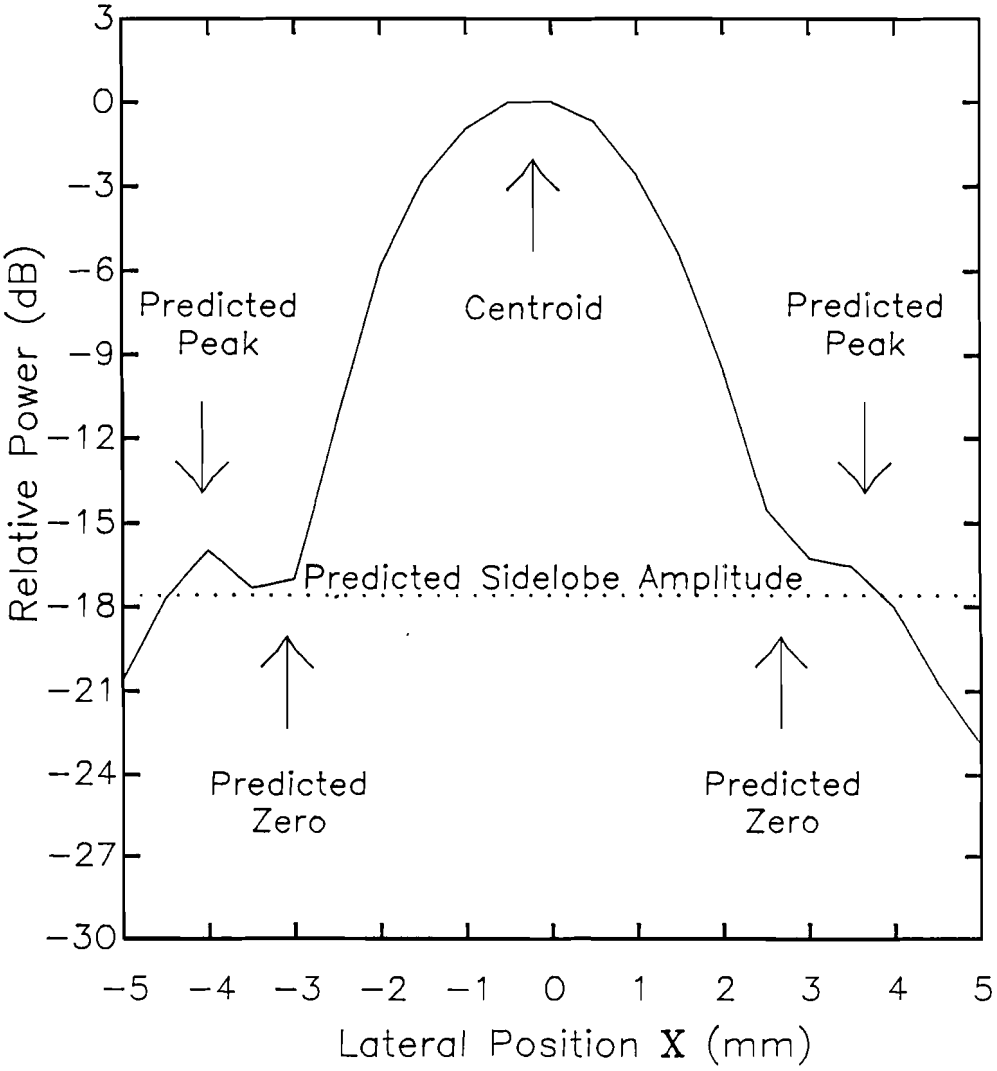

Figure 3. One-dimensional graph of the power measured at 5 MHz by the receiver elements lying along Y=0, showing locations of predicted peaks and zeroes.

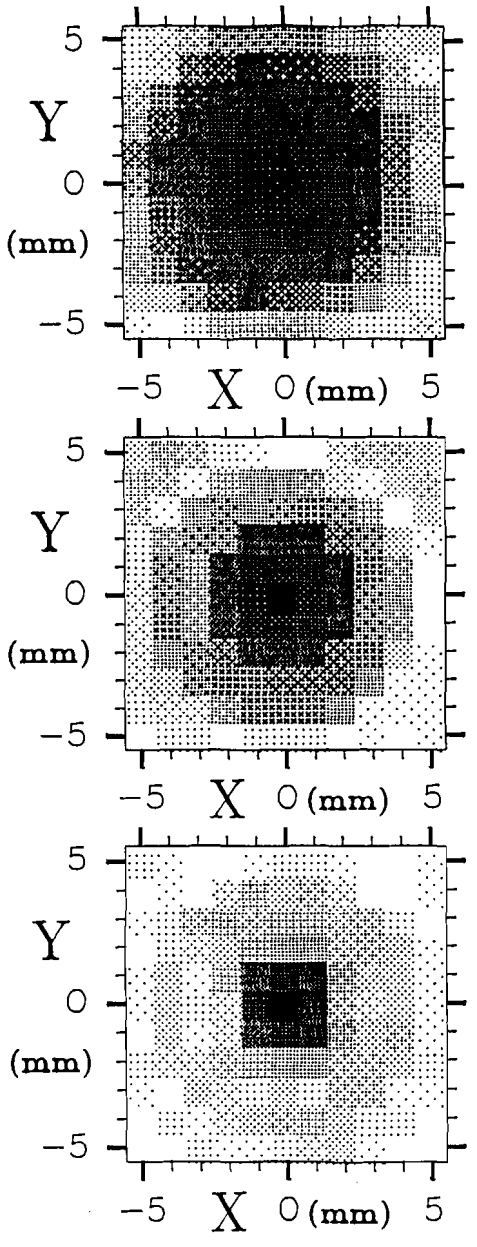

Figure 4. Gray-scale representation of the spatial power distribution at 2, 5, and 8 MHz as measured by an 11 × 11 element simulated two-dimensional array. The tables of beam parameters are based on spatial moments calculated using a 12-dB cutoff level.

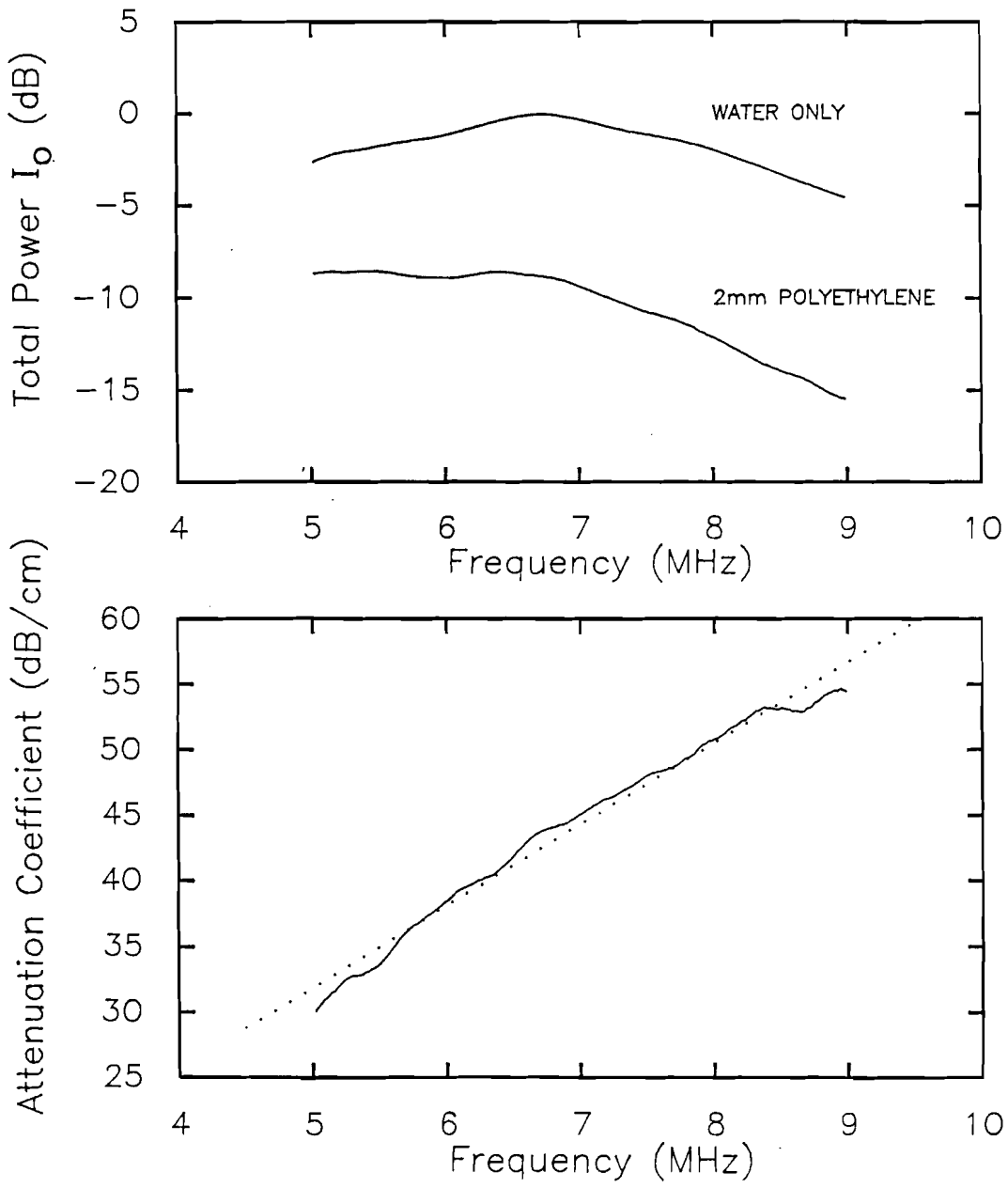

Figure 5. Measurement of attenuation coefficient using zeroth moment.

In order to illustrate the use of the first spatial moment to identify lateral deviations of the transmitted beam, the 2-mm polyethylene plate was rotated in the path of the beam to an incident angle of approximately 45 degrees from the normal. The refraction suffered by the 5-MHz beam during passage through the plate is illustrated in grayscale format in Figure 6. In the upper panel is an image of the beam after transmission through a water-only path. Below is an image after the insertion of the polyethylene plate at 45 degree incidence. The corresponding beam parameters calculated from the two-dimensional spatial moments are shown to the right of the images. We note a significant shift of the beam to the left after the polyethylene plate is inserted at 45 degree incidence. The magnitude of the shift is determined to be approximately 1 mm on the basis of the change in value of c_x, a result in good agreement with the result noted by visual inspection of the grayscale images.

In the discussion accompanying Figure 2 we noted that the beam width decreases with frequency. In order to assure that the width w calculated from the two-dimensional spatial moments of the beam reliably indicates beamwidth, a threshold criterion must be applied to the data prior to calculating the spatial moments. We will now describe the physical basis of the necessity for this cutoff procedure.

A two-dimensional moments calculation is very sensitive to the value of power measured by receiver elements far away from the origin (0,0). To illustrate this, consider a function F(r) defined from 0 to R in one-dimension. The nth one-dimensional moment of F(r) is

$$M_n = \int_0^R r^n F(r)\, dr. \qquad (2)$$

Hence the values of moments M_1, M_2, ... are increasingly more sensitive to the value of power measured at greater distances r from the origin. If the same function is rotated to produce a cylindrically symmetric two-dimensional function, the nth two-dimensional moment is

$$M_n = \int_0^R r^n F(r)\, 2\pi r\, dr. \qquad (3)$$

Thus, the value F(r) at any distance r from the origin is weighted by an additional factor $2\pi r$ in the two-dimensional integral [Eq. (3)] as opposed to the one-dimensional integral [Eq. (2)].

For the case of a transmitted beam considered here, the weighting factor in the two-dimensional moments substantially magnifies the relative importance of the sidelobes and noise level measured at some distance from the center of the beam. Practical transducers have bandpass characteristics, so that at some frequencies there may be two sidelobes above the noise level, while at other frequencies there is one or none above the noise. This variable signal-to-noise ratio over frequency may confuse the interpretation of two-dimensional spatial moments for the

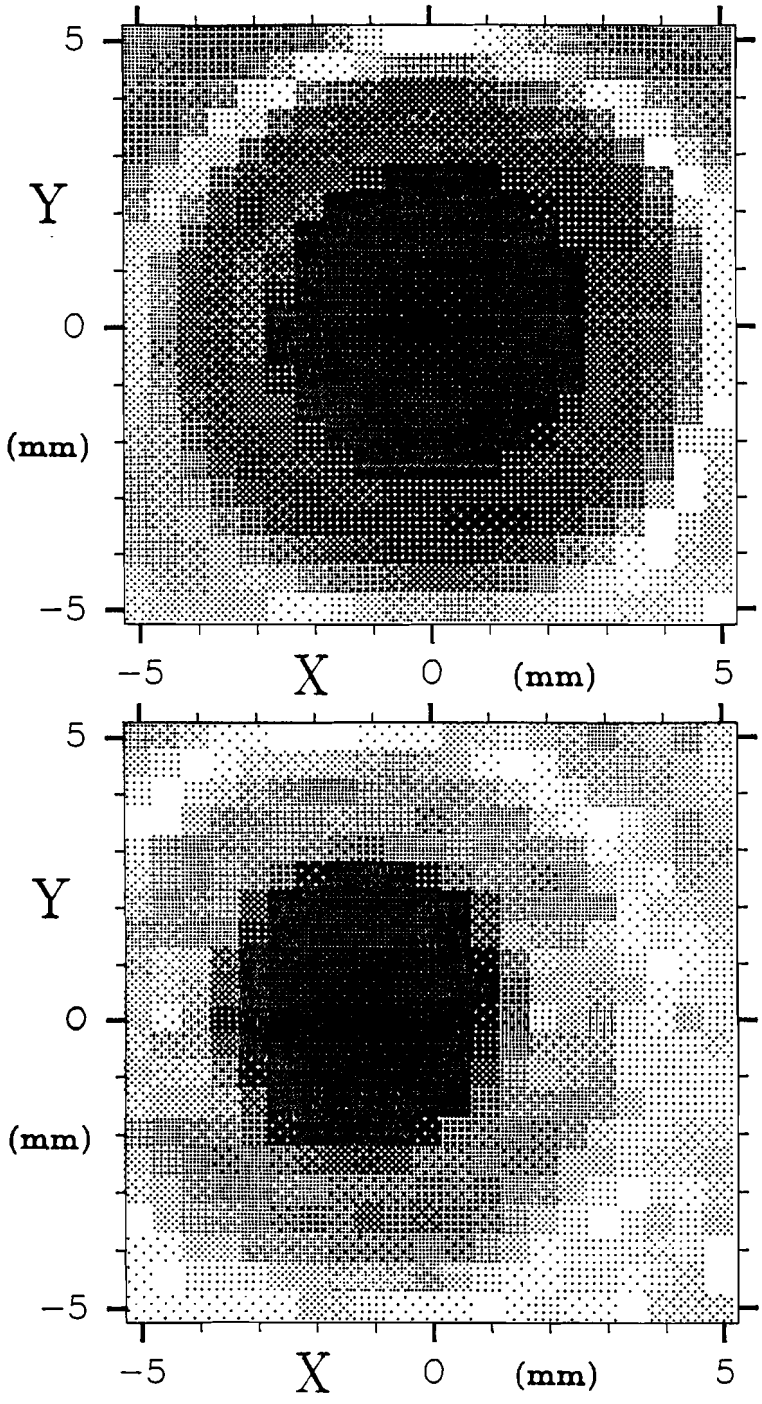

WATER PATH

I_o = 0.0 dB
c_x = 0.1 mm
c_y = 0.0 mm
w = 1.3 mm

2mm POLY.
PLATE: 45°

I_o = −13.6 dB
c_x = −1.0 mm
c_y = −0.1 mm
w = 2.0 mm

Figure 6. Illustration of the detection of the centroid of the spatial power distribution at 5 MHz using the first two-dimensional spatial moment.

received beam in broadband transmission measurements. Furthermore, because the beamwidth varies with frequency, a two-dimensional receiving array of finite size, say 1 cm, will capture a variable fraction of the total transmitted power, depending on the ratio of beam width to size of the aperture. These considerations indicate that it is necessary to truncate the beam function at some level above the noise level prior to calculating the spatial moments, and that care must be taken to restrict the range of frequencies measured in accordance with the size of the aperture.

In order to illustrate the effects described above, we shall plot the beam width calculated from simulated receiving array data using a set of threshold-cutoff levels ranging from 3 dB to 21 dB. In Figure 7 we show a one-dimensional scan line through a 5 MHz beam showing the cutoff points to be used in two-dimensional moments calculations below.

In Figure 8 we show the 5-MHz beam width calculated from data taken by a simulated 11 x 11 receiver array with 1.0 mm spacing, plotted as a function of the cutoff level used. In this and the remaining figures, the value of width calculated using no threshold is plotted as a 30-dB value. Also indicated are the levels at which the peaks of the first and second sidelobes occur, and the noise level exhibited by the system during this measurement. The width calculated using a 3-dB cutoff is relatively small, because only the very top of the power distribution is used. The beam width increases smoothly as the cutoff level is increased. Between 15 dB and 18 dB, however, the calculation picks up the effects of the first sidelobe of the power distribution, and reflects this in an abrupt increase in the rate of rise of beam width as a function of cutoff level. As the cutoff level is increased beyond 21 dB, the entire aperture is included, so the width value becomes constant.

In Figures 9 and 10 we illustrate the effect of signal-to-noise ratio on the selection of cutoff level. In Figure 9 we show the width calculated for an 8-MHz beam in a case of very good signal-to-noise ratio. The measured beam width is represented as the solid line. The noise level of approximately 29 dB is marked with a dash-dot line. Using the width w_5 determined at 5 MHz at each cutoff and an assumed inverse-frequency dependence for width, a predicted beam width w_8 calculated according to $w_8 = (8/5)w_5$ is shown as the dashed curve. The measured beam width follows the predicted dependence well up to 18 dB.

In Figure 10 we depict a case analogous to that in Figure 9, but with a relatively poor signal-to-noise ratio. The measured beam width is again plotted as a solid line, with the noise level indicated as a vertical dot-dash line and a predicted beamwidth based on the measured 5-MHz width is shown as a dashed line. In this case the estimated width deviates dramatically from the predicted width below a cutoff of 12 dB. This effect arises from the heavy weighting of the noise which is measured by pixels away from the center and which begin to be included at this cutoff level.

A related effect resulting from the relative size of the beam and the receiving array aperture is illustrated in Figure 11. Here the beam width calculated for 2 MHz is shown versus cutoff level. The width w_2 predicted from the measured 5-MHz data as $w_2 = (2/5)w_5$ is shown as a dashed

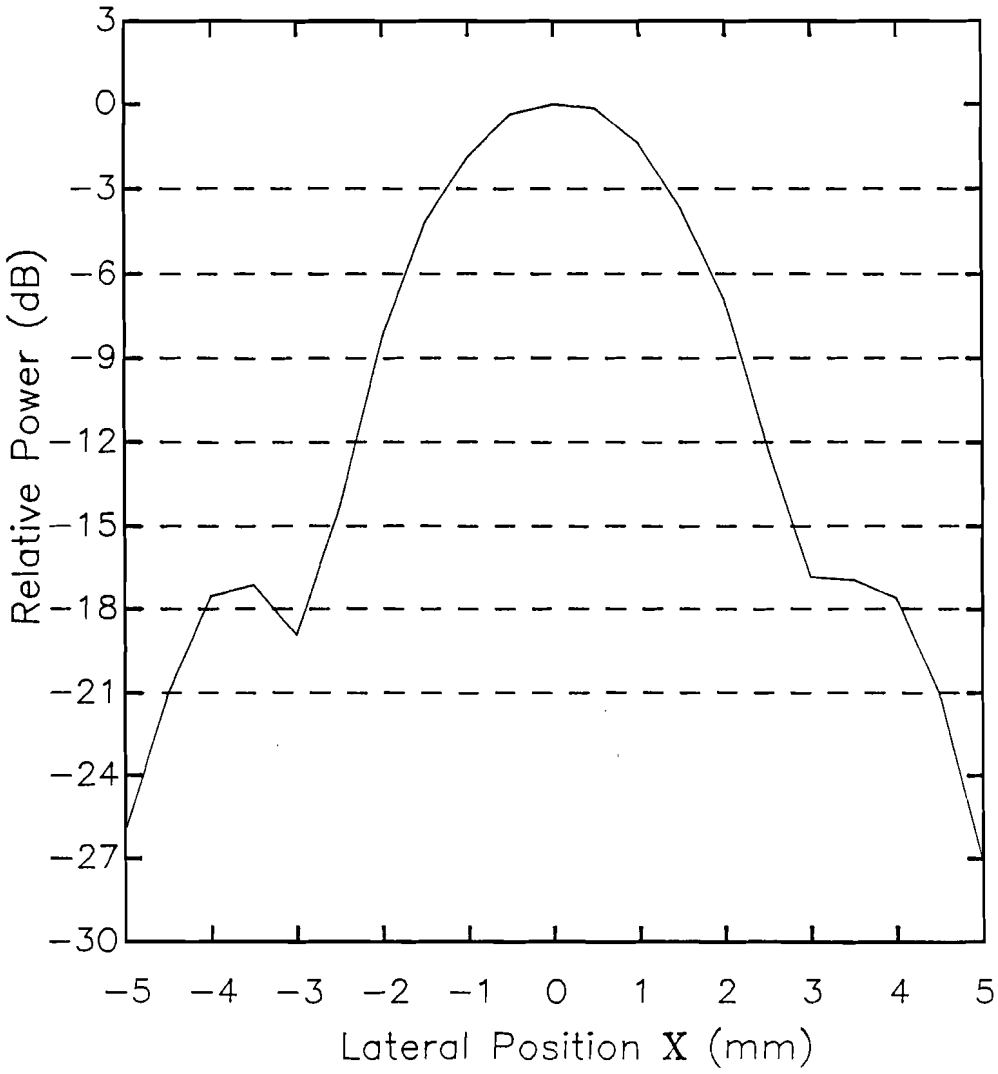

Figure 7. Cutoff levels for spatial moment calculations displayed across a representative 5 MHz scan line, i.e. signal for receiver elements along Y=0.

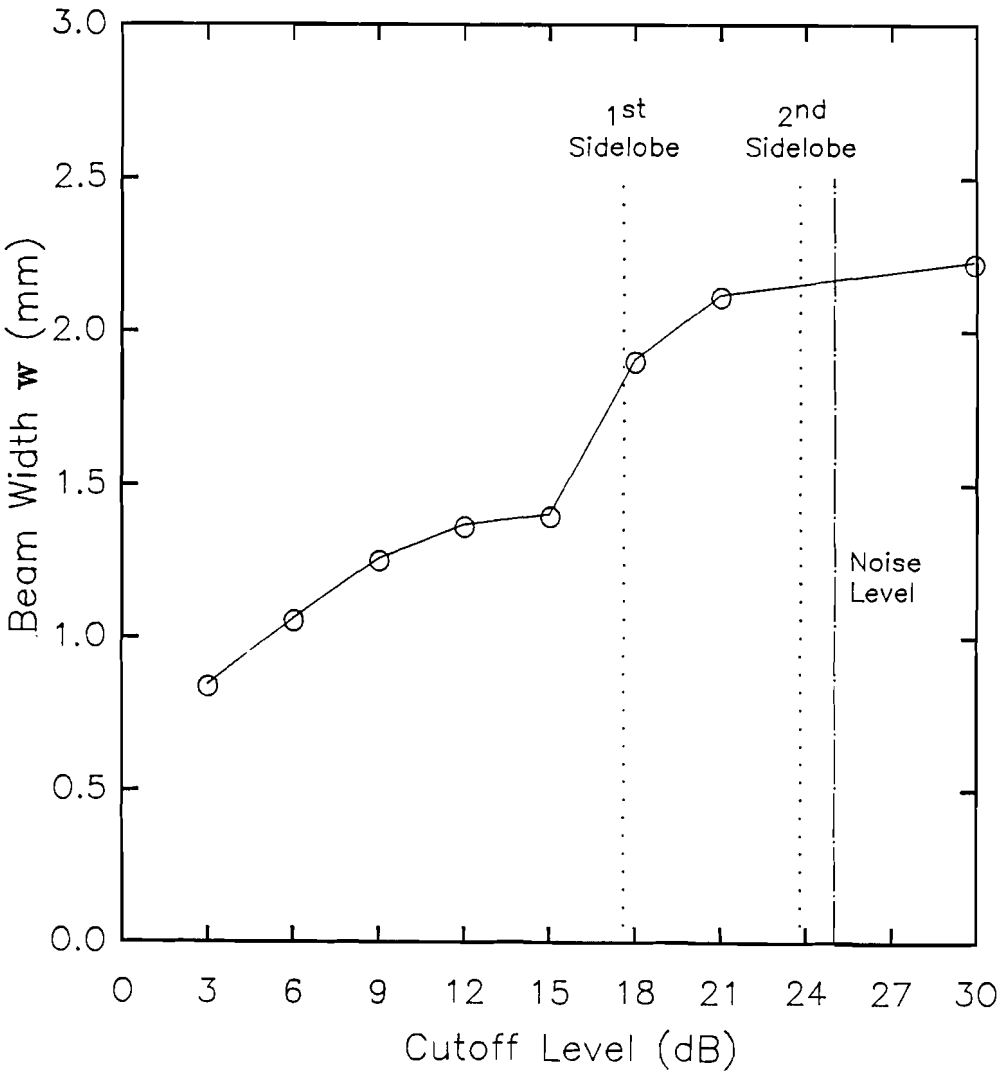

Figure 8. Plot of beam width w based on two-dimensional spatial moments of received power at 5 MHz in a water path versus cutoff level applied.

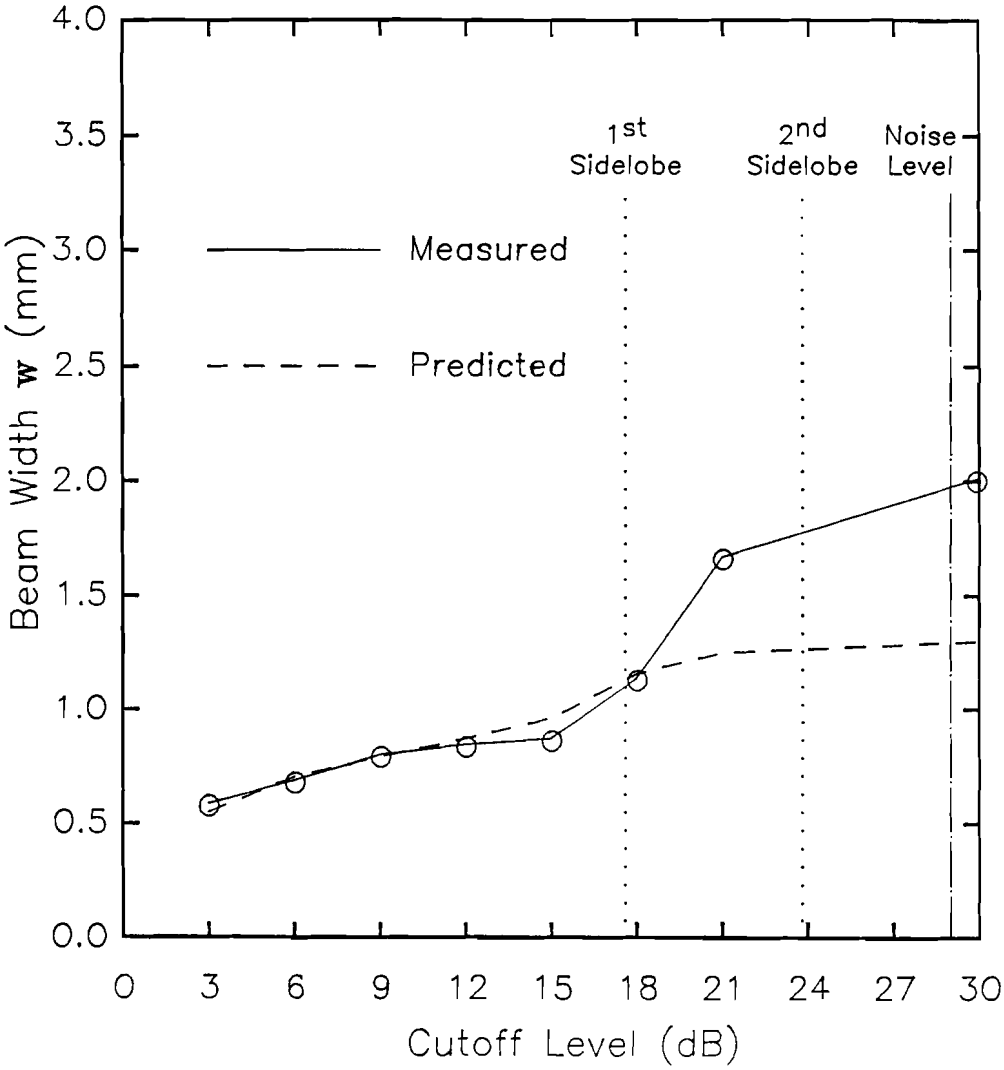

Figure 9. Plot of beam width w based on two-dimensional spatial moments of received power at 8 MHz in a water path with good signal-to-noise ratio, versus cutoff level applied.

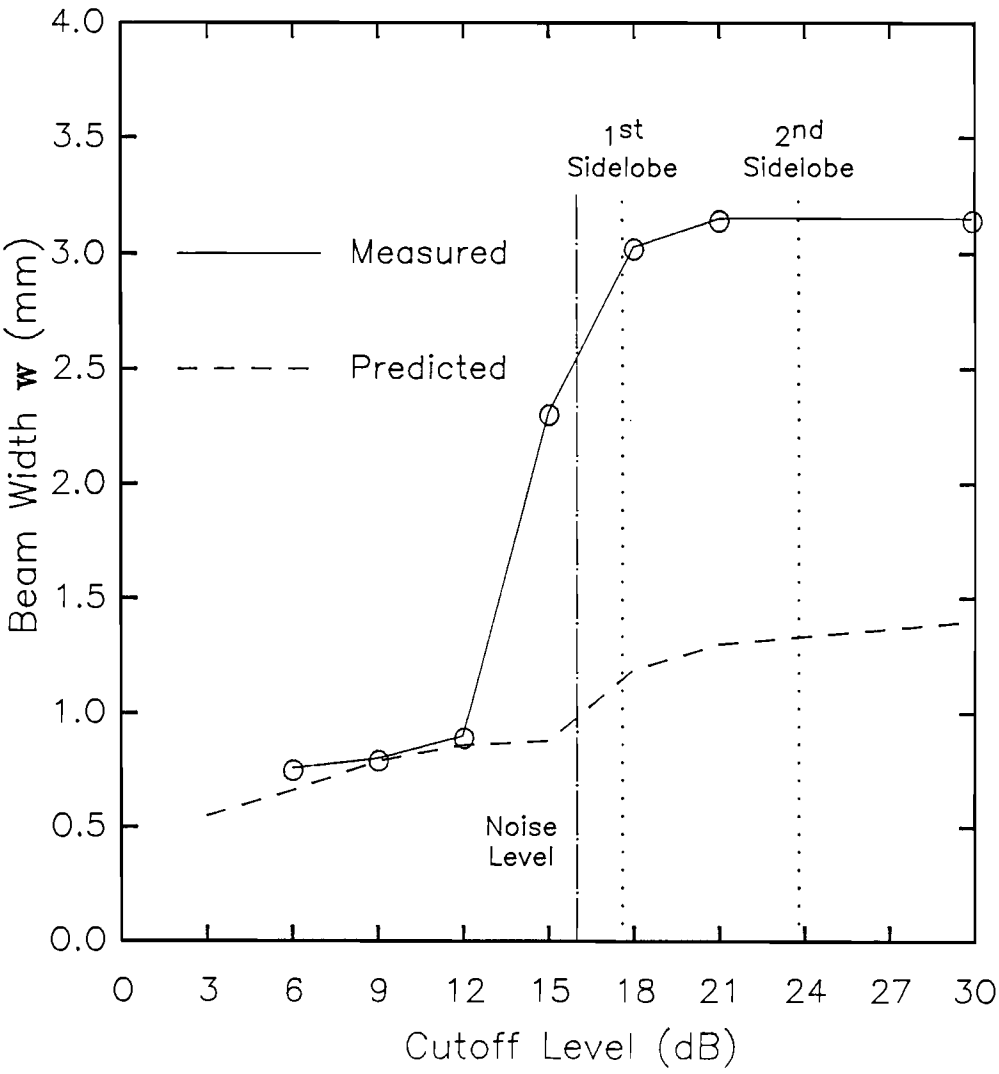

Figure 10. Plot of beam width w based on two-dimensional spatial moments of received power at 8 MHz in a water path with poor signal-to-noise ratio, versus cutoff level applied.

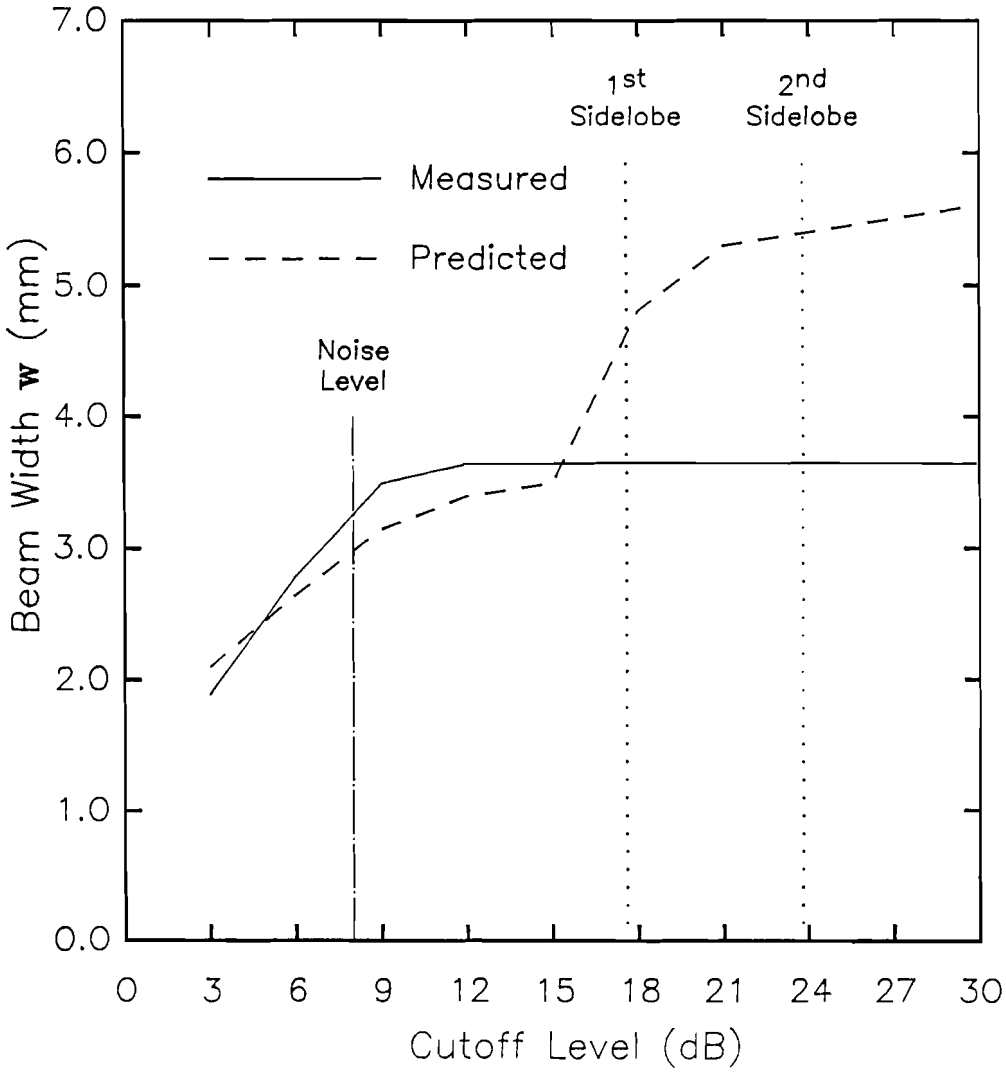

Figure 11. Plot of beam width w based on two-dimensional spatial moments of received power at 2 MHz in a water path with poor signal-to-noise ratio, versus cutoff level applied.

line for comparison. The measured beam width rises with increasing cutoff in reasonable agreement with the predicted curve up to about 9 dB, after which the value remains constant. All the receiver elements received power within 12 dB of the peak because the main lobe of the beam fills the aperture. The square shape of the receiver aperture artifactually truncates the power distribution, and thus distorts the estimated beam width.

The overall approach to quantitative ultrasonic imaging based on information derived from the spatial moments of the received ultrasonic field continues to look very promising. Work is continuing along several parallel lines, including an investigation of the interdependences among the size of simulated array aperture, frequency bandwidth, truncation level, and signal-to-noise ratio.

B-5. The Electroacoustic Transfer Function of Linear Transducer Arrays

Personnel: R. M. Arthur, BCL
S. R. Broadstone, BCL
M. L. Seiger, B.S., Electrical Engineering

Support: RR 01362
Washington University

Transducer behavior must be taken into account in order to make quantitative ultrasonic measurements (PR 19, B-6). The energy transmitted or received by a transducer element is dependent on signal frequency and on the angle of propagation or incidence. It is also affected by cross-talk from nearby elements. A scanner was added to the processing environment (B-7) to permit mapping the pressure fields generated by individual elements of transducer arrays and to capture the signal received by the element when its transmitted beam is scattered by a reflector moved through its field of view. Broadband pulses were used to excite transducer elements in order to calibrate the element for quantitative pulse-echo imaging.

The excitation pulse, the pressure field recovered by a hydrophone, and the scattered signal received by the element itself were recorded as a function of hydrophone or scatterer range and angle. Signals were sampled at 50 MHz with 8 bits of precision. Spectra were determined by Fourier transform. By comparing the received signals to the excitation pulse we calculated the ability of the element to insonify and its sensitivity to scatterers in a given region of its field of view. We are now applying this technique to elements of 3.5 and 5 MHz, 32-element linear arrays, composed of piezo-electric material.[1]

These studies may also permit development of a phenomenological model for the transfer function of the transducer element itself, i.e. the relation between the electrical excitation and the motion of the face of the transducer. We hope to be able to infer transducer vibration modes by removing diffraction effects from the calibration studies described above. To characterize the transfer function of a given transducer we propose to model each element as a collection of facets or subelements. The diffraction patterns of these facets will be calculated using the impulse-response method employed in our model for studying phased-array resolution (B-6). Calculations will be compared to the calibration measurements in order to fix facet motion on a least-squared-error basis.

1. R. M. Arthur, M. L. Sieger, and D. W. Stein, "Assessing Ultrasonic Arrays for Imaging Tissue Properties," Ultrasonic Imaging, vol. 6, p. 209, 1984.

B-6. Diffraction-Limited Lateral Resolution of Ultrasonic Phased Arrays

Personnel: R. M. Arthur, BCL

Support: RR 01362
Washington University

The objective of this study was to determine the diffraction-limited resolution of an ultrasonic linear phased array as a measure of the maximum number, that is as a limit on the number, of independent scan lines appropriate for tissue characterization. The approach was to simulate a linear array, so that its ability to separate two point targets located on an arc in regions throughout the field of view of the array could be calculated (PR 19, B-5).

The simulated transducer was composed of 16 rectangular elements. Its center frequency was 2.25 MHz. In terms of wavelength in the medium, each element was 0.9 of a wavelength wide and 12 wavelengths high. The spacing between element centers was 1.8 lambda. The height and width of the array were 8 and 19.4 mm, respectively. Each element was driven by a sinusoid at the center frequency (2.25 MHz) with an exponential envelope. The excitation was applied to the elements of the array with delays to produce point focus and beam steering. The receive signal was formed using the same delays, that is, the focal point of the array was the same on both transmit and receive.

The impulse response of an element in an infinite baffle which undergoes uniform logitudinal motion can be readily calculated using the method of Lockwood and Willette.[1] The impulse response is proportional to the pressure in the medium. The signal received by the array upon scattering from two point targets was found, again using the impulse

response of the array. The impulse response from target to array is the same as that from array to target. The array output was the sum of the signals from each of the targets in the medium.

In this study the focal points on transmit and receive were moved together along an arc for various separations of two point targets which were also on the arc. A scan was generated from the peak of the received signal for a given look direction. In Figure 1 we see two scans. The dashed lines indicate the position of the point targets. As expected, the scan at 20 mm (the width of the array) is symmetric about the axis because the targets are symmetrically placed about the axis. In the scan for targets in the vicinity of 30 degrees at 100 mm, which is 5 times the width of the array, the peaks of the received signals are roughly an order of magnitude smaller than the peaks of v(t) at 20 mm. Signal amplitude falls off both with an increase in radius and with an increase in off-axis angle. In order to resolve the two targets, the peaks in the scans must be distinct. In this study the criterion used was that the smaller peak must be at least 3 dB above the minimum between the two peaks.

For that criterion we find the angular resolution shown in Figure 2. Angular resolution gets better then converges with an increase in radius. For radii equal to or greater than 3 times the width of the array, angular resolution as a function of off-axis angle is about the same. It is roughly linear and undergoes about a 2:1 change from 0 to 45 degrees. The angular resolution curves were used to find the number of independent scan lines in the 45-degree field of view of the 16-element array which was simulated.

Simulations of 32-element arrays with element width the same or half as wide as that of the 16-element array showed that array width was the primary determinant of resolution and that the number of independent scan lines in the field of view of a linear array beyond a range two to three times the width of the array, the number of independent lines in the field of view is nearly constant.

1. J. C. Lockwood and J. G. Willette, "High-Speed Method for Computing the Exact Solution for the Pressure Variations in the Nearfield of a Baffled Piston," Journal of the Acoustical Society of America, vol. 53, pp. 735-741, 1973.

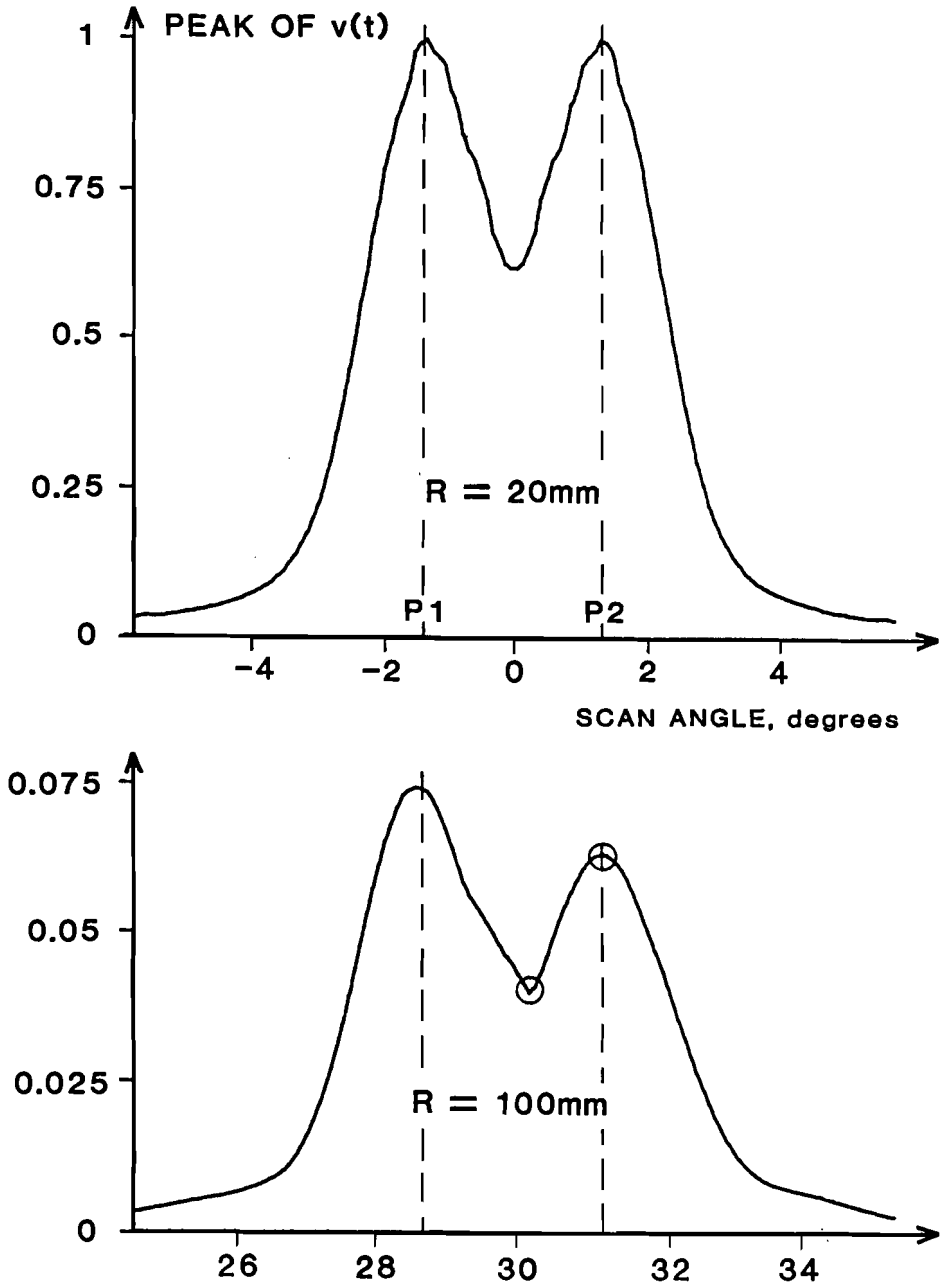

Figure 1. Scans at constant radius.

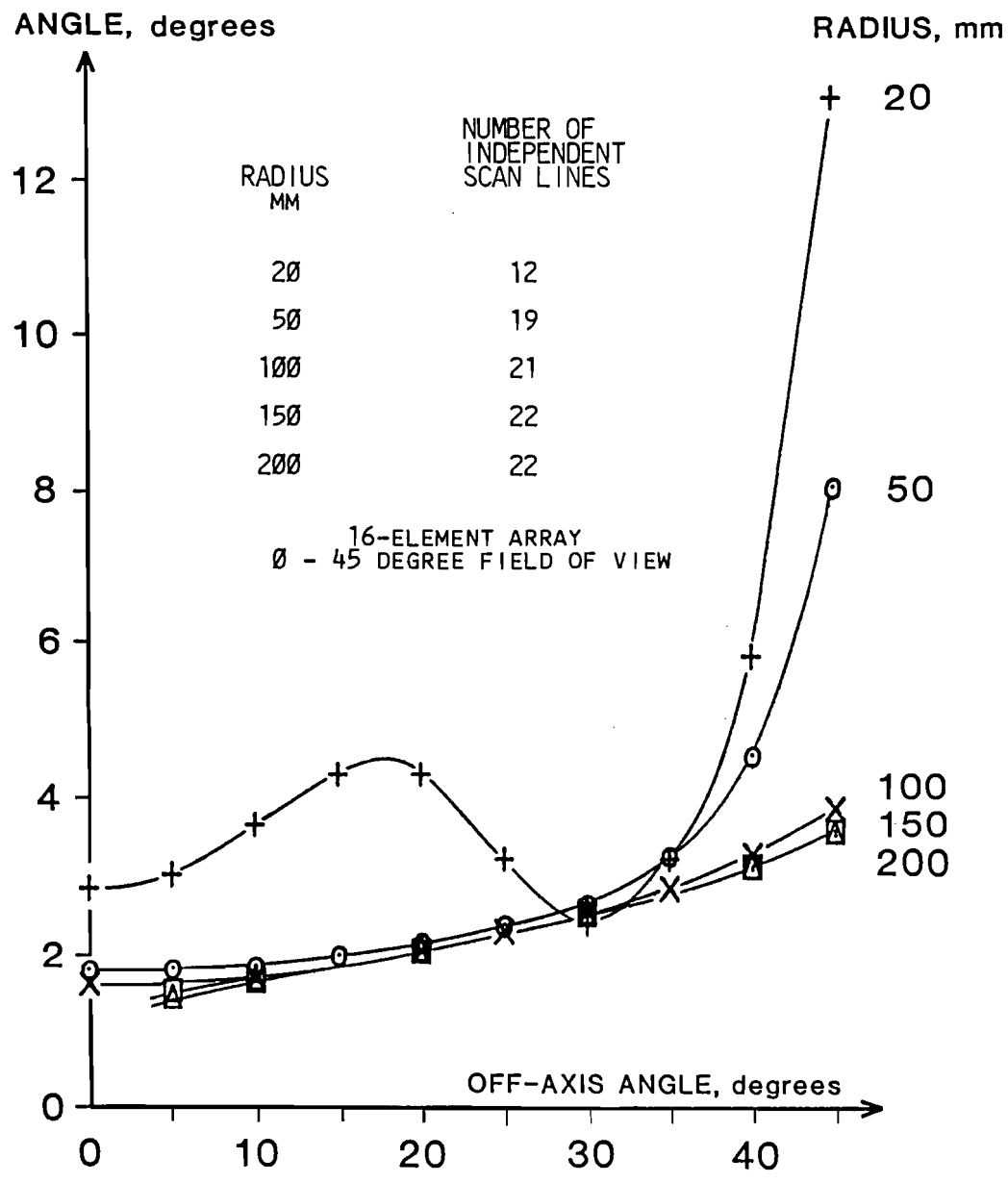

Figure 2. Angular Resolution.

B-7. The Processing Environment for Ultrasonic Tissue Characterization

Personnel: R. M. Arthur, BCL
S. R. Broadstone, BCL
P. H. Johnston, BCL
J. G. Miller, BCL
J. G. Mottley, BCL
D. W. Stein, Jr., BCL
L. J. Thomas, Jr., BCL

Support: RR 01362

Major modification and upgrading of the processing environment for the tissue-characterization project (PR 19, B-7) is now complete. The processing environment is built around a DEC LSI-11/23 microcomputer, which is interfaced to: 1) two 50-megabyte disk drives to provide programming storage; 2) an FPS 100E array processor to significantly improve execution time for both simulations and data analysis; 3) a 9-track, industry compatible tape drive for backup storage; 4) an electrostatic printer/plotter; 5) a digital plotter; 6) a 16-bit parallel input/output port for connection to a video display; 7) six serial lines; 8) analog-to-digital and digital-to-analog converters; and 9) an IEEE-488 bus for communication with instrumentation, such as our data-acquisition circuitry.

This year we added a Winchester drive with a total of 111 M bytes of storage. It houses our operating systems and signal and image processing libraries, which are too large for the RK05 drives. It also has sufficient capacity to store a typical tomographic or linear-array scan. In addition we added a scanner which can rotate and translate a linear array, to determine the behavior of individual elements throughout its field of view, as well as to collect signals for two-dimensional imaging with reflected ultrasound. Driver software for the Biomation recorder, stepper motors, and other hardware of the scanning systems is now operational. We can fully support acquisition of both transmitted and reflected ultrasound on the LSI-11/23.

C. Quantitative Imaging: Radiation Treatment Planning

About half of all cancer patients are treated with ionizing radiation during the course of their disease. The goal of radiation therapy is to control the malignant disease by delivering adequate radiation dose to the tumor volume while minimizing the dose to the surrounding normal tissues.

Treatment planning in radiation therapy is a procedure for appropriately selecting and placing sources of ionizing radiation so that their combined effect yields an optimal spatial distribution of absorbed dose in a particular region of the body. In the presence of tissues with inhomogeneous scatter and absorption properties, presently available methods of absorbed-dose calculation are approximate. Thus, their real utility in radiation-treatment planning is limited. We and several other groups have recognized for a number of years that computed tomography (CT) may provide a remedy for the shortcomings of present methods of absorbed-dose calculation. Accordingly, in 1977 we began the development of a new approach to absorbed-dose prediction that is based on fundamental physical principles and takes advantage of information provided by CT scanning.

The general objectives of this project are to develop algorithms for computing three-dimensional dose distributions within inhomogeneous tissue regions valid for radiation fields of arbitrary shape and size, and to apply advanced computer technology in the implementation of these algorithms to render them clinically useful. A specific objective of our initial work was to investigate the validity of the physical basis of the mathematical model on which our method depends. Comparison between measured and calculated dose in complicated geometric phantoms and in the Rando phantom show excellent agreement (C-1). In addition, a new investigation into treatment verification using our dose calculation algorithm has been started (C-1). This may provide an effective way to verify that the planned treatment is actually delivered to the patient, which is as important as developing an effective plan in the first place. An integrated circuit to perform the ray-tracing part of the dose calculation has been designed (C-2) and is being fabricated, and preliminary work is in progress for display of information to aid treatment beam placement and display of calculated dose distributions to aid treatment plan evaluation (C-3).

C-1. Algorithm Development for Radiation Treatment Planning

Personnel: J. W. Wong, Ph.D., Radiology
K. B. Larson, BCL
F. U. Rosenberger, BCL and Computer Systems Laboratory
E. D. Slessinger, B.S., St. Louis University

Support: RR 01380
RR 01379

Imperative in any radiation treatment planning (RTP)system is a method of accurate dose calculation. As mentioned in our last progress report, we have implemented on a VAX-11/780, a new delta-volume algorithm based on the work by Wong and Henkelman.[1,2] We have demonstrated that, in stringent phantoms irradiated by cobalt-60 beams, the calculation of correction factors agrees with measurements, usually to within one percent. During the past year we have continued our evaluation of the algorithm for cobalt-60 irradiations and are close to the completion of the important "photon-transport phase" of the RTP project where the incorporation of electron-transport for dose calculations is not necessary (e.g. cobalt-60 or equivalent radiation beams). The work can be described in two parts: voxel-based dose calculations; and methods for treatment verification.

We have performed verification studies in the more realistic Alderson Rando anthropomorphic phantom. X-ray CT scans of the Rando phantom in the upright position were made. In this manner, contiguous scan data at the desired x-ray beam width could be obtained without data interpolation and scan artifacts between the transverse sections of the phantom. The Rando phantom was irradiated anterior-to-posterior in the thoracic region with a 15 cm x 15 cm cobalt-60 beam. Dose measurements were made with high precision thermoluminescent dosimeters[3] placed primarily in the lungs and mediastinum of the Rando phantom. For dose calculations, the CT numbers were converted to electron densities determined by narrow-beam cobalt-60 transmission measurements through sections of the phantom composed of the various materials used in the phantom construction. Comparison of the calculations and measurements are shown in Figure 1 as a histogram distribution of percent differences. Linear interpolation of calculated values was used to account for the unavoidable positioning mismatch between the dosimeters and the calculation grid. The average difference of 60 samples of comparison was $-0.25\% \pm 2.96\%$.

The agreement is excellent considering the discrepancies in the positions of the measurements and calculations, and the errors introduced due to the finite dimensions of the input voxel data.

This study demonstrates that we are able to perform accurate dose calculations based on actual CT pixel-based input data and is the first time that such a truly three-dimensional dose calculation has been attempted. With our prototype delta-volume implementation, actual clinical cobalt-60 dose calculations can now be made within the limitations of the

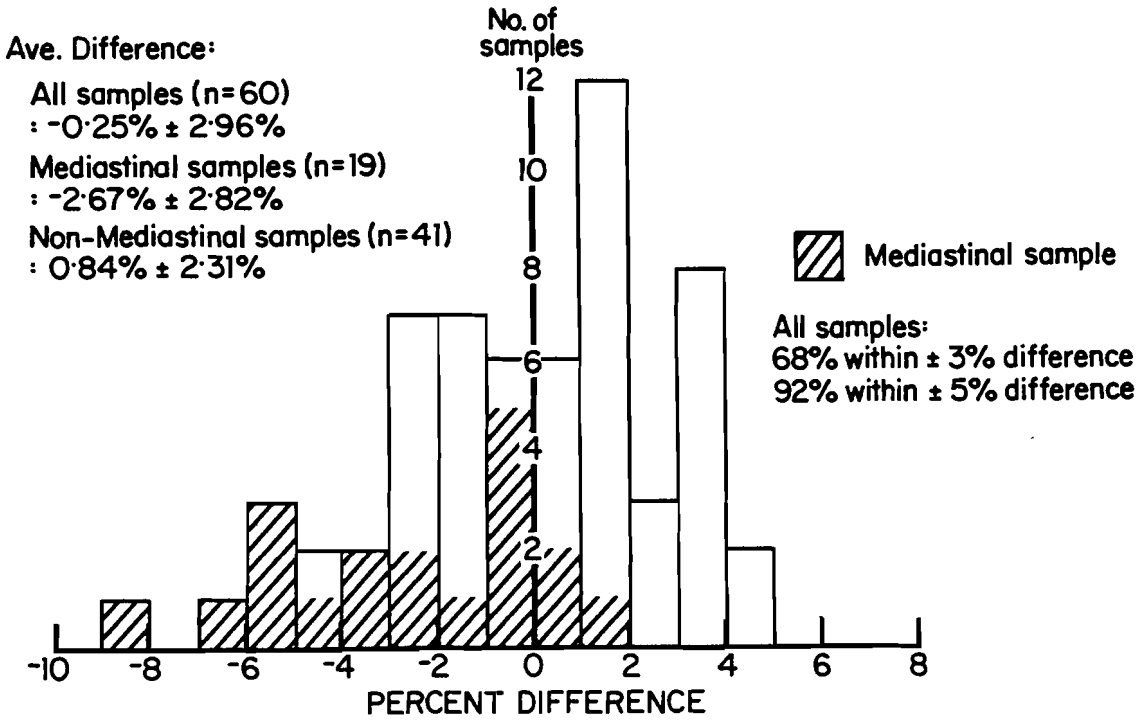

Figure 1. Comparison of TLD Measurements with Δ-Volume Calculations

present algorithmic design such as field dimensions, grid spacing, and computation time.

Verification that the intended treatment plan is carried out is as important as development of the plan. While we may be able to arrive at an optimized treatment plan for the patient based on the delta-volume calculations, we have been concerned that to date, there is a paucity of non-invasive techniques to verify the execution of the plan. The customary practice of exposing port films with the irradiating beam on the exit side of the patient merely provides a test of the geometric reproducibility without verification of the dose calculations. Recently, we have begun investigating a new approach to treatment verification based on the comparison of the calculated and measured exit-dose distribution. Provided that the patient set-up remains the same for dose calculations and treatment, a necessary condition for treatment planning, such comparison should yield good agreement. A study was conducted using the phantom geometry shown in Figure 2a. The calculated correction factors for this phantom (i.e., the ratio of dose in medium to the dose in water) agreed very well with measurements. The average difference was 1.8% ± 1.4%. In Figure 2b, only two points of comparison show a difference larger than 3%, one of which is probably due to positioning error of the dosimeter (see axis (b)) and the other is located in the more rapidly changing penumbral region (see axis (a)).

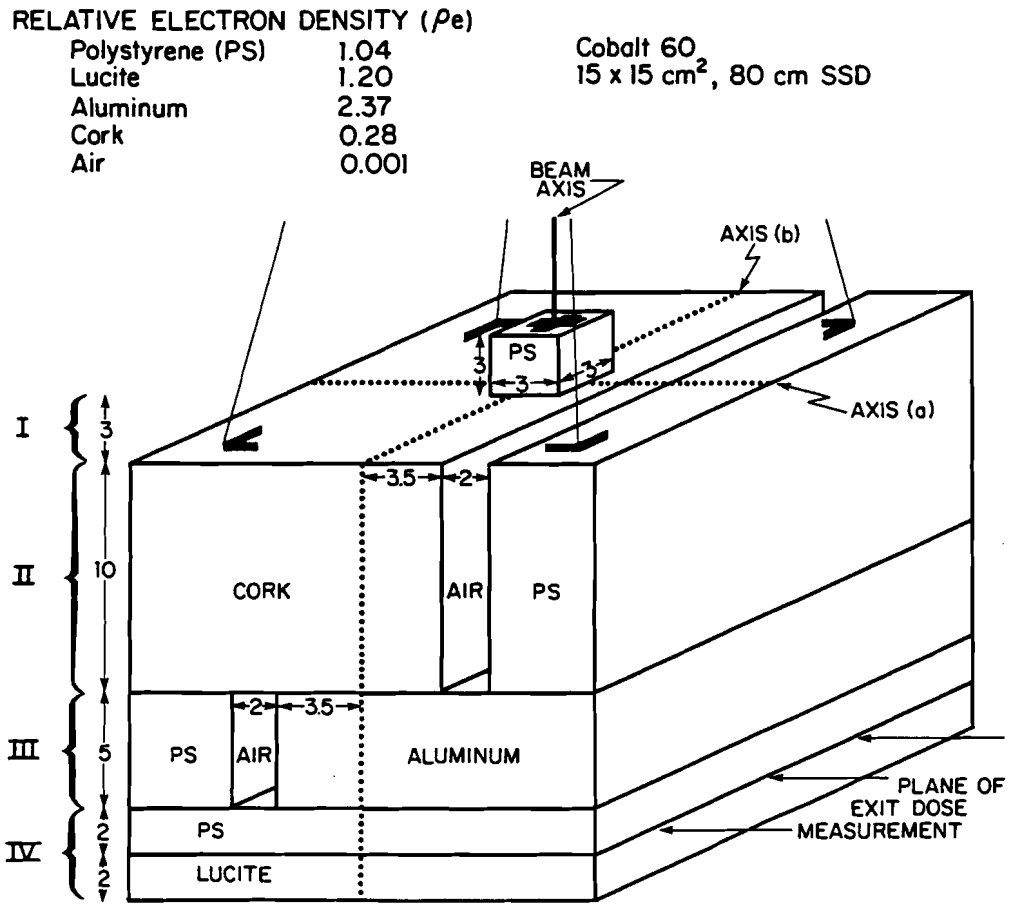

Figure 2a. Phantom Geometry

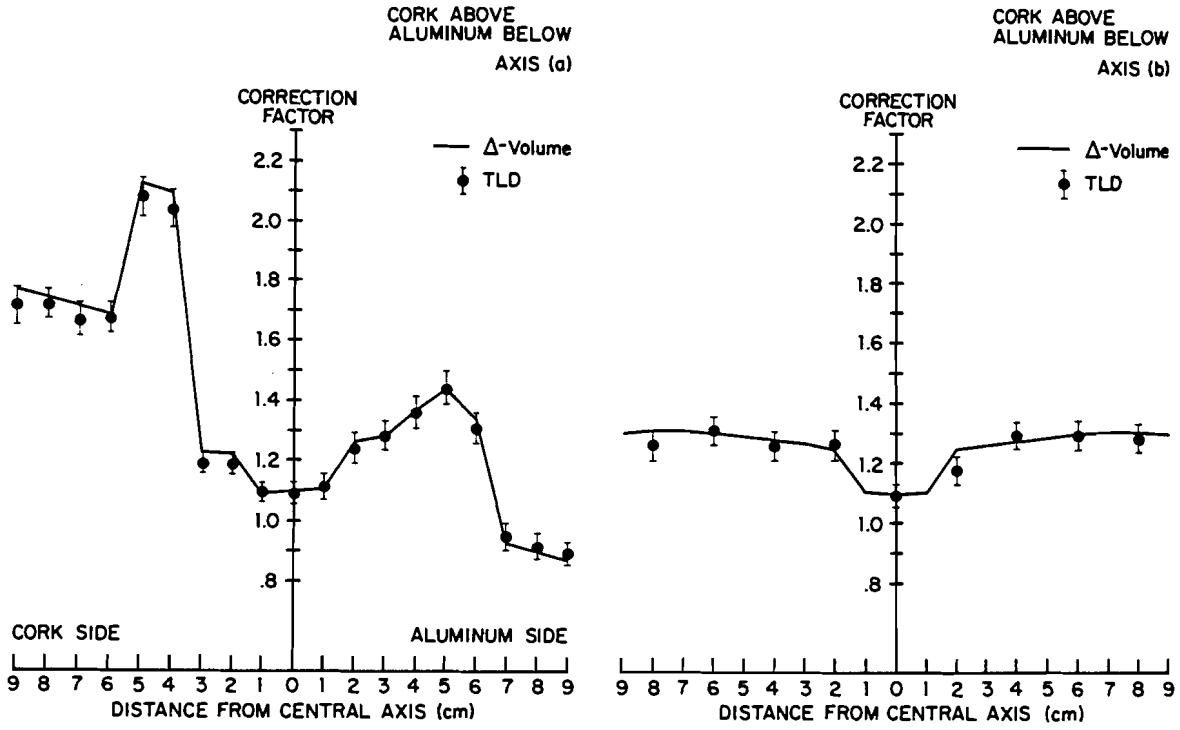

Figure 2b. Comparison of Calculated and Measured Values

Encouraged by these results, we proceeded to apply this verification approach in the more realistic Rando phantom. Profiles of correction factors were measured at the exit side of the phantom using an ionization chamber. Figure 3 shows the results of two profiles 5 cm superior and inferior to the horizontal axis of the beam. The measurements and calculations are shown as continuous and dashed lines respectively. Excellent agreement was obtained. Of the 57 points used for direct comparison, 80% agreed to within ± 3%. Largest errors occurred, once again, in the mediastinal and penumbral regions. The study suggests that accurate prediction of the exit dose distribution may be used for non-invasive treatment verification, a level of quality control that has not been attempted before. We hope that in the future, with a better detection device, and appropriate methods for data analysis (see Section C-3 for the gray-scale images of the exit-correction factors distribution), such an approach will place treatment planning closer to the clinical setting and help to enhance treatment accuracy.

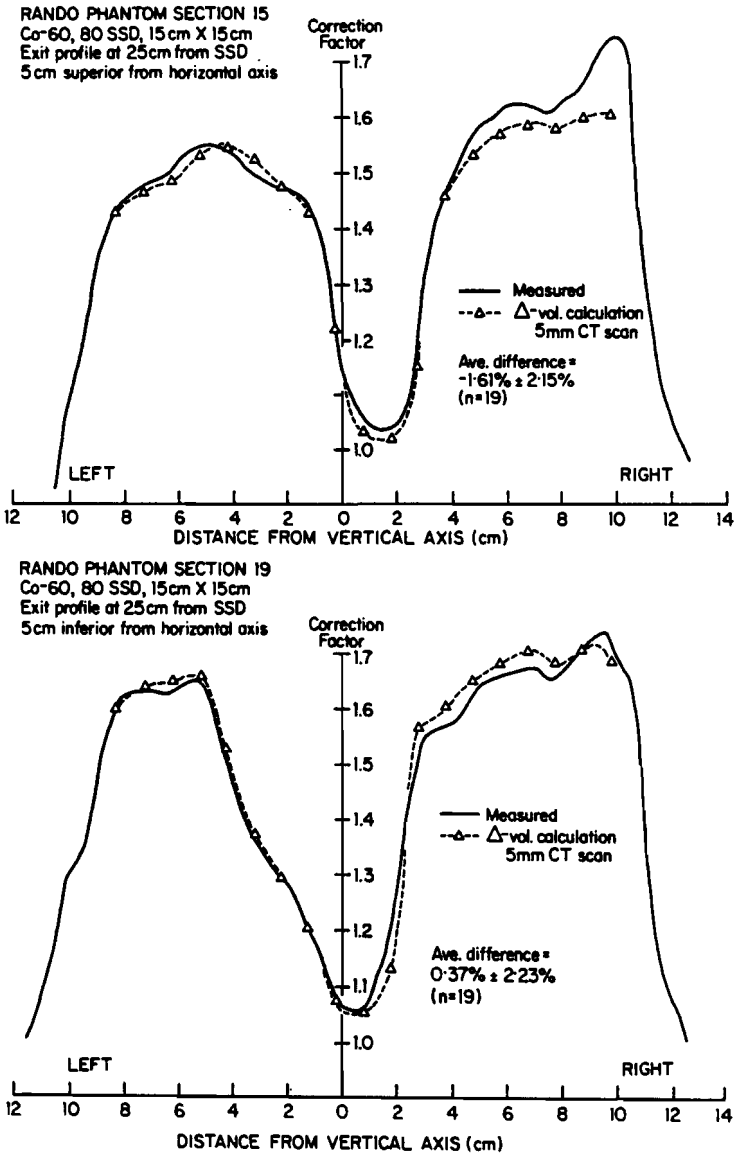

Figure 3. Comparison of Measured and Calculated Exit Dose

Next, we intend to:

(1) Initiate the "photon-electron-transport" phase of the RTP project in order to extend the algorithm to higher photon energies.

(2) Increase or modify the resolution of the primary intensities and dose calculation grids of our prototype algorithm for more appropriate comparisons with measurements and verification studies in high dose-gradient region, and to accommodate larger field dimensions.

(3) Perform actual clinical dose calculations, including exit dose verification studies based on film dosimetry, for patients receiving cobalt-60 irradiations in the head and neck, and thoracic regions.

(4) Examine different methods of data (or image) analysis such as image subtraction so as to quantify our exit-dose treatment verification technique.

(5) Investigate the subtraction from the digitized exit dose distribution obtained from port films of the calculated scattered dose contributions so as to improve the usually poor contrast of the port-films.

1. J. W. Wong and R. M. Henkelman, "A New Approach to CT Pixel-Based Photon Dose Calculations in Heterogeneous Media," Medical Physics, vol. 10(2), pp. 199-208, March/April 1983.

2. J. Wong, "A New Approach to Photon Dose Calculations in Radiotherapy Treatment Planning," Ph.D. Thesis, Department of Medical Biophysics, University of Toronto, July 1982.

3. M. K. Keller, E. D. Slessinger, J. W. Wong, J. Van Dyk, and P. M. K. Leung, "A Practical Method for Precise Thermoluminescent Dosimetry," Journal of the American Association of Medical Dosimetrists, vol. 8(3), pp. 22-26, 1983.

C-2. Integrated Circuit Implementation for Absorbed-Dose Computation in Radiation Treatment Planning

Personnel: F. U. Rosenberger, BCL and Computer Systems Laboratory
G. J. Blaine, BCL
T. J. Chaney, M.S., Computer Systems Laboratory
J. D. Collins, B.S., Computer Systems Laboratory
R. D. Edelman, B.S., Computer Systems Laboratory
E. T. Macke, M.S., Computer Systems Laboratory
W. J. Thomas, M.S., Electrical Engineering
J. W. Wong, Ph.D., Radiology

Support: RR 01380
RR 01379
Washington University

The design of two integrated circuits for ray-tracing and attenuation calculation for absorbed-dose calculations has been completed and both circuits have been submitted for fabrication, one to MOSIS[1] and one to VLSI Technology Incorporated (VTI). We expect to receive the fabricated circuits and to start testing and evaluating them in August or September. The two circuits implement different versions of the ray-tracing algorithm for dose calculations. The first IC, which is being fabricated by VTI, uses a fixed voxel size for attenuation calculations, and as a result, requires a long time for dose computation in large volumes. After initialization and loading of associated memory by a host, it calculates the sum of the augmented first-scatter dose at each voxel in the volume from each voxel. The circuit includes about 12,000 field-effect transistors, 168 cell definitions, and is about 6.5 mm by 6.1 mm with 5 micron feature sizes. Figure 1 shows a plot of the finished design.

The second IC, which was designed as a class project in EE563, calculates dose contribution from a volume of 8 by 8 by 10 voxels to a single voxel upon a command from the host. However, the IC can be used to calculate the dose with 1 cm voxels, 2 cm voxels, 4 cm voxels, etc. until the dose contribution from an entire volume has been calculated. This allows a much smaller number of attenuation calculations than the first method by using lower resolution for the scattering volume that is further away from the dose point. The time savings for calculation of first scatter dose using this technique is about an order of magnitude for volumes of 32 voxels per side.[2] This circuit includes about 6300 field-effect transistors, 117 cell definitions, and is about 3.6 mm by 6.6 mm with 4 micron feature sizes. This second circuit requires less area because of the smaller feature size and because it requires more frequent attention from its host. However, under typical operating conditions, it will compute for about 10ms intervals before requiring a few words of data transfer to and from the host.

The design of these two ICs has been a difficult and time-consuming experience and although we have learned much as a result, it is clear that a less labor intensive technique is required to provide new designs with less effort and to allow modifications and corrections to be incorporated

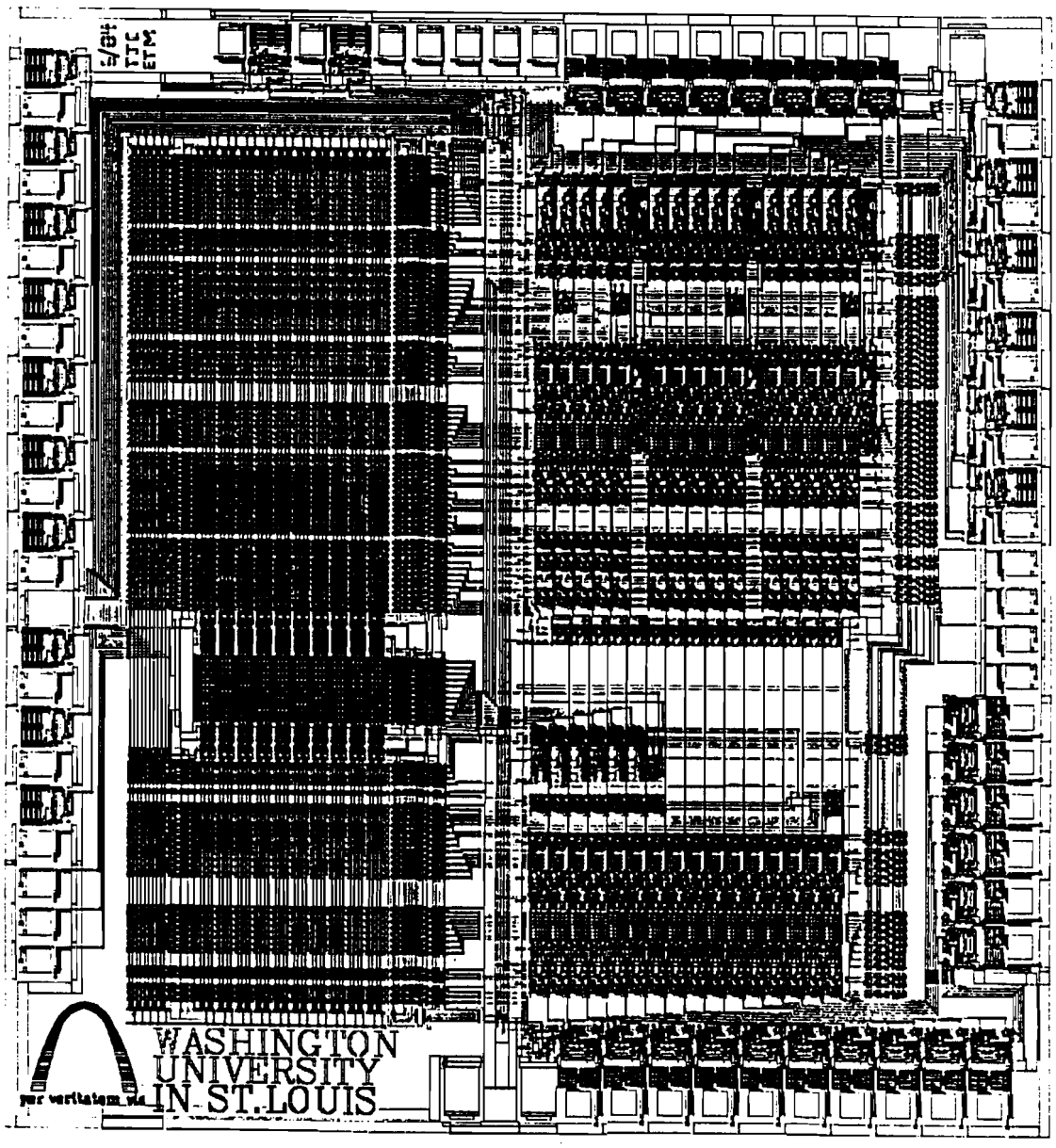

Figure 1. Plot of Δ-Volume Ray-Tracing Integrated Circuit

more easily into completed designs. We are obviously not the only organization encountering such difficulties and significant effort is being expended by other universities and by industry to reduce the time required for design and modification of integrated circuits. We presently have a preliminary version of the VIVID system being developed by the Microelectronics Center of North Carolina and expect to get a significantly improved version within a month or two. VIVID allows design to be completed without explicit specification of dimensions or absolute position, only relative position. When the design is complete, a program adds absolute coordinates and attempts to compact the circuit to remove

unneeded and wasted space. This makes initial design and subsequent changes much quicker and easier than design that uses absolute coordinates.

1. D. Cohen and G. Lewicki, "MOSIS -- The ARPA Silicon Broker," Proceedings of the Second Caltech Conference on VLSI, pp. 29-44, January 1981.

2. F. U. Rosenberger, K. Krippner, D. Stein, Jr., and J. W. Wong, "Implementation of the Delta-Volume Dose Calculation Algorithm," Proceedings of the Eighth International Conference on the Use of Computers in Radiation Therapy, pp. 78-82, July 9-12, 1984.

C-3. Displays for Radiation Treatment Planning

Personnel: R. E. Hermes, BCL
J. W. Wong, Ph.D., Radiology

Support: RR 01380

Experimental displays of conventional treatment plans were demonstrated using the MMS-X system and reported on last year (PR 19, C-2). These displays were used to demonstrate their usefulness and practicality for improving the interpretation and development of radiation treatment plans. The displays utilized stroke graphics to represent isodose contours and outlines of anatomical features.

Our Lexidata system has been used to display and photograph calculated and measured exit dose distributions (C-1) to allow subjective evaluation of the effectiveness of exit dose calculations. Figures 1a and 1b show measured and calculated exit dose data as displayed for comparison and evaluation. The qualitative comparison is good, with the major difference due to the calculation being performed at only half the resolution of the measurements.

The MASSCOMP MCS-500 has stimulated work toward implementing raster displays similar to those achieved on the MMS-X. We are presently implementing a generalized set of display software for the graphics system to provide support for a variety of applications including the development and evaluation of displays for planning beam placement and for evaluating calculated dose distributions.

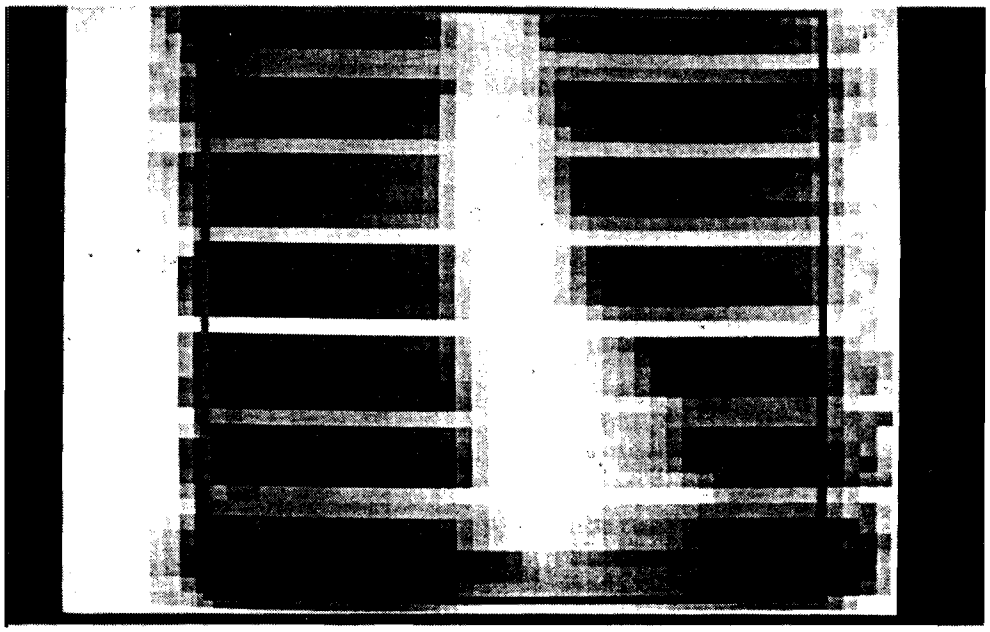

Figure 1a. A gray-scale image of the digitized measured correction factor profiles from our Rando study.

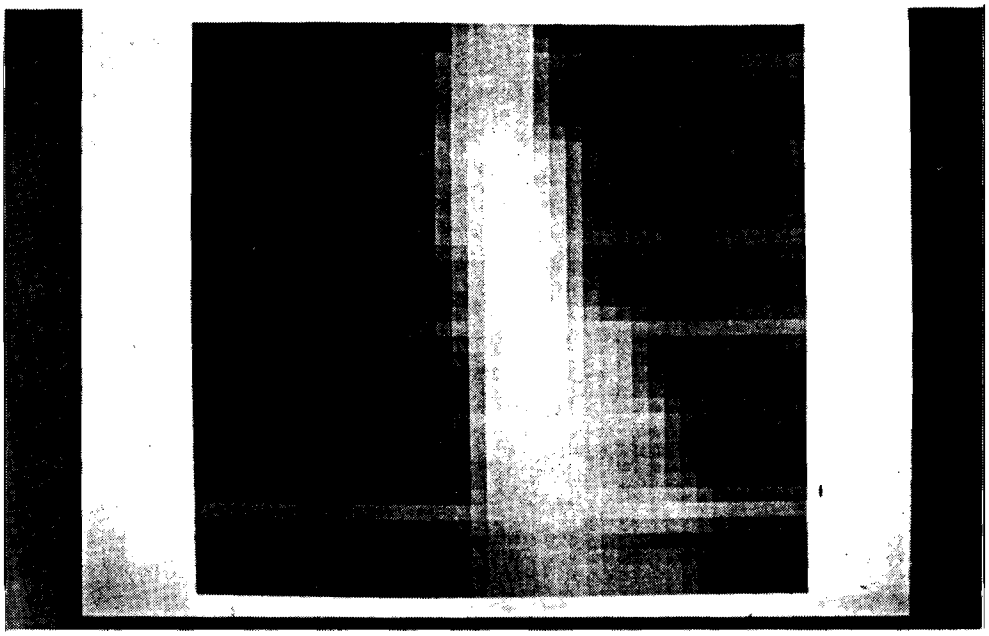

Figure 1b. The corresponding calculated correction factor image of a 25 x 25 matrix, linearly interpolated for comparison to the 50 x 50 matrix of the measured image.

D. Quantitative Imaging: Positron-Emission Tomography

Stimulated by the clinical impact of the EMI transmission tomographic scanner in 1973, experimental studies were initiated in collaboration with the Division of Radiation Sciences to evaluate positron coincidence-detection as a method for emission reconstruction tomography. This collaborative activity resulted in a prototype scanner called PETT (Positron-Emission Transaxial Tomograph). Extensive studies in patients and animals were conducted with the PETT III scanner in collaboration with the divisions of Neurology and Cardiology. A subsequent scanner, PETT IV, utilized concepts developed with its predecessor but incorporated a novel technique for the simultaneous collection of four tomographic slices from a single set of detectors. PETT IV is now located in the Cardiac Care Unit for use in the SCOR project for the quantification of regions of myocardial ischemia and infarction (D-1, D-2). Subsequent scanners have been developed that permit more rapid data collection and improved spatial resolution. One of these, PETT V, was used in experimental studies in dog hearts. PETT VI became operational during the summer of 1980 and employs fast detectors and an entirely circular motion for rapid data acquisition. Further experimental and clinical studies with this system occurred over this past year (D-3, D-4). One of the most exciting recent developments for emission tomography results because of new developments in crystal technology and high-speed electronics. These now permit the propagation time of each of the two photons created in an annihilation to be measured. Theoretical and experimental studies of tomography systems that utilize this new information continued, and the software and hardware needed to realize the predicted benefits were developed (D-5 to D-11); the new system is called Super PETT I. Studies of ways to improve the detector electronics for the improved measurement of time-of-flight continued during the year (D-12). Work was initiated on a new approach for estimating parameters in dynamic studies using list-mode data (D-13) and on using side information, such as CT and MR data, to improve PET reconstructions (D-14). A study of finite-register effects in implementing reconstructions from PET data has been initiated as a necessary step for special processor design (D-15). A new time-of-flight instrument for neurological studies is under development (D-16, D-17). A reconstruction algorithm for single-photon tomography is being studied for use with data collected with a multiview gamma camera (D-19).

D-1. PETT Experimental Studies

Personnel: S. R. Bergmann, Ph.D., Medicine
K. A. A. Fox, M.B., Ch.B., Medicine
R. M. Knabb, Ph.D., Medicine
J. Markham, BCL
B. E. Sobel, M.D., Medicine
M. M. Ter-Pogossian, Ph.D., Radiology
M. J. Welch, Ph.D., Radiology

Support: HL 13851
HL 17646

The overall goal of this project is to implement and evaluate procedures required to translate into intact animals the results obtained with selected positron-emitting tracers used to characterize myocardial metabolism and perfusion in isolated hearts and anesthetized, closed-chest dog studies performed with the Isolated Probe Data Acquisition System (Project A-6). Utilizing positron-emission tomography with PETT VI, the distribution of tracer and the time course of its uptake and clearance from the myocardium can be quantified. Such studies are intimately related to the clinical studies using positron-emission tomography.

During the past year, we have demonstrated that using $H_2{}^{15}O$ ($t_{1/2}$ = 2.1 min) and a modification of the classical Kety-Schmidt autoradiographic approach, quantification of myocardial blood flow in anesthetized dogs was possible. The approach was adapted for use with PET by estimating the myocardial content of radiolabeled H_2O after intravenous infusion of 20-30 mCi of $H_2{}^{15}O$, corrected for vascular radioactivity with the use of tomographic data obtained after the administration of $C^{15}O$ by inhalation to label red blood cells. Tomograms obtained in vivo in six dogs with either normal or reduced regional blood flow correlated closely with tomographically detectable distribution of ^{68}Ga-labeled microspheres ($r = 0.93$) and with postmortem microsphere distribution ($r = 0.95$). The technique thus accurately reflects regional myocardial blood flow and should permit improved objective assessment of nutritional blood flow in patients with medical and surgical interventions designed to augment perfusion. Absolute measurement of myocardial blood flow will necessitate correction of motion artifacts with gating, and algorithms for correction of partial volume and spillover effects.[1]

In pilot studies performed within the past year, we extended this technique to demonstrate that non-invasive determination of regional myocardial blood flow in response to pharmacologically induced vasodilation can permit detection of functionally significant coronary stenoses without coronary angiography. We used PETT VI to characterize myocardial blood flow before and after dipyridamole (1 mg/kg i.v.) in closed-chest dogs with 50-70% reduction of LAD diameter produced by intraluminal placement of Teflon cylinders (i.d. 0.6-1.1 mm). Relative flow was determined following i.v. bolus injections of 40-60 mCi $H_2{}^{15}O$ with correction for vascular tracer with $C^{15}O$ and compared to the distribution of simultaneously administered radiolabeled microspheres. Control tomograms were homogeneous

whereas relative myocardial blood flow was markedly diminished in tomograms after dipyridimole. Although absolute myocardial flow distal to the stenoses increased after dipyridamole, relative flow determined with PET was only 43 ± 10% of normal, and correlated closely with the distribution of microspheres measured in vitro (r = .85). These studies demonstrated that the manifestations of coronary stenosis insufficient to cause resting ischemia can be detected by PET with dipyridamole-induced vasodilation. The approach developed should be applicable to noninvasive diagnosis and localization of stenoses in patients.

We previously demonstrated that PET can be used to estimate the salutary response to coronary thrombolysis. These studies have continued during the current project year. Even though restoration of vessel patency after reperfusion is demonstrable angiographically, it has been reported that myocardial blood flow (MBF) declines below 20% of normal at 24 hours of reperfusion. To evaluate the extent to which externally measured MBF is maintained after coronary thrombolysis, occlusive thrombus was induced by placing a copper coil into the LAD in closed-chest dogs. One and one-half to two hours after thrombosis, lysis was induced with streptokinase. PET following i.v. administration of $H_2{}^{15}O$ and inhalation of $C^{15}O$ was performed during ischemia, after streptokinase, and 24 hours after reperfusion. Radio-labeled microspheres were administered simultaneously at each interval. Myocardial blood flow was 11% of normal during ischemia, increased to 80% of normal immediately after reperfusion, and was 49 ± 17% of normal at 24 hours despite continued angiographic patency. From these studies, we concluded that MBF is reduced 24 hours after reperfusion and that sequential evaluation of MBF can be achieved conveniently with PET.[2] In the last year, we also studied the beneficial effects of coronary thrombolysis on myocardial metabolism as well as perfusion. In eight closed-chest dogs subjected to LAD coronary thrombus, perfusion was evaluated with the $H_2{}^{15}O$ technique, and metabolism was assessed after i.v. injection of ^{11}C-palmitate one to two hours after induction of thrombus. Tomographic data were acquired in the dynamic acquisition mode (2-minute scans). In normal regions, ^{11}C-palmitate accumulated within two to four minutes, and the turnover of ^{11}C-activity from five to fifteen minutes was exponential with a $t_{1/2}$ of 13 ± 5 minutes. In the regions supplied by the LAD, perfusion was diminished to 22% of normal and clearance of ^{11}C-palmitate increased ($t_{1/2}$ = 26 ± 4 minutes) indicating substantial recovery of metabolism. These results indicated that sequential PET permits prompt assessment of the responses of metabolism and perfusion to coronary thrombolysis.[3]

In addition, we have continued our studies of the salutary effects of coronary thrombolysis induced with tissue-type plasminogen activator. PET documented the recovery of metabolism and perfusion after thrombolysis induced with t-PA, suggesting that this promising agent which does not induce a systemic thrombolytic state, has salutary effects on perfusion and metabolism.[4,5]

The studies completed during the past year have demonstrated the utility of PET for the evaluation of myocardial metabolism and perfusion and are currently being implemented in patient studies being designed to evaluate the efficacy of coronary thrombolysis utilizing Super PETT I.

During the coming year, we plan to continue our evaluation of the effects of coronary thrombolysis on the restoration of myocardial perfusion and metabolism with PET to better characterize the response to this promising intervention. Furthermore, we plan to evaluate algorithms, after institution of cardiac and respiratory gating, to correct for the effects of partial volume effects and count-spillover. This will enable measurements of perfusion in absolute terms.

1. S. R. Bergmann, K. A. A. Fox, A. L. Rand, K. D. McElvany, M. J. Welch, J. Markham, and B. E. Sobel, "Quantification of Regional Myocardial Blood Flow in Vivo with $H_2{}^{15}O$ and Positron Emission Tomography," Circulation, in press.

2. R. M. Knabb, M. A. Burnes, B. E. Sobel, K. A. A. Fox, and S. R. Bergmann, "Myocardial Perfusion Following Coronary Thrombolysis Assessed with Positron Emission Tomography (PET) with $H_2{}^{15}O$," Federation Proceedings, vol. 43, p. 709, 1984 (abstract).

3. S. R. Bergmann, K. A. A. Fox, R. M. Knabb, M. A. Burnes, and B. E. Sobel, "Effects of Coronary Thrombolysis on Regional Myocardial Perfusion and Metabolism Assessed with Positron Emission Tomography," Journal of the American College of Cardiology, vol. 3, p. 527, 1984.

4. S. R. Bergmann, K. A. A. Fox, A. L. Rand, D. Collen, and B. E. Sobel, "Recovery of Metabolism and Perfusion Assessed with PET after Coronary Thrombolysis with Plasminogen Activator," Circulation, vol. 68, pp. III-38, 1983 (abstract).

5. F. Van de Werf, S. R. Bergmann, K. A. A. Fox, H. DeGeest, C. F. Hoyng, B. E. Sobel, and D. Collen, "Coronary Thrombolysis with Intravenously Administered Human Tissue-Type Plasminogen Activator Produced by Recombinant DNA Technology," Circulation, vol. 69, pp. 605-610, 1984.

D-2. PETT IV Cardiac Studies

Personnel: E. M. Geltman, M.D., Medicine
H. D. Ambos, BCL
T. R. Baird, Medicine
D. E. Beecher, BCL
A. S. Jaffee, M.D., Medicine
J. Markham, BCL
B. E. Sobel, M.D., Medicine
M. M. Ter-Pogossian, Ph.D., Radiology
M. J. Welch, Ph.D., Radiology

Support: RR 01380
HL 13851
HL 17646

This project was designed to determine the utility of positron-emission tomography (PET) for the assessment of myocardial metabolism after the intravenous injection of ^{11}C-palmitate in patients with a variety of cardiac diseases. During the current grant-interval, patients were studied with ischemic heart disease and congestive cardiomyopathy of various etiologies to determine the extent of metabolic derangements and their response to therapeutic interventions.

To determine whether coronary thrombolysis benefits the heart directly, we utilized positron-emission tomography with ^{11}C-palmitate to characterize regional myocardial metabolism in 17 patients with initial infarction. That was performed immediately after admission, again after intracoronary streptokinase given within 18 hours, and 7 to 10 days later. Clots were persistent in 9 patients, despite a mean dose of 336,000 units and marked fibrinogen depletion. Only 2 of these patients exhibited improved regional metabolism (a decrease in defect size greater than 20%) in late, compared with early, tomograms. Without lysis, mean metabolic-impairment increased by $4 \pm 18\%$ (SD). In contrast, all of the 8 patients who manifested lysis (mean time to lysis = 5.75 hrs after the onset of pain) exhibited improved metabolism with 75% exhibiting more than 20% reduction in defect size in late compared with early studies, and a mean improvement of $28 \pm 2\%$ ($p < 0.01$) in the group as a whole. Results were comparable in patients with anterior and inferior infarction. Thus, clot lysis induced by intracoronary streptokinase exerts salutary effects on myocardial metabolic integrity and viability assessed with positron emission tomography.

Work initiated previously to study the differentiation of ischemic from nonischemic cardiomyopathy by positron-emission tomography has been continued during the current grant-interval. We have now analyzed data from 12 patients with ischemic cardiomyopathy for comparison with 10 patients with nonischemic cardiomyopathy. All patients were studied with positron-emission tomography after the intravenous injection of 15-20 mCi of ^{11}C-palmitate intravenously. The spatial characteristics of the distribution of ^{11}C-palmitate within myocardium of the 10 new patients with nonischemic congestive cardiomyopathy were virtually identical to the

spatial characteristics of our 17 patients with nonischemic congestive cardiomyopathy previously studied. In contrast, the distribution of ^{11}C-palmitate in the myocardium of the 12 patients with ischemic cardiomyopathy were distinct from patients with nonischemic congestive-cardiomyopathy. Large defects encompassing more than 15% of the area of a transverse tomographic reconstruction, representing depressed accumulation of ^{11}C-palmitate, were seen frequently in patients with ischemic cardiomyopathy. Ten of the 12 patients with ischemic cardiomyopathy demonstrated such a defect. None of the patients with nonischemic cardiomyopathy demonstrated these defects. When analyzed employing statistical methods previously described, the number of noncontiguous regions summed for 7 isocount thresholds was 12.1 ± 0.6 for patients with ischemic cardiomyopathy compared to 17 ± 0.6 among patients with nonischemic congestive cardiomyopathy. The frequency distribution of the relative myocardial content of ^{11}C-palmitate was shifted towards lower values in patients with nonischemic congestive cardiomyopathy compared to the non-infarcted zones of patients with ischemic cardiomyopathy or to normal subjects. Thus, positron-emission tomography, after the intravenous administration of ^{11}C-palmitate, permits the objective identification of patients with ischemic from patients with nonischemic congestive cardiomyopathy, a finding which may have significant therapeutic implications.

Positron-emission tomography is also being employed in the analysis of other interventions designed to salvage ischemic myocardium. It is being used as an endpoint for studies of the efficacy of nifedipine, a calcium channel blocker, for the salvage of ischemic myocardium in the setting of acute myocardial infarction. To date, over 40 patients have been studied in this randomized, double-blind trial. However, data have not been analyzed, since 5 additional patients are required before the study is terminated and the code can be broken. These data should be available for the next progress report.

Positron-emission tomography is also being employed as the primary endpoint for studies of tissue plasminogen activator (tPA) as a new thrombolytic agent for use in the setting of acute myocardial infarction. To date, a total of 7 patients have been studied with tPA derived from a melanoma cell line and, subsequently, 7 patients have been studied with tPA derived from recombinant DNA technology and studied under an IND provided by Genentec, Inc. Tomographic data indicate that the reduction in the size of the defect in accumulation of ^{11}C-palmitate observed with positron-emission tomography when lysis is achieved with tPA is at least comparable to that observed when lysis is achieved with streptokinase. Since lysis appears to be achieved more quickly with tPA, ultimately salvage may be greater, but definitive analysis will require the acquisition of more patient data.

Studies in progress should complete the analysis of the effects of nifedipine on myocardial infarct size and the effects of tPA on the ultimate extent of infarction with positron-emission tomography as the primary endpoint. Additional studies are in progress which are designed to study the relationship between defects and cardiac metabolism detected by positron-emission tomography and abnormalities in proton spin resonance

detected by magnetic-resonance imaging. These data will help clarify the impact of partial volume effects and wall-motion abnormalities in the genesis of regions of decreased apparent myocardial content of ^{11}C-palmitate in patients with ischemic heart disease and congestive cardiomyopathy.

D-3. In-Vivo Measurements of Regional Blood Flow and Metabolism in Brain

Personnel: M. E. Raichle, M.D., Neurology and Radiology
D. C. Ficke, B.S., Radiology
P. T. Fox, M.D., Neurology and Radiology
M. H. Gado, M.D., Radiology
R. L. Grubb, Jr., M.D., Neurological Surgery
P. Herscovitch, M.D., Neurology and Radiology
K. B. Larson, BCL
J. L. Lauter, Ph.D., Central Institute for the Deaf
J. Markham, BCL
M. A. Mintun, M.D., Neurology
W. J. Powers, M.D., Neurology and Radiology
D. L. Snyder, BCL
A. G. Swift, B. A., Radiology
M. M. Ter-Pogossian, Ph.D., Radiology
M. J. Welch, Ph.D., Radiology

Support: RR 01380
HL 13851
HL 25944
NS 06833
ECS 8215181
Washington University

Because of the previously noted (PR 19, D-3) deficiencies of compartmental models for estimating cerebral blood flow with PET using radioactive water as a tracer, we have been led to the formulation and testing of distributed models for this purpose. The distributed models we have investigated take into account longitudinal gradients of tracer concentration along the capillaries but assume that transverse gradients are zero. The resulting conservative conditions take the form of sets of partial differential equations in the concentrations, with axial distance and time as independent variables and with capillary and cellular permeabilities, surface areas, volumes, and thermodynamic activity coefficients as parameters. On the basis of solutions of these equations, we have constructed simulated residue curves and have compared these with high-temporal-resolution experimental radiowater residue histories obtained following intracarotid injections of tracer in rhesus monkeys. A two-barrier distributed model was found to provide a realistic simulation of the experimental curves using plausible assignments of parameter values. With the same assignments, all other models tested failed to perform as

satisfactorily. We are therefore encouraged to believe that our two-barrier distributed model can provide insight into the nature of in-vivo water transport in brain and will allow us to devise simplified versions suitable for use in our tomographic clinical applications.

Studies of brain receptors have been performed using PET and labeled spiperone. A three-compartment model, developed previously to describe the kinetics of spiperone in brain tissue (PR 19, D-3), was used to evaluate the PET-acquired time-activity curves of various regions of the brain after injection of ^{18}F-spiperone in twelve baboons. These studies demonstrated the repeatability of the method and the sensitivity of the procedure to a decrease in the number of receptors available for binding due to previous injections of unlabeled spiperone. Parameter values estimated from these data agreed with published values of blood-brain-barrier spiperone permeability and brain-receptor density. Specialized techniques are under development for estimation of the parameters for temporal data in each pixel of the PET reconstruction images. These techniques are based on sensitivity analysis relating variations in the tissue-activity curves calculated from the spiperone model to variations in the values of the parameters. Utilization of the relationships between the tissue-activity curves and the parameters should permit rapid and accurate estimation of the parameters and, consequently, generation of an image of receptor distribution in the brain for each study.

D-4. Maximum-Likelihood Image Reconstruction for PETT VI

Personnel: J. D. Gorman, BCL
M. A. Mintun, M.D., Neurology
D. L. Snyder, BCL

Support: RR 01380
RR 01379
HL 13851
ECS 8215181

The maximum-likelihood image reconstruction algorithm for non-time-of-flight PETT VI data was implemented on two general purpose computers (DEC PDP-11, Perkin-Elmer 3240), and found to produce better images than those obtained from the filtered back-projection algorithm. Increases were observed in the signal-to-noise ratio and resolution, and background artifacts were decreased in the maximum-likelihood images as compared to images obtained with the linear-filtering algorithm. This is consistent with earlier studies done for Super PETT I data using a maximum-likelihood reconstruction algorithm that incorporates time-of-flight (TOF) information.[1]

The maximum-likelihood algorithm has also been applied to Super PETT I data where the TOF information has been suppressed. Images obtained

by using the non-TOF maximum-likelihood algorithm with Super PETT I data appear to be better in preliminary studies than those obtained with the confidence-weighting algorithm which does use TOF information. This indicates that the non-TOF maximum-likelihood algorithm may have applications in TOF PET studies where the TOF information would be used to improve the quality of the measured data by randoms rejection, and then suppressed for reconstruction. Processing times per seven-slice study on a VAX-class machine are on the order of seven hours for the non-TOF algorithm (which operates on two-dimensional data) and 630 hours for the TOF algorithm (which operates on three-dimensional data).

1. D. G. Politte and D. L. Snyder, "Results of a Comparative Study of a Reconstruction Procedure for Producing Improved Estimates of Radioactivity Distributions in Time-of-Flight Emission Tomography," IEEE Transactions on Nuclear Science, vol. NS-31, no. 1, pp. 614-619, February 1984.

D-5. Data-Acquisition for Super PETT I

Personnel: D. E. Beecher, BCL
D. C. Ficke, B.S., Radiology
T. J. Holmes, BCL

Support: RR 01380
HL 13851
HL 17646
HL 25944

The software development for Super PETT I as described in PR 19, D-5 has continued to be useful in prototype studies of the instrument. The list-mode, projection-array, and hybrid list-mode data collection protocols have remained unchanged over the past year and are in routine use. Auxiliary software to utilize the slice processors as offline array processors is still under consideration; however, this is not considered essential to the successful use of Super PETT I in the clinical research environment.

D-6. Time-of-Flight Data Acquisition System Development for Super PETT I

Personnel: T. J. Holmes, BCL
G. J. Blaine, BCL
D. C. Ficke, B.S., Radiology
S. R. Phillips, BCL
D. A. Schwab, BCL
M. M. Ter-Pogossian, Ph.D., Radiology

Support: RR 01380
HL 13851
HL 17646

The data acquisition system[1] of Super PETT I consists of high-speed digital electronics for processing positron-annihilation positional-measurements as they occur. When operating in the "list mode," the digitally encoded measurements are routed as they occur, at a maximum rate of 200,000 per second, to disk storage and are retrospectively retrieved for imaging. When operating in the "pre-processing mode," the measurements are processed as they occur at a maximum rate of 380,000 per second to construct conventional projection arrays while using the time-of-flight measurements to reject most of the random-coincidences (D-10). In the "hybrid list-mode" the raw digital code of each measurement is transformed into fields representing angle, distance, and time-of-flight while correcting for calibration of the time-of-flight measurement and a physical translation of the photon-detector array. These corrected measurements are then transferred to disk storage as in the list-mode while they occur at a maximum rate of 200,000 per second. The pre-processing and hybrid list-mode are made possible by seven microcoded "slice-processors".[2]

The Super PETT I instrument became operational in the list mode during May of 1982 and has since been used for medical research studies. At the present time, the seven slice-processors have been installed, and microcode for both the pre-processing and hybrid list modes has been written and tested. Preliminary tests with phantom radioactivity sources have shown occasional artifacts in the pre-processing mode. We have determined these artifacts to be due to capacitive signal coupling and transmission-line reflections on the busses which transfer the measurements between various data-acquisition devices. Our current efforts are in addressing these bus anomalies while continuing to test the reliability of the instrument.

Current plans for the utilization of the system are as follows. The pre-processing mode is to be used for obtaining calibration data mentioned in PR 19, D-13 and for obtaining conventional emission-images within a few minutes following data collection. Images reconstructed by the time-of-flight method[1] will be obtained from list-mode data. The hybrid list-mode may be used in the future if it becomes necessary to enhance the data-processing efficiency of the instrument.

1. G. J. Blaine, D. C. Ficke, R. E. Hitchens, and T. J. Holmes, "Data Acquisition Aspects of Super-PETT," IEEE Transactions on Nuclear Science, vol. NS-29, no. 1, pp. 544-547, February 1982.

2. T. J. Holmes, R. E. Hitchens, G. J. Blaine, D. C. Ficke, and D. L. Snyder, "A Dedicated Hardware Architecture for Data Acquisition and Processing in a Time-of-Flight Emission Tomography System (Super-PETT)," IEEE Transactions on Nuclear Science, vol. NS-30, no. 1, pp. 170-174, February 1983.

D-7. A Reduced Angle Reconstruction Algorithm for Super PETT I

Personnel: D. G. Politte, M.S., Radiology
D. E. Beecher, BCL
D. C. Ficke, B.S., Radiology
G. R. Hoffman, B.A., Radiology

Support: RR 01380
HL 13851
HL 17646

A new software reconstruction system which uses the "reduced-angle" technique has been designed, implemented, and tested during the past year. This technique is due to Tomitani,[1] who showed by simulation that the angular sampling requirements of time-of-flight tomography are less than those of conventional tomography.

The angle reduction occurs because of the way the data are organized into a three-dimensional array of measurement points. Previously, the data had been organized into an array with three indices representing 96 distinct angles, 128 distances from the center of the scanner, and 40 differential time-of-flight values. In the new reduced angle scheme, data from 16 groups of 6 adjacent angles are coalesced so that the angle index of the measurement array now takes on 16 values. When the data are parsed into the 16 group angles, the distance and time-of-flight values are adjusted so that the location in space of the measurement point is unaffected, to within the quantization error. This reduced-angle measurement array is then reconstructed as before.

The memory requirements of the new 16-angle measurement array are only one-sixth as great as that of the 96-angle array. Therefore, data from several image slices can be accommodated in memory simultaneously. With the current memory of the Perkin-Elmer 3230 host computer, only two passes through the list-mode data file are required. (The first pass processes image slices 1 through 4; the second pass finishes with slices 5 through 7). In addition, some of the subsequent processing steps, such as confidence-weighting and the coordinate transformation and superposition which form the preimage, are angle dependent and the time needed for their

computation scales linearly with the number of angles. The time to process 7 slices of emission data with approximately one million counts per slice has been reduced from two and one half hours to forty-five minutes, assuming that the processing of the blank and transmission scans (used for calibration and data correction) has already been done.

Images reconstructed from data organized into measurement arrays with 96 and 16 angles have been shown by Ficke to be of comparable quality.[2]

1. T. Tomitani, "Simulation Study of Reconstruction with Practical Writing Functions and Noise Evaluation in Time-of-Flight Assisted Positron Computed Tomography," Proceedings of the Workshop on Time-of-Flight Tomography, IEEE Catalog No. 82CH1791-3, Washington University, St. Louis, Missouri, pp. 117-124, May 1982.

2. D. C. Ficke, D. E. Beecher, G. R. Hoffman, T. J. Holmes, and M. M. Ter-Pogossian, "Recent Developments in Image Reconstruction Using a Time-of-Flight Assisted Positron Emission Tomograph: Super PETT I," IEEE Transactions on Nuclear Science, vol. NS-31, no. 1, pp. 605-608, February 1984.

D-8. A Comparative Study of Image-Reconstruction Approaches for Super PETT I

Personnel: D. G. Politte, M.S., Radiology
D. L. Snyder, BCL

Support: RR 01380
RR 01379
HL 25944
ECS 8215181

We have compared the performance of two image-reconstruction algorithms for time-of-flight tomography, the confidence-weighting (CW)[1] algorithm and the estimated posterior-density weighting (EPDW) algorithm.[2] The EPDW algorithm is a non-linear iterative approach, and predicting its performance analytically has proven intractable. Therefore, our approach for comparison has been to implement both algorithms on real and simulated data in order to compare specific performance-metrics. The results have been reported;[3,4] we briefly summarize them below.

Resolution. The CW algorithm uses an adjustable filter which controls the resolution of the images. The resolution is a measure of the smallest features which are distinct. The best resolution obtainable by the CW algorithm is limited by the geometric resolution, which is a function of the detector size and placement. However, we have found that

features as small as half of the geometric resolution can be made distinct with the EPDW algorithm.

Signal-to-noise ratio. We find that the EPDW algorithm improves the signal-to-noise ratio in the myocardium of a simulated left ventricle by at least 2.1 db over the CW reconstruction. The amount of gain is dependent on the resolution of the image and is greatest when the resolution is best.

Contrast. The EPDW algorithm provides superior contrast between the simulated left ventricle and its blood pool.

Background artifact. Registration of activity in regions where there is none is lessened with the EPDW algorithm.

Reconstruction time. Computation of images with the EPDW algorithm is approximately 100 times slower than the computation of images with the CW algorithm.

The current implementations of the EPDW algorithm are too slow for routine clinical use. Further research is needed to explore methods for speeding its computation.

1. D. L. Snyder, L. J. Thomas, Jr., and M. M. Ter-Pogossian, "A Mathematical Model for Positron-Emission Tomography Systems Having Time-of-Flight Measurements," IEEE Transactions on Nuclear Science, vol. NS-28, no. 3, pp. 3575-3583, June 1981.

2. D. L. Snyder and D. G. Politte, "Image Reconstruction from List-Mode Data in an Emission Tomography System Having Time-of-Flight Measurements," IEEE Transactions on Nuclear Science, vol. NS-30, no. 3, pp. 1843-1849, June 1983.

3. D. G. Politte and D. L. Snyder, "Results of a Comparative Study of a Reconstruction Procedure for Producing Improved Estimates of Radioactivity Distributions in Time-of-Flight Emission Tomography," IEEE Transactions on Nuclear Science, vol. NS-31, no. 1, pp. 614-619, February 1984.

4. D. G. Politte, "Reconstruction Algorithms for Time-of-Flight Assisted Positron-Emission Tomographs," Department of Electrical Engineering, Washington University, St. Louis, Missouri, December 1983 (M.S. Thesis).

D-9. Count Normalization for Conventional and Time-of-Flight Tomography

Personnel: T. J. Holmes, BCL
D. C. Ficke, B.S., Radiology
D. L. Snyder, BCL

Support: RR 01380
HL 13851
HL 17646
ECS 8215181

Two of the fundamental operations of a positron-emission tomograph are the sorting and counting of discrete recordings of positron-annihilation events according to measurement vectors which they carry. Part of the reconstruction process includes the normalization of these counts with respect to scintillation-detector efficiency, spatial-sampling density, and photon absorption. There are several ways to combine and normalize these counts during the image-reconstruction process. We have performed a statistical analysis on these methods to determine their relative performance. The combined, normalized counts are treated as parameter estimators, and the metrics of their performances are their biases and variances. These results have been published,[1] and have implications on the complexity of the reconstruction process.

1. T. J. Holmes, D. L. Snyder, and D. C. Ficke, "A Statistical Analysis of Count Normalization Methods Used in Positron-Emission Tomography," IEEE Transactions on Nuclear Science, vol. NS-31, no. 1, pp. 521-526, February 1984.

D-10. Modeling of Random-Coincidence Detections in Time-of-Flight Tomography

Personnel: T. J. Holmes, BCL
D. C. Ficke, B.S., Radiology
D. L. Snyder, BCL

Support: RR 01380
HL 13851
HL 17646
ECS 8215181

A random coincidence is defined as the erroneous registration of two photons, originating from separate positron annihilations, as having originated from the same positron annihilation. Previous analyses which did not consider random coincidences indicated that for a certain radioactivity distribution a gain in image signal-to-noise ratio of about

5 dB is achieved by the time-of-flight method over the conventional method. Subsequent experiments[1] have validated this prediction in low counting rate situations. For higher, typical counting rates these experiments showed a significantly larger gain of about 9 dB, which was attributed to the way in which the time-of-flight method suppresses the degrading effects of random coincidences.

We have developed and published an analytical model[2] which extends a previous model[3] to consider random coincidences. Calculations of signal-to-noise ratio, using this model, compare well with the experiments and show that the additional gain is indeed due to the treatment of random coincidences. An understanding of the model leads to an intuitive explanation of the gain mechanism and a determination of an effective coincidence-timing window that is achieved by the time-of-flight method.

1. M. Yamamoto, D. C. Ficke, and M. M. Ter-Pogossian, "Experimental Assessment of the Gain Achieved by the Utilization of Time-of-Flight Information in a Positron Emission Tomograph (Super PETT I)," IEEE Transactions in Medical Imaging, vol. MI-1, pp. 187-192, November 1982.

2. T. J. Holmes, D. L. Snyder, and D. C. Ficke, "The Effect of Accidental Coincidences in Time-of-Flight Positron Emission Tomography," IEEE Transactions in Medical Imaging, to appear.

3. D. L. Snyder, L. J. Thomas, Jr., and M. M. Ter-Pogossian, "A Mathematical Model for Positron-Emission Tomography Systems Having Time-of-Flight Measurements," IEEE Transactions on Nuclear Science, vol. NS-28, pp. 3575-3583, June 1981.

D-11. Effects of Positron-Emission Tomography Scintillation Detectors on Resolution and Sensitivity

Personnel: T. J. Holmes, BCL
D. C. Ficke, B.S., Radiology
M. M. Ter-Pogossian, Ph.D., Radiology

Support: RR 01380
HL 13851
HL 17646

In addition to improvements in signal-to-noise ratio, the trends in positron-emission tomography have been toward images of higher resolution. The fundamental parameter that determines this metric is the width of the scintillation-detector crystal. With linear-filtering reconstruction methods, a resolution of approximately 0.6 of the detector width is typically achievable at the center of the image. This value is

approximately equal to the full-width at half-maximum (FWHM) of the line-spread function seen in the center of a conventional projection array.

This FWHM is not constant throughout the profile. It is significantly greater at the edges of the profile, manifesting a degradation in image resolution, because the geometry of the scintillation detectors is such that the gamma-photons penetrate a crystal and are erroneously absorbed by adjacent crystals. The chosen crystal-geometry and inter-crystal septa have an impact on this phenomenon and on the detector sensitivity, which depends upon the radiation's angle of incidence.

Exploiting the methods of Lecomte et al,[1] we have analyzed various high-resolution scintillation detectors for resolution and sensitivity. In particular, the effects of using a triangle-shaped face and inter-crystal septa are studied for both BaF_2 and BGO crystals. The results indicate that usage of the tungsten septa alone causes an improvement in resolution in areas away from the center of the image but also causes a degradation in sensitivity in those areas, and that usage of a triangle face alone causes no improvement in resolution, while usage of septa and a triangle face in combination causes a similar resolution improvement with a lesser degradation in sensitivity. Current plans are to analyze a wider range of detector geometries at various angles of incidence.

1. R. Lecomte, D. Schmitt, and G. Lamoureux, "Geometry Study of a High Resolution PET Detection System Using Small Detectors," IEEE Transactions on Nuclear Science, vol. NS-31, no. 1, pp. 556-561, February 1984.

D-12. Studies of Detector Electronics for Time-of-Flight Tomography Systems

Personnel: R. O. Gregory, BCL
G. L. Engel, BCL

Support: RR 01380
RR 01828
Washington University

During this time period, work was initiated on a novel gamma ray detector. In time-of-flight positron-emission tomography machines, such as Super PETT I and II, gamma photons are detected via their interaction with a scintillator crystal and a photomultiplier tube. The intent of the novel detector is to combine the scintillator and photomultiplier tube in one structure, with a view towards an improvement in time and space resolution of the time-of-flight measurement. A proposal to the Department of Health and Human Services in Spring 1983 describes the proposed structure in detail.[1]

Work carried out subsequent to July 1, 1983 has been mainly in the area of photocathode deposition. We have been depositing thin films of antimony and alkali metals, including cesium, sodium, and rubidium, on glass substrates and measuring their photoemissive characteristics. These materials, deposited in the proper proportions, constitute the bulk of commercial photocathodes described in the literature. Development of this technique was felt to be necessary because photocathodes, once deposited, are extremely sensitive to trace amounts of oxygen or water vapor and so are not transportable outside of an ultra high vacuum environment. We have deposited photocathodes with what appears to be adequate quantum efficiency; however, we have not been able to obtain photocathodes whose photo-emission does not deteriorate with time. We have concluded that the reason for this is because we have been depositing the photocathodes in a large, demountable vacuum system with attainable vacuums in the $5x10^{-7}$ to $5x10^{-6}$ range. Although these vacuum values are within the range considered appropriate for this work,[2] in large systems the attainable vacuum is strongly dependent on the pumping rate and a high capacity pump may mask leaks that would be apparent in a smaller or non-pumped enclosure. The solution is to move to a small, bakeable envelope, which is in fact the technique used in ordinary photomultiplier construction where evaporation takes place from sources placed within the tube itself. Although we are reluctant to do so because our available volume is small, it appears that we will have to move to this technique also; and so we are in the process of assembling suitably small emission sources and arranging with a glass blower for the necessary envelope.

1. "A New Approach to Fast Gamma-Radiation Detection," Grant Application to DHHS under the BRP Small Grants Program for Pilot Projects, January 27, 1983.

2. A. H. Sommer, Photoemissive Materials: Preparation, Properties, and Uses, John Wiley, New York, 1968.

D-13. Maximum-Likelihood Estimation of Parameters in Dynamic Tracer Studies

Personnel: J. M. Ollinger, BCL
D. L. Snyder, BCL

Support: RR 01380
RR 01379
ECS 8215181

The primary advantage of positron emission tomography over other imaging modalities is its ability to provide information on physiological and biochemical processes. Although this information is both temporally and spatially dependent, conventional reconstruction-algorithms suppress

The temporal aspects and display only the spatial variations of the data. The goal of this research is to utilize the time-dependency of the data to estimate physiological parameters of interest.

Analyses of biological processes using compartmental models represent the tracer activity distribution (intensity) as a linear combination of the solutions to a set of linear differential equations. Physiological parameters of interest, e.g. blood flow or blood volume, appear as coefficients in these equations. The intensity can therefore be represented as a sum of decaying exponentials convolved with an input function:

$$\lambda(t) = i(t) * \sum_{m=1}^{M} \frac{A_m}{\tau_m} \exp(-t/\tau_m),$$

where the input function, i(t), is proportional to the tracer concentration within the blood, and is assumed to be known. Snyder[1] proposed a method which estimates the A_m and τ_m of this equation. The analytical solution of the differential equation can then be used to solve for the physiological parameters of interest.

The method can be summarized as follows. After a number of images have been reconstructed, regions of interest are specified in each. Data from the images are then used to weight each event in the list-mode data with the probability that it occurred in the region of interest. The EM algorithm of statistics, as discussed by Dempster, Laird, and Rubin,[2] is then used to find the maximum-likelihood estimates of the parameters from histograms formed from the weighted list-mode data. The number of reconstructed images is small, perhaps only one in some clinical studies. The principal advantage of the EM algorithm over other maximum-likelihood techniques is that it decouples the set of equations which must be solved.

Evaluation of the method to date has concentrated on the estimation step. Testing of the histogram-generation step will be done in the near future.

The algorithm was evaluated for a bolus input-function by comparing it to a gradient method of maximum-likelihood estimation proposed by Markham,[3] which in turn was compared favorably to several other methods.[3] The EM algorithm always converged to a unique solution, even for very poor initial estimates. The variance of the estimation error and the bias were consistently lower than that of the gradient method, and were considerably better for small numbers of bins. This algorithm is, therefore, an attractive approach for an impulsive input-function.

The extended algorithm for arbitrary input functions is of greater practical interest, since non-bolus input functions are frequently encountered in practice. This algorithm is currently being evaluated. Issues to be addressed include the uniqueness of the solution, sensitivity to poor starting values, and the incorporation of side information in the

form of physiological parameters measured in other tests. This version of the algorithm could be applied to several experiments currently being performed at the Mallinckrodt Institute of Radiology if these issues are satisfactorily resolved.

1. D. L. Snyder, "Parameter Estimation for Dynamic Studies in Emission Tomography Systems Having List-Mode Data," IEEE Transactions on Nuclear Science, no. 2, pp. 925-932, April 1984.

2. A. P. Dempster, N. M. Laird, and D. B. Rubin, "Maximum Likelihood from Incomplete Data via the EM Algorithm," J. R. Statistical Society, vol. 39, pp. 1-38, 1977.

3. J. Markham, D. L. Snyder, and J. R. Cox, Jr., "A Numerical Implementation of the Maximum-Likelihood Method of Parameter Estimation for Tracer-Kinetic Data," Mathematical Biosciences, no. 28, pp. 275-300, 1976.

D-14. Utilization of Side Information in Image Reconstruction

Personnel: D. L. Snyder, BCL

Support: RR 01380
RR 01379
ECS 8215181

Anatomical information derived from x-ray and magnetic-resonance tomographic sections is useful for producing more accurate reconstructions of radioactivity distributions in the same section from emission-tomography data. Additionally, attenuation information acquired for calibration in emission tomography is necessary for producing accurate reconstructions of activity. An algorithm based on the maximum-likelihood method of statistics has been identified for utilizing both of these forms of side information.[1]

1. D. L. Snyder, "Utilizing Side Information in Emission Tomography," IEEE Transactions on Nuclear Science, vol. NS-31, no. 1, pp. 533-537, February 1984.

D-15. Effects of Finite-Precision Arithmetic on the Maximum-Likelihood Algorithm for PETT Image Reconstruction

Personnel: J. D. Gorman, BCL
D. L. Snyder, BCL

Support: RR 01380
RR 01379
ECS 8215181

Since the introduction of the maximum-likelihood algorithm for PET image reconstruction,[1,2] there has been increasing interest among researchers to use this algorithm for reconstruction in clinical studies. Although the algorithm has produced better images than other available PET reconstruction techniques,[3] it is also more computationally burdensome. Reconstruction times for the maximum-likelihood algorithm implemented on a VAX-class machine are too long for the algorithm to be of practical use clinically. A specialized hardware processor, perhaps implemented using VLSI,[4] could supply the additional computational speed needed to make the algorithm useful in the clinical environment.

A study has been initiated to investigate the effects of finite-length registers and finite-precision arithmetic on the algorithm. Knowledge of the effects of fixed-point arithmetic and tradeoffs in image quality as a function of register sizes are the first steps toward an efficient hardware implementation of the algorithm.

1. L. A. Shepp and Y. Vardi, "Maximum-Likelihood Reconstruction for Emission Tomography," IEEE Transactions in Medical Imaging, vol. MI-1, no. 2, pp. 113-121, October 1982.

2. D. L. Snyder and D. G. Politte, "Image Reconstruction from List-Mode Data in an Emission Tomography System Having Time-of-Flight Measurements," IEEE Transactions on Nuclear Science, vol. NS-30, no. 3, pp. 1843-1849, June 1983.

3. D. G. Politte and D. L. Snyder, "Results of a Comparative Study of a Reconstruction Procedure for Producing Improved Estimates of Radioactivity Distributions in Time-of-Flight Emission Tomography," IEEE Transactions on Nuclear Science, vol. NS-31, no. 1, pp. 614-619, February 1984.

4. C. E. Molnar, "VLSI Systems for Time-of Flight PET," Proceedings of Workshop on Time-of-Flight Tomography, IEEE Catalog No. 82CH1791-3, Washington University, St. Louis, Missouri, pp. 167-170, May 1982.

D-16. Slice Processor Selection for Super PETT II

Personnel: D. E. Beecher, BCL
D. C. Ficke, B.S., Radiology

Support: RR 01380
HL 13851

The motivation for the utilization of seven slice-processors is a result of considerable experience gained in the design, fabrication, and use of Super PETT I, which uses the list-mode data collection and time-of-flight information in the image-reconstruction process. While these two concepts have proven to be useful and desirable, they both place high demands on the supporting computer system.

The incorporation of list-mode data-collection requires list-mode events first to be buffered in computer memory and then transferred to disk as they occur. If 100K events/second is used as a target goal for the count rate in each slice, the computer system's I/O throughput capacity must be able to sustain 1.4M bytes/second, and the disk subsystem must be able to sustain a 700K event/second rate.

In addition, the proper incorporation of the time-of-flight information and its associated correction factors for the "confidence weighted" pre-image and the subsequent two-dimensional filtering to form final images are formidable CPU intensive tasks. This problem is compounded by processing seven simultaneously collected slices from the event list.

In the development of Super PETT I, it was recognized that auxiliary processing power was necessary to use the time-of-flight information effectively. For this reason, seven specialized slice-processors were designed and built to form attenuation arrays and aid in on-the-fly data corrections before recording the data in the event list. From this experience it was apparent that the design, fabrication, debugging and software development involved in such specialized hardware components was a formidable task and has yielded results which are less than desirable, although at that time this approach was perhaps the only available. In Super PETT I, the event rate is limited to about 400K events/second in the list-mode, and post processing requires about 35 minutes for a set of seven slices, each containing about 1 million events.

Recently however, several commercially available 32-bit processors were introduced which we felt could be used successfully in this environment, and we began to explore these possibilities for Super PETT II. There are several reasons why this particular approach is very attractive. The general scheme consisting of individual low-cost processors and disks for each slice very much improves total system event-rates since each slice is serviced by a single processor and disk. This implies no contention between slices for DMA input and storage. The reconstruction process is also enhanced by allowing each slice processor to reconstruct one slice in parallel with the other six. Another very important point lies in the fact

that these systems are equipped with the total complement of support software found on larger machines which greatly reduces the software development time associated with the slice processors. Vendor supplied systems can also be placed under maintenance contracts to avoid excessive down time due to hardware and software related problems.

Several systems were examined and tested to determine their potential usefulness. They were: Perkin-Elmer 3205, Digital Equipment Corporation (DEC) Micro-VAX, and Hewlett-Packard (H-P) 9000. Due to our existing in-house expertise with Perkin-Elmer, we were somewhat predisposed to a Perkin-Elmer solution if indeed it proved to be competitively cost-effective. However, we realized that it could be advantageous to switch to DEC or H-P if conditions dictated. In an evaluation effort, we designed a specialized interface to simulate event generation from Super PETT II and ran a series of tests involving the list-mode data transfer and the ability to do on-the-fly processing. We ran these tests initially on the Perkin-Elmer 3205 and obtained good results with the ability to collect approximately 200K bytes/second of event data per slice. With proper hardware preprocessing each event may be reduced to 2 bytes yielding 700K events/second for the entire system. For instance, one preprocessing strategy reduces each event to 5 bits of angle information, 4 bits of time-of-flight information, and 7 bits of displacement information.

Similar tests on a Micro-VAX system yielded only 120K bytes/second from a single slice which translates into 420K events/second for the total system. This drop in effective throughput was deemed unacceptable given that the Micro-VAX and 3205 are comparably priced. The H-P 9000 was not directly tested. However, we did speak at length with H-P technical personnel and discovered that the 9000 did not readily allow the incorporation of custom-designed interfaces; and the machines cost was substantially higher than that of the Micro-VAX or the 3205.

The combination of price, performance, and compatibility indicated that the 3205 was the best choice for this application. The Perkin-Elmer 3205 processor is implemented as a single-board CPU with built-in hardware floating point, a high-speed DMA port, and memory which can be expanded on the single board to 1 megabyte. An additional memory board can be added to expand the total memory to 4 megabytes. A second board contains the medium-speed multiplexor bus, a multiple peripheral controller, universal clock, watchdog timer, loader storage unit, 8-line communications multiplexor, line printer interface, and high-speed data handling capabilities. Figure 1 shows the internal configuration of a single slice processor. Each 3205 is also configured with an 80 megabyte fixed disk drive for data storage and a dual-port option for intersystem communication. Figure 2 illustrates the entire proposed configuration to support Super PETT II for neurological studies.

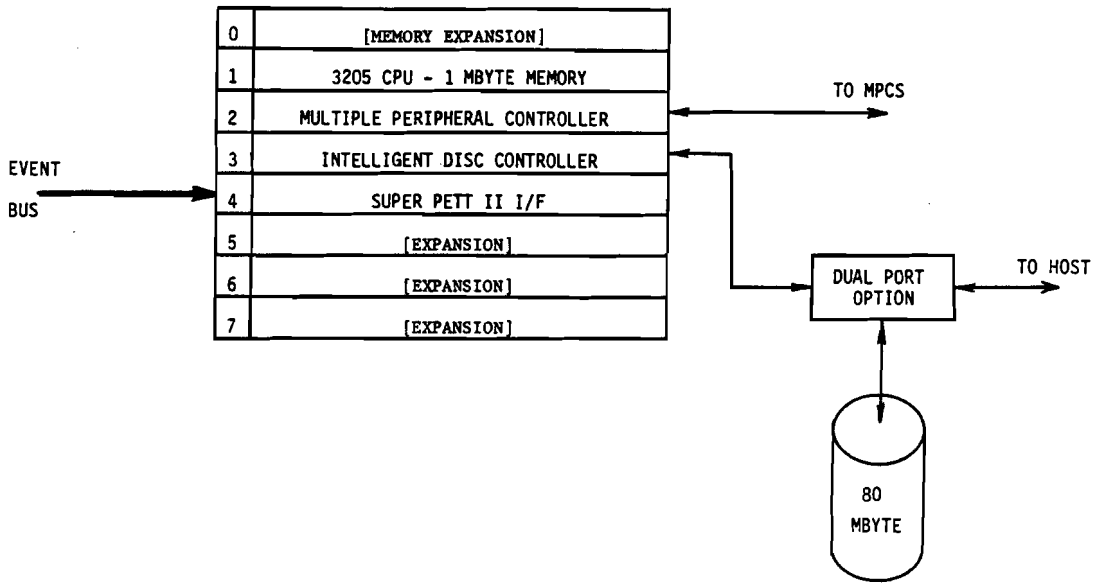

Figure 1. Slice Processor Configuration

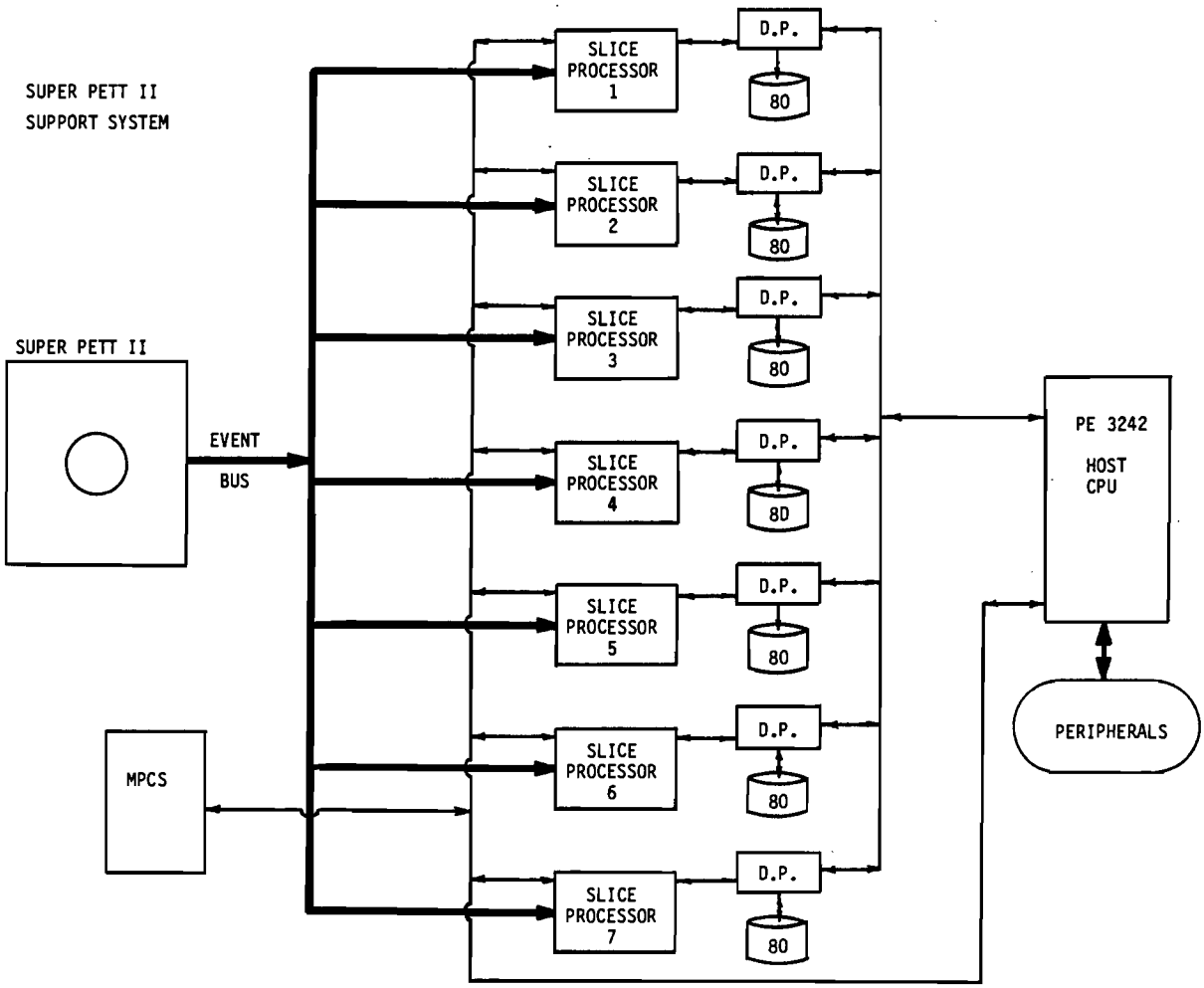

Figure 2. Super PETT II Support System

D-17. Super PETT II Detector Design

Personnel: D. C. Ficke, B.S., Radiology
T. J. Holmes, BCL
J. T. Hood, B.S., Radiology
M. M. Ter-Pogossian, Ph.D., Radiology

Support: RR 01380
HL 13851

A new detector module has been designed, fabricated, and tested for use in Super PETT II, a time-of-flight assisted positron-emission tomograph which is currently being developed.

The detector module as shown in Figure 1 consists of eight barium-fluoride scintillation-detectors coupled to five high speed photomultiplier tubes. In this arrangement, four tubes are each coupled to two detectors for the purpose of photon timing and energy information, while the central tube is coupled to four detectors for resolving the photon positional information by an electronic coincidence detection scheme with the timing tubes.

When this module is tested by scanning a line source, the response as shown in Figure 1 is obtained which indicates a spatial resolution of 4 mm FWHM.

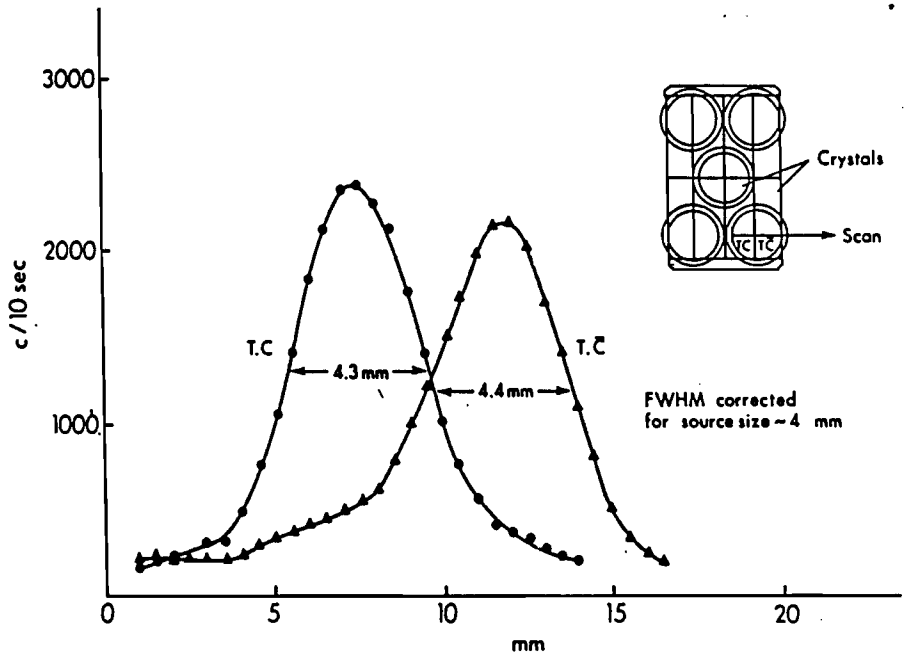

Figure 1. The Super PETT II detector module is shown with its measured spatial resolution.

D-18. Three-Dimensional Image Construction and Display

Personnel: D. E. Beecher, BCL
J. R. Cox, Jr., BCL
L. J. Thomas, Jr., BCL

Support: RR 01380
HL 13851

Work has continued on the research as described in (PR 19, D-6) and the results of this research have been published.[1] Further research is planned in the following areas:

1. Three-Dimensional Object Definition

Current techniques employ a simple thresholding algorithm to define the object(s) of interest in a scene. Although this technique has proven to be useful in pilot studies, new techniques are being explored in order to define three-dimensional objects more effectively. Gradient techniques which define object boundaries based on changes in a local neighborhood may yield superior results. Also transparency techniques may prove to be quite effective in alleviating the need to do any object definition.

2. Parallelism

The algorithm as described in (1) has a very high degree of parallelism which may be exploited via a custom-designed VLSI implementation. This may make real-time shaded-surface display possible.

3. Shading Algorithms

Initial efforts in this area were very simplistic in that only a depth cue was utilized to produce the three-dimensional effect. Much work is planned in this area to improve the visualization by enhancing the shading algorithm used in view generation. The concept of local neighborhoods will be studied to determine the orientation of planes which may exist within the object. This information when combined with angle information, should substantially improve the views generated.

4. Generation of Non-Orthogonal Views

The system as originally implemented generates only orthogonal views of the voxel volume. Generation of non-orthogonal views will require slight modifications of the original algorithm but should not substantially increase view generation time.

5. Multiple-Intensity Level Displays

The current scheme thresholds at a single intensity level to determine an object space. However if color is used as a secondary cue, multiple intensity levels can be displayed simultaneously which should improve the contextual information contained in the visualization.

1. D. E. Beecher, J. R. Cox, Jr., and L. J. Thomas, Jr., "A New Voxel-Model Approach for Three-Dimensional View Generation," Proceedings of the Eighth Conference on Computers in Radiology, St. Louis, Missouri, May 23-25, 1984, in press.

D-19. Maximum-Likelihood Estimation for Single-Photon Emission Computed Tomography

Personnel: D. L. Snyder, BCL
M. I. Miller, BCL
T. R. Miller, Radiology

Support: RR 01380
HL 17646
RR 01379
ECS 8215181

An algorithm is being developed for producing maximum-likelihood estimates of activity distributions for emission-tomography systems which employ tracers that emit single photons. This algorithm takes into account both the depth-dependent point spread function of single-photon detectors and the non-uniform attenuation of photons from the emission point to the detector. More accurate quantitative reconstructions of activity distributions should result compared to algorithms in present use.

E. Systems for Specialized Biomedical Studies

This section reports on a variety of instruments, systems, and methods which are not easily grouped under the major report headings. There is one common thread; much of the work relates directly to the nervous system. For example, the data recording system described in PR-19 (E-3) is being combined with a versatile and remotely controllable signal amplifier and conditioner. This should find general application in future projects. In a related study large-scale electrode arrays receive signals from the brain which are then analyzed by computers.

Electrical concomitants of nervous system activity are no longer the only minimally invasive method of studying the functional anatomy of the brain. The PETT system shows promise of displaying a variety of responses to sensory stimulation and software for this purpose is under development.

Studies of the auditory nervous system are helped by the application of statistical methods originally designed for use in nuclear medicine, whilst a computer is providing information on the responses of the eye to colored stimuli. This is finding clinical use in cases with retinal or optic nerve diseases. The remaining neurological project has been the introduction of the autoradiographic analysis method, using computer imaging of silver grains, to the Laboratory for Neuro Imaging (LONI) where it is co-located with larger computer systems.

There are a number of projects which involve the development of specialized mathematical algorithms especially related to biomedical imaging and work continues on the application of computer technology to DNA restriction mapping.

E-1. An Automated Autoradiographic Analysis System for Neuroanatomical Studies

Personnel: R. E. Hermes, BCL
E. G. Jones, M.D., Ph.D., Anatomy
S. R. Phillips, BCL
J. L. Price, Ph.D., Anatomy
A. W. Toga, Ph.D., Neurology

Support: RR 01380
NS 15070

The silver grain counting system developed several years ago for automated analysis of neuroanatomical autoradiographs (PR 18, C-1; PR 19, E-1) was moved to the Laboratory for Neuro Imaging (LONI). The LONI laboratory consists of a VAX 11/750 with an image display system. An Eikonix flat bed scanner for digitizing images of interest is interfaced to the VAX. The LONI system serves as a general resource for neuroanatomist and other researchers. Placement of the silver grain counting system in close proximity to the LONI system has made use of the system more convenient for users of both systems.

The silver grain counting system has a well designed data acquisition and image display system. Data analysis software on the system is very specialized for the task of counting silver grains. The specialized nature of the analysis software has prohibited use of the system for other data analysis problems which could take advantage of the data acquisition system. The current proximity of the LONI system makes possible the connection of the two systems where data may be acquired on the specialized system, and subsequent data analysis, display, and archiving may be conducted on the larger system.

E-2. DNA Restriction-Mapping

Personnel: J. G. Dunham, BCL and Electrical Engineering
M. S. Frank, M.D., Genetics
M. V. Olson, Ph.D., Genetics
M. R. Weber, Electrical Engineering

Support: RR 01380
GM 27889
GM 28232
Washington University

The DNA mapping project, under the direction of M. V. Olson of the Department of Genetics, will generate approximately 5000 fragments of DNA randomly sampled from a particular yeast. These fragments will be cloned using recombinant DNA techniques, completely digested with a restriction enzyme run on an agarose gel using electrophoretic techniques and photographed. An automated gel reading system was developed by BCL to determine the location of bands on the gel and has been reported.[1]

One effort has been to characterize the noise introduced by digitizing the gel photographs for further analysis. M. Weber has obtained a characterization of the system.[2] To summarize, an analysis of the various noise sources within the CCD camera of the digitizer suggests that the overall noise is a combination of Poisson and Gaussian components. Since these noises are quantized, the overall noise should appear as a quantized Gaussian whose variance is a linear function of the input light intensity. A histogram at 12 bits showed that the output was roughly a quantized Gaussian. In time, they were found to be uncorrelated, and hence independent. When viewing a single sample, one gets approximately 6 bits of useful information while temporal averaging of 32 samples yields 8 bits of useful information, useful in the sense that the true value is obtained with probability 0.95 or higher. After proper normalization, all the pixels seemed to consistently reflect the input intensity level on the average. However, a few pixels had a large variance, tending to fluctuate widely about the mean value. These wide fluctuations suggests that such pixels are unreliable and perhaps should be noted in later stages of processing the digitized gel photographs.

Accurate band detection and estimation of location is critical to the success of the overall reconstruction of the yeast genome from the clones. A review early in the progress report period found that the original band detection algorithm was unsatisfactory for several reasons. Two approaches were undertaken to improve the band detection algorithms, an ad hoc approach by M. Frank and an analytic method based upon a statistical model of the overall gel photography by M. Weber.

The ad hoc approach by M. Frank reads the gel at two light intensity levels and attempts to compensate for nonuniform light intensities across the gel. First, peaks are detected which potentially correspond to bands. Next, several properties of the band shape are used to determine if a band is an isolated band or a cluster of bands. If an isolated band is found,

then it is determined whether it is a singlet, doublet or triplet. If a cluster of bands is found, then further work is performed to determine how many bands are in the cluster and then their locations are estimated. The algorithm was implemented and found to yield improved performance over the original algorithm.

Another approach was undertaken by M. Weber based upon a model described in Reference 2. Briefly, the model shows that the concentration of DNA from a band is approximately:

$$C(x) = C_o \, e^{-\alpha x} e^{(x-\mu)^2/2\sigma^2}$$

where x is the distance down the gel lance, C_o is the actual DNA concentration, 2 is a factor related to gel mobility and the amount of time a gel is run, μ is the true location of the band and σ^2 is the variance of the band shape. Since a negative is taken, the transmittance of the film is roughly proportional to $1/C(x)$ and implies that large concentrations appear as small transmittances. Some experimental work described in Reference 2 provides a partial verification of the model.

Based upon the model for the digitizer noise process and the model for the band DNA concentration, a detector was developed using ideas from statistical detection and estimation theory. Two filters were developed, one to locate the center of bands and the other to estimate the concentration of DNA. Applying the filter to real data indicated that the approach has potential for estimating band location and concentration. Several potential problems were also observed. First, since a negative was taken, the digitized image must be numerically inverted and accuracy becomes a problem when using a linear analog/digital converter. Second, the large dynamic range of the light on the gel suggests that the gel needs to be scanned at a multiple number of intensities, a conclusion independently reached by M. Frank. Third, not all gels give consistent results, for equimolar DNA samples. The cause of this problem has not been identified at the present time. Possible explanations include reciprocity failure of the film, incorrect film exposure and light-source problems.

1. A. J. Gray, D. E. Beecher, and M. V. Olson, "Computer-Based Image Analysis of One-Dimensional Electrophoretic Gels Used for the Separation of DNA Restriction Fragments," Nucleic Acids Research, vol. 12, pp. 473-491, 1984.

2. M. R. Weber, "Band Detection for DNA Electrophoretic Gels," Master of Science thesis, Department of Electrical Engineering, Washington University, St. Louis, Missouri, 1984.

E-3. Development of Multi-Channel Analog Data Recorder

Personnel: H. W. Shipton, BCL
S. R. Broadstone, B.A., B.S., Electrical Engineering

Support: RR 07054
Washington University

The prototype model described in PR-19 has been re-engineered and an improved filter system incorporated. The system has been tested in this new form but extensive trials in a realistic environment await the completion of the data acquisition system (E-4) with which the system will be packaged.

E-4. Development of a Data Acquisition System

Personnel: H. W. Shipton, BCL
S. R. Broadstone, B.A., B.S., Electrical Engineering

Support: Washington University

Most biological amplifiers are direct descendants of the differential amplifiers developed early in the vacuum tube era and few systems exist which take advantage of the stability and reliability of solid state amplifiers. An investigation has been carried out into the desirable features of a "universal" biophysical amplifier than can be produced simply and incorporated into many different devices. The desirable features include low input-stage noise and the ability to accept high-impedance electrodes. They must also be capable of operating with considerable offset potentials since in clinical practice these often approach 200 millivolts.

It is desirable that gain and filter settings be capable of control from devices (e.g. computers) which are located away from the biological preparation.

The problem of common mode rejection ratio is frequently misstated. Obtaining ratios of the order of 130 db is trivial in a laboratory but neither necessary nor practicable under operational conditions. It is of considerable importance that CMRR should be preserved with 10-15% electrode impedance imbalances and also that it should not vary over the frequency range of the amplifier.

Consideration of these factors led to the design of a system in which the input stage is a low gain JFET differential amplifier with a constant current injected into the source so as to stabilize the working point. It was found difficult to obtain a repeatable design owing to wide tolerances of obtainable commercial components. This stage is followed by

an instrumentation amplifier which has switch controllable gains in the sequence 1, 2, 5. Unfortunately, no available silicon switches have sufficiently low "on" resistances to permit them to be used to set the instrumentation amplifier. The necessity of using reed relays or DIP switches complicates gain control. It is understood that early next year at least one manufacturer will produce an instrumentation whose gain can be controlled by a typical computer bus. Samples of this are not yet available.

A major advantage of the present system is that up to the output of the instrumentation amplifier, the system is directly coupled so that only one high pass filter occurs in the system. This has great advantages in minimizing blocking time, undesirable phase shifts and frequency dependent CMRR. The system can be adjusted over the entire range of commonly measured biophysical measurements by the adjustment of no more than one resistor and two capacitors.

A multi-channel version of the system is currently undergoing tests and will form part of the analog tape system described in E-3.

E-5. Color Perimetry Studies

Personnel: W. M. Hart, Jr., M.D., Ph.D., Ophthalmology
K. W. Clark, BCL

Support: RR 01380
EY 03703

During the past year the color perimetry video system has been in clinical use at the Department of Ophthalmology. The system has been used for visual field evaluation of patients with known or suspected optic nerve and retinal diseases. The perimetry device consists of a color video tangent screen with a diagonal size of 19 inches which is placed at a distance of 10 inches from the patient's eye. Colored test objects which are square in shape and variable in size are presented on the tangent screen under real-time control by a graphics tablet. The test objects are of various colors and are presented in a background of a neutral gray color. Luminance values for the gray background and for the colored test objects are calibrated by means of a digital video photometer which is used to generate a lookup table in the memory of a microcomputer (Motorola Exorset). Colored test objects are matched to a constant-luminance white surround through the use of heterochromatic flicker photometry. Test objects are then varied only in their size and degree of color saturation.

Clinical studies[1,2] over the past year have revealed that visual field defects resulting from retinal and optic nerve diseases, when plotted by color contrast perimetry, are identical in shape and size to those plotted by conventional luminance increment perimetry. No significant

difference was found either between the use of red or green vs blue test objects. Studies during the subsequent project year will involve the use of a yellow color for the adapting surround with test objects that are modulated in the blue direction from yellow passing through white into fully saturated blue. This strategy has been chosen because neurophysiologic studies of the primate visual system have revealed that the blue-yellow color-opponent channel is the only one that can be expected to be completely isolated from luminance difference detection mechanisms.

1. W. M. Hart, Jr., R. K. Hagen, and K. W. Clark, "Color-Contrast Perimetry," Investigative Ophthalmology and Visual Science, vol. 25, pp. 400-413, 1984.

2. W. M. Hart, Jr., and M. O. Gordon, "Color Perimetry of Glaucomatous Visual Field Defects," Ophthalmology, vol. 91, pp. 338-346, 1984.

E-6. Isolated-Scintillation-Probe Data Acquisition System

Personnel: D. E. Beecher, BCL
H. D. Ambos, Medicine
R. E. Hermes, BCL

Support: RR 01380
HL 13851
HL 17646

Hardware and software development has been initiated and continued over the past year using the newly acquired LSI 11/23 system configuration as described in PR-19, E-8.

Software system development is now close to completion and will allow protocols not possible with the current configuration. The software system is highly modular which will allow the completed system to be easily maintained and modified in the future. Specifications are not yet complete for the analysis portion of the system, but will be developed shortly after the prototype has been finished.

A new hardware probe interface has recently been developed and is now being tested on the new system. It utilizes a DMA interface to the LSI 11/23 and will enable real-time acquisition and display of the probe data. This will enable experiments to be aborted quickly if initial probe data curves are not promising.

E-7. Software Development for Neurological Sciences

Personnel: D. E. Beecher, BCL
P. T. Fox, M.D., Neurology and Radiology
M. A. Mintun, M.D., Neurology

Support: RR 01380
NS 06833
McDonnell Center for Studies of Higher Brain Function

Work is currently underway on two separate neurology projects involving visual evoked response as measured by PET and redesign of a pre-existing software system to analyze PET images.

The software for visual evoked response is separated into three distinct subsystems. The first is a variable sized checkerboard pattern which has a user-selectable background and foreground colors. The remaining subsystems involve the generation of moving targets. The first generates a box of a specified size which can be moved at a user-selected rate. The moving target subsystems also have user-selectable background and foreground colors.

The software system redesign involves a software analysis system which has been in place for several months. Although modifications are needed, the system is very large and the design is such that modifications to the existing code are very difficult. For this reason it was decided to redesign the system using structured design techniques in order to make modifications and maintenance much more manageable than they are at present. Current efforts are concentrated on the development of libraries of low-level routines to handle the bulk of the device-dependent I/O functions necessary in a system of this size. Final system development should proceed rather quickly after completion of the library primitives.

E-8. Maximum-Likelihood Estimation Applied to Electron-Microscopic Autoradiography

Personnel: M. I. Miller, BCL
K. B. Larson, BCL
J. E. Saffitz, M.D., Pathology
D. L. Snyder, BCL
L. J. Thomas, Jr., BCL

Support: RR 01380
Washington University

For electron-microscopic (EM) autoradiography thin tissue sections containing beta-emitting radioactive material are overlayed by a crystalline layer of emulsion. Beta particles leave the tissue sections

and pass through the emulsion layers where they give rise to latent images which are subsequently developed into silver grains. The unused emulsion is dissolved, leaving final specimens consisting of thin sections containing silver grains, the positions of which are a function of the distribution of radioactive tracer in the underlying tissue sections. The production of these autoradiographs at the electron microscopic level is a technique of growing importance as the tracer distributions offer a wealth of information about the sites and activity levels of metabolic and pharmacologic processes of the subcellular organelles. We have developed new algorithms for localizing and quantifying, within ultrastructural features, the radioisotope source distributions which are reflected in the observed silver grain measurements.

The quantitative analysis of EM autoradiographs used for identifying the distribution of radioactive sources must be a statistical one because of the nature of radioactive processes and the low number of radioactive events involved. Due to the nature of the radioactive emission spread, it is not possible to assume a priori that a particular silver grain originated from radioactivity in the particular organelle over which it lies. Analytical methods taking both emission spread and cellular anatomy into account are essential for estimating the relative concentrations of tracers in various cell compartments. One such analysis is the mask-analysis technique of Salpeter and Bachmann[1] which may be used with the computer algorithm of Land and Salpeter.[2] The mask-analysis algorithm utilizes a set of transparent plastic overlays (masks) containing 288 equally probable source-grain pairs, each denoting the relative hypothetical positions of a point source of radiation and a silver grain resulting from that point source. The hypothetical source-grain pairs are generated from a grain-distribution point-spread function that is characteristic of a given autoradiographic system and depends upon variables including isotope type, section thickness, emulsion type and thickness, and photographic parameters.[1,3] The masks are manually placed over individual photographs and the tissue structures over which hypothetical source-grain pairs occur are recorded. The information derived from the mask technique defines the relative sizes and juxtapositions of the tissue structures and is utilized to generate a table of transition probabilities which we call $P(m|i)$. All the algorithms proposed to date are similar in that they require this table of transition-probability estimates (Blackett and Parry[4] call them cross-scatter estimates; Williams [5]calls them cross-fire estimates; Salpeter and coworkers[3] call them source-to-grain probability pairs). The transition probabilities $P(m|i)$ may be viewed as an estimate of the probability that a given disintegration occurring in one structure i may give rise to a silver grain measurement within some structure m.

Once the table of transition probability estimates has been generated, the silver grain measurement statistic N_m in each organelle may be computed using the circle method of Williams.[5] The silver grain statistic N_m is generated by combining across all of the micrograph slices the number of silver grains located in a particular organelle structure m. So that the N_m statistic becomes approximately Gaussian, there should be at

least 8-10 silver grains measured in any one organelle type. The Land and Salpeter routine minimizes the sum of the squared errors between the actual silver grain measurement statistics N_m and a linear weighted sum of the hypothetical estimates of the underlying sources of radioactivity. The squared-error statistic that is minimized is generally assumed to be Chi-squared, and it is for this reason that experiments are designed so that there are a minimum of 8-10 silver grains in any one organelle. The distribution of radioactive-source estimates that minimizes the squared error statistic becomes the best guess of the distribution of the underlying radioactivity.

One of the important features of the mask-analysis algorithm is that data derived from any one micrograph are not preserved and processed individually for each EM slice. Rather, the silver grain measurement points are added within any one organelle structure across all of the slices to generate the single measurement statistic N_m. Also, the transition probabilities are generated not for each slice geometry separately, but rather by applying to all of the different micrographs the mask method and then averaging these together to get estimates of the transition probabilities. It occurred to us that since the geometry of every EM slice is different, algorithms which use the EM data obtained from each micrograph separately, may have a higher performance than those algorithms which average the measurement points together. Also, in using the mask method there are many overlays which must be applied to the large number of micrographs in order to obtain estimates of the transition probabilities. The errors in the radioactive-intensity estimates are due partly to statistical variations in the table of transition-probability estimates. These vary due to the random nature of the micrograph geometries and the limited sampling of the hypothetical source-grain pairs. Another issue which is of concern to us is that the mask method must be modified as the geometries of the cellular organelle structures change.[6,7] Of particular difficulty are linear source compartments like cell membranes. Modifications to the point-spread function and mask setup must be included for proper utilization of the mask-analysis algorithm.[7]

From our study we have identified an algorithm using the technique of maximum-likelihood estimation based on Poisson emission and measurement statistics. Unlike present algorithms, our's uses knowledge of the number of measurements as well as the particular source geometry from which these measurements arose and then processes the data from each micrograph separately rather than the summed count statistic N_m. It maximizes the likelihood function of the data based on a recursive algorithm which is a nonlinear functional of the observed data and requires no minimum data collection in order for it to provide valid estimates of the radioactive intensities. Our algorithm does not use the mask analysis, nor does it generate the table of transition probabilities; what it requires is the form of the universal point-spread function describing the beta-particle emission spread. The maximum likelihood estimation scheme does not depend on the source geometries; particular geometries are included as side constraints.

The new maximum-likelihood algorithm which we have developed for analyzing electron-microscopic autoradiographs is based on maximizing the likelihood of observing the data by using a recursive procedure first introduced by Dempster, Laird and Rubin.[8] This approach was then used by Shepp and Vardi[9] and Snyder and coworkers[10,11] for estimating radioactivity distributions in positron-emission tomography. The method we propose utilizes information about the detected locations of the silver grain measurements to which the probability-density function representing the measurement uncertainty resulting from emission spread is applied. The algorithm then recursively computes the most probable locations of the radioactive sources based on the maximum-likelihood method of statistics. The universal curves worked out empirically by Salpeter and coworkers[1,3] and analytically by us for isotopes used in autoradiography are used to describe the probability density of the measurement uncertainties. It exploits the a priori knowledge that we obtain from source modeling of the silver-grain emissions and measurements; i.e., the Poisson statistical distribution of the emissions and the limit in measurement precision due to the finite silver-grain size and image spread. The results indicate that the data-acquisition requirements for the maximum-likelihood algorithm are more extensive than those necessary for the mask-analysis algorithm, although our method does lend itself to computer-assisted data acquisition. The wide variation in geometries in the different micrographs dictates that the measurements from each micrograph slice must be processed individually before estimates of the radioactive intensity within particular structures are derived from the array of micrographs.

1. M. M. Salpeter, and L. Bachmann, "Autoradiography," in Principles and Techniques of Electron Microscopy, Biological Applications, M. A. Hayat, ed., Van Nostrand Reinhold, New York, 1972.

2. B. Land, and E. E. Salpeter, "Basis for Computer Program for Mask Analysis of EM Autoradiographs," Journal of Cell Biology, vol. 76, p. 142, 1978.

3. M. M. Salpeter, F. A. McHenry, and E. E. Salpeter, "Resolution in Electron Microscopic Autoradiography - IV; Application to Analysis of Autoradiographs," Journal of Cell Biology, vol. 76, pp. 127-145, 1978.

4. N. M. Blackett, and D. M. Parry, "A New Method for Analyzing Electron Microscope Autoradiographs Using Hypothetical Grain Distributions," Journal of Cell Biology, vol. 57, p. 9, 1973.

5. M. A. Williams, "Electron Microscopic Autoradiography: Its Applications to Protein Biosynthesis," in Techniques in Protein Biosynthesis, P. N. Campbell and J. R. Sargent, eds., vol. 3, Academic Press, London and New York, 1973.

6. N. M. Blackett, and D. M. Parry," A Simplified Method of Hypothetical Grain Analysis of Electron Microscope Autoradiographs," Journal of Histochemistry and Cytochemistry, vol. 25, no. 3, pp. 206-214, 1977.

7. M. M. Salpeter, C. D. Smith, and J. A. Matthews-Bellinger, "Acetylcholine Receptor at Neuromuscular Junctions by EM Autoradiography Using Mask Analysis and Linear Sources," Journal of Electron Microscopy Techniques, vol. 1, pp. 63-81, 1984.

8. A. D. Dempster, N. M. Laird, and D. B. Rubin, "Maximum Likelihood from Incomplete Data Via the EM Algorithm," Journal of the Royal Statistical Society, vol. B-39, pp. 1-37, 1977.

9. L. A. Shepp, and Y. Vardi, "Maximum-Likelihood Reconstruction for Emission Tomography," IEEE Transactions on Medical Imaging, vol. MI-1, pp. 113-121, 1982.

10. D. L. Snyder, and D. G. Politte, "Image Reconstruction from List-Mode Data in an Emission Tomography System Having Time-of-Flight Measurements," IEEE Transactions on Nuclear Science, vol. NS-30, pp. 1843-1849, 1983.

11. D. L. Snyder, "Utilizing Side Information in Emission Tomography," IEEE Transactions on Nuclear Science, vol. NS-31, pp. 533-537, 1984.

E-9. Maximum-Likelihood Estimation of Auditory Nerve Fiber Responses

Personnel: M. I. Miller, BCL
W. R. Bosch, M.S., Computer Systems Laboratory
C. E. Molnar, Sc.D., Computer Systems Laboratory

Support: RR 01380
GM 07564
RR 01379

Many investigators have inferred details about intra-cochlear mechanisms by collecting data from the responses of single cochlear nerve fibers. These histograms are in general distorted by the existence of neural refractoriness; that is, the occurrence of a spike decreases the likelihood of a succeeding spike. Gray[1] demonstrated that the relative frequency of discharge conditioned on the time r since a previous spike rises monotonically with r and levels off after 20-25 msec. Gray interpreted this as indicating a gradual recovery of the nerve fiber's excitability over an approximately 25 msec interval following a spike discharge. He concluded that the conventional PST histogram reflected the combination of both the characteristics of the stimulus related function and the refractory characteristics of the nerve fiber resulting in the observed recovery effects. More recently, Gaumond and coworkers[2] have demonstrated significant differences between post-stimulus-time (PST) histogram estimates and estimates of the stimulus related function which have compensated for the recovery based distortion. Johnson and Swami[3] have shown that for simulated point-process models of neural discharge

which contain recovery functions that are similar in form to those measured by Gray and Gaumond, distortion is introduced that depends on both the signal being estimated and the recovery function.

For any studies which formulate mathematical and physical models of the cochlea based on neural discharges, it would be desirable to have histograms for which the recovery related distortion has been removed. Gaumond has developed and applied a method for this compensation by separating post-spike recovery from the important stimulus related function that results from intracochlear mechanics. His model for neural discharge basically contains two components. The first results from the excitation of the fiber, which is closely related to the mechanical motion of cochlear structures and the resulting action of the hair cells. The second component is related to the refractory properties of the nerve fiber and results in the neurons demonstrating recovery effects; i.e., an increase in the probability of discharge as the time since the previous spike increases. He denotes these functions as s(t) and r(r) respectively and demonstrates that a reasonable model for the probability of discharge of the nerve fiber at time t is the product of these two functions. From this model, estimates can be derived for the s(t) and r(r) functions separately by maximizing the joint likelihood equations of having observed the neural event process. The likelihood equations of Gaumond that arise are based on a Markov-chain model of neural discharge in which the probability of transition from a state in the Markov-chain is dependent on both the acoustic stimulus during that time (s(t)) and on the time since the previous discharge of the nerve fiber (r(r)). The equations that must be maximized are quite complex and to date a closed form solution for both s(t) and r(r) has not been identified. In order to get explicit estimates of the stimulus related function s(t) from the likelihood equations, Gaumond first obtains separately derived estimates of the recovery function r(r), and than maximizes the equation with respect to s(t) based on the previous estimate of r(r).

Under the assumptions of the Gaumond model for separating the refractory related aspects of neural discharge from their time-varying rate of discharge due to the applied stimulus, Johnson and Swami[3] have taken an alternative approach to solving for the maximum-likelihood estimate (MLE) of s(t). Assuming an a priori knowledge of the recovery function r(r) they have derived the likelihood equation of the observed histogram based on an intensity description of the point process. The key concept for this alternative approach is that the Markov-chain can be considered as a self-exciting point-process in which the intensity depends on response of the nerve fiber. Following Johnson's previous work,[4] Johnson and Swami compute what they call the "maximum-likelihood PST histogram" of the responses of a model neuron to a periodic stimulus which compensates for the distortion introduced by the relative refractoriness of neural discharge. They define relative refractoriness to occur when the recovery function is known and is non-zero for all r, they show their histogram estimate to be an unbiased estimate of s(t); Johnson and Swami conclude that the distortions introduced by relative refractory effects are removed. They note, however, that this technique can not remove the effects of absolute refractoriness (i.e., the distortion introduced when the recovery function r(r) is zero).

The new approach which we have established has been motivated by the joint estimation equations of Gaumond under the condition that there is not a separate a priori knowledge of the recovery function r(r). If in different nerve fibers and under varying stimulus conditions the recovery function changes ,then an algorithm based on an a priori knowledge of r(r) derived from a previous estimation procedure is unacceptable. A scheme which from a single data set collected under a single stimulus condition provides estimates for the recovery function r(r) and the stimulus-dependent function s(t) jointly is therefore invaluable. In order to solve the likelihood equations for s(t) and r(r) simultaneously when the recovery function is not known, we have formulated the estimation problem using an intensity description. This approach has allowed us to independently verify the MLEs derived by Gaumond and coworkers[2] under conditions when the recovery function is known. By maximizing the likelihood-function with respect to s(t) under the constraint that the stimulus-related function s(t) is periodic we have also been able to derive estimates of the stimulus-dependent cochlear output function which does not suffer from absolute recovery related distortion in the same way as Johnson and Swami's recovery corrected PST histogram does. The technique of deriving MLEs subject to constraints, has been recently used and elaborated by Snyder.[5] Finally, by adopting an intensity description of the process we have been able to adopt a recursive algorithm, introduced in the statistics literature as the "EM" algorithm,[6] for deriving the maximum-likelihood estimates of both the stimulus related function s(t) and the recovery-related components in the response histograms.

We are excited about the suitability of the recursive algorithm for the removal of the distortion in cochlear histograms under conditions when the recovery function is unknown. This algorithm has been studied extensively for maximum-likelihood estimation in positron-emission tomography and has desirable global convergence properties. For maximizing the exponential family (Poisson as an example) of likelihood equations the recursive algorithm will in general converge. We show that under very mild conditions a unique maximizer of the likelihood equations arising from neural refractoriness exists and starting from any initial estimate the recursive algorithm will converge to that maximizer.

1. P. R. Gray, "Conditional Probability Analyses of the Spike Activity of Single Neurons," Biophysical Journal, vol. 7, pp. 759-777, 1967.

2. R. P. Gaumond, C. E. Molnar, and D. O. Kim, "Response of Cochlear Nerve Fibers to Brief Acoustic Stimuli: Role of Discharge History Effects," Journal of the Acoustical Society of America, vol. 74(S), pp. 1392-1398, 1983.

3. D. H. Johnson, and A. Swami, "The Transmission of Signals by Auditory-Nerve Fiber Discharge Patterns," Journal of the Acoustical Society of America, vol. 74, no. 2, pp. 493-501, 1983.

4. D. H. Johnson, "The Relationship of Post-Stimulus Time and Interval Histograms to the Timing Characteristics of Spike Trains," Biophysical Journal, vol. 22, pp. 413-430, 1978.

5. D. L. Snyder, "Utilizing Side Information in Emission Tomography," IEEE Transactions on Nuclear Science, vol. NS-31, pp. 533-537, 1984.

6. A. D. Dempster, N. M. Laird, and D. B. Rubin, "Maximum Likelihood from Incomplete Data Via the EM Algorithm,," Journal of the Royal Statistical Society, vol. B39, pp. 1-37, 1977.

E-10. An Automated System for the Monitoring of Patients with Epidural Electrode Arrays

Personnel: J. S. Massey, BCL
S. Goldring, M.D., Neurological Surgery
E. M. Gregorie, M.D., Neurological Surgery
P. Lombardo, B.A., Neurological Surgery

Support: RR 01380
NS 14834

The purpose of this project as detailed in PR 18, E-14 and PR 19, E-9 is to develop a system which will permit simultaneous recording of the EEG and somatosensory evoked response (SER) from patients in whom epidural electrode arrays have been implanted for the purpose of localizing an epileptogenic focus.

The CAESER system (computer-aided extraction of somatosensory evoked responses) consists of a sixteen-channel EEG amplifier, a sixteen-channel analog-to-digital converter, a Digital Equipment Corporation (DEC) MINC microcomputer, and a video module which displays the evoked responses on standard television monitors.

Initially, the CAESER system used the sixteen Grass Instrument Company 8A5 EEG amplifiers in our EEG machine. This meant that the EEG machine could not be used to monitor the patient for seizures while SER's were being acquired. In August 1983, sixteen Grass Model 12 Computer Interface Amplifiers were installed in the CAESER system, making it possible to obtain patient SERs while simultaneously monitoring the patient for seizures.

During the past year, a number of improvements were made to the original version of the software. The user is now able to view the signals coming from the EEG amplifiers on the CAESER displays, so that adjustments can be made to the amplifier settings before the acquisition of SERs begins. The software variables which the user sets for each run are now reported in a clearer fashion, new informational messages have been added

at several points, and error messages have been expanded and clarified. In addition, the MINC's original LSI-11/02 processor was replaced with a DEC LSI-11/23, resulting in a noticeable improvement in system performance.

The system has been used to gather SER data from ten patients since December 1982. In four of these cases, SERs were obtained simultaneously with seizure monitoring.

F. Resource Development Activities

Resource development activities are those which contribute to the goals of more than one major program of the laboratory, address the needs of individual users who can benefit from the expertise of the BCL staff and the inventory of computing and specialized test equipment, or identify new technologies which may become appropriate foundations for new experimental tools. Service to users does not follow the usual computation-center pattern with an established fee schedule and a highly centralized facility. Rather, senior laboratory staff members consider requests for assistance from investigators who must address a particular biomedical computing problem. If an appropriate technology exists, investigators may be referred to commercial vendors or fee-for-service organizations when these are available. In other cases, problems may be approached by the laboratory provided that the effort complements other activities of the laboratory. Many times the project can be assigned to a staff member with appropriate experience and completed in a short time. The investigator then has his or her results, and a short note describing the work will appear in the annual report and perhaps the open literature. A few projects, however, may develop into major initiatives within the laboratory. Most of the major projects began in this fashion and the opportunities that supporting activities provide are valued.

The broad spectrum of projects reported on in this section may be categorized as biomedical applications, system development aids, digital hardware designs, and ad hoc studies. The biomedical applications represent new initiatives in which basic explorations are being conducted, some having potential for becoming major, long term programs.

System development aids primarily benefit BCL staff, but may also be used by others. Examples include microprocessor development support, RSX-11 system enhancements and extensions to the MASSCOMP raster graphics workstation. System software developments reported here also are widely utilized in a variety of projects.

Many digital hardware designs are one-time, special purpose projects. Others may have wide appeal and construction of multiple copies is envisioned, examples being the TERRANET local network and the image buffer.

The topics of the studies reported in this section are quite varied. Some are theoretical and address a highly specific problem; others are more properly thought of as feasibility studies.

F-1. Microprocessor Development Support

Personnel: S. M. Moore, BCL
R. E. Hermes, BCL
S. R. Phillips, BCL

Support: RR 01380
HS 03792

Locally developed FORTRAN-based cross-assemblers (FOCRAS) and intelligent consoles continue to play important roles in hardware and software development activities for 8-bit microprocessor-based systems. Porting of FOCRAS to a PDP-11/RSX system was completed and verified by transferring TERRANET software from a TI-980 to the RSX system. Future software will be done under RSX, FOCRAS support on the TI-980 system will be discontinued.

Program development support for 16-bit Motorola M68000 (M68K) exists in many forms. The UNIX V7 operating system has been ported to the M68K based VERSAmodule system (F-8) which supports program development. C language programs can be entered, compiled and run directly on the system. C language compilers and cross-assemblers also exist on both PDP-11/34 and VAX-750 systems for developing stand-alone software for the M68K.

Computer controlled PROM programming capabilities are currently limited to 2 Kbyte EPROMs using the Intelligent Console and current FOCRAS software. Larger EPROMs can be programmed by reading and concatenating data from several smaller PROMs and then transferring to larger PROMS using the DATA I/O universal PROM/PLA programmer. The Data I/O programmer will be integrated into the FOCRAS system under RSX to allow larger PROMS to be programmed automatically.

F-2. Information Systems Group

Personnel: J. R. Cox, Jr., BCL and Computer Science
G. J. Blaine, BCL
S. M. Moore, BCL
S. R. Phillips, BCL
L. J. Thomas, Jr., BCL

Support: HS 03792
Washington University

The Information Systems Group provided the collaborative structure within which participants from the Department of Computer Science, the Computer Systems Laboratory, the School of Medicine, and the Biomedical Computer Laboratory addressed the development of a methodology for the design of composite medical-information systems. The development activities were divided into four major categories: model, design studies, implementation and Neonatology Database. The more theoretical portions of the work on a design methodology fall in the first category and the more applied tasks in the second. The Neonatology Database provided a relevant context for testing concepts, models and implementations.

The primary goals of the group, supported by the NCHSR research grant HS 03792, are now complete. The accomplishments are summarized here for reference:

1) a powerful data model, ADS;

2) implementation of a data language consistent with the ADS model;

3) experiments with special hardware implementations for ADS memory;

4) testing in a clinical database application;

5) performance studies of three software implementations of ADS;

6) demonstration of ADS as an intermediate language for database translation.

A final report contains specific details of these accomplishments and future plans.[1]

1. J. R. Cox, Jr., and K. F. Wong, "A Medical Information Systems Design Methodology," HS 03792 Final Report, July 1984.

F-3. Studies in the Design of a Coprocessor for Pattern Matching

Personnel: S. M. Moore, BCL
G. J. Blaine, BCL
J. R. Cox, Jr., BCL and Computer Science

Support: RR 01380
HS 03792

A version of ADS was implemented in C under UNIX to provide experimental tools for:

1) studying the feasibility of implementing a truly usable version of the ADS data model,

2) gathering initial workload and performance data to use as a guide for the design of a production version and customized hardware,

3) trying different algorithms, and

4) studying software portability issues.

Examination of the performance of the ADS system suggested that a hardware pattern matcher might be necessary to speed operation in a production version of ADS. An algorithm was found which allows the data to be searched in time that is linear with the size of the data, and several architectures for implementing this algorithm were studied. One architecture was used as the basis for a processor which was designed and built using commercially available integrated circuits and wire-wrap technology.

The search processor serves as a coprocessor in the Motorola M68000 (M68K) VERSAbus system (F-8). In addition to the search processor, a dual-ported memory was built to provide I/O for the processor. One port can be accessed by the M68K system through the VERSAbus and the other by the search processor.

A simple data retrieval system was designed on the M68K system using the pattern matcher as the search mechanism. A similar system was built which implemented the search algorithm in software. Comparisons between the two systems showed that the hardware search was 500 to 1200 times faster than the software search on the M68K. The pattern matcher searched memory 85 to 180 times faster than the ADS implementation on a VAX-750 on a per node basis. Other comparisons showed the speed of the pattern matcher to be nearly equivalent to the speed of other hardware-based searchers.[1]

1. S. M. Moore, "A Pattern Matcher for Searching Binary Trees," Master of Science thesis, Department of Electrical Engineering, Washington University, St. Louis, Missouri, May 1984.

F-4. An Experimental Local-Area Network: TERRANET

Personnel: S. M. Moore, BCL
G. J. Blaine, BCL
J. R. Cox, Jr., BCL and Computer Science
R. E. Hermes, BCL
S. R. Phillips, BCL
D. F. Sandel, BCL
D. A. Schwab, BCL

Support: RR 01380
Computer Services Corporation
Washington University

In the past year, TERRANET has gone from a successful experiment in local-area networking to an important part in the day-to-day operations of BCL. TERRANET provides terminal-to-computer and computer-to-computer communications for most of the time-sharing computer systems in the laboratory. The current network configuration utilizes each of the possible 30 stations. These stations include 15 terminals, 11 computer connections to 7 different machines, and 4 modem or other network gateway connections. Usage of the network is quite heavy and has indicated that the overall number of stations in the system should be increased. Design studies are now in progress to determine how best to realize this increase. Possibilities include a second TERRANET network or increasing the number of stations on the current network by increasing the capacity of the network or by decreasing the data rate per channel.

No major revisions have been made in the hardware configuration of tap units or insert units. Minor changes were made to one tap unit with appropriate changes in software to facilitate modem control. Several more general software changes were made to improve flow control in tap units connected to modems, terminals, and serial printers. Other software modifications were done for an experiment which demonstrated that TERRANET could be connected to and implement the protocol of the GANDALF switch at the main computing facilities on the Hilltop Campus. All TERRANET software was moved from the TI-980 system to the PDP-11/RSX system to take advantage of better software development and backup utilities available under RSX.

Experiments for integrating voice with data communication on the network were conducted using the test bus (PR 19, F-6). Three tap units were modified to accommodate the voice transmission. Two units were used for communication while the third unit was used to monitor the network and to evaluate the stability of the system. Initial results show that voice communication is possible with the current design, but more revisions may be necessary to decrease noise and the cost of the tap units.

Higher level software to provide network services is currently being developed. A PDP-11/UNIX system will be used to monitor network activity. Station-to-station connect time will be measured and used to determine future tap unit allocation as the TERRANET system expands. UNIX file

transfer utilities were modified at the Hilltop Campus to recognize TERRANET and will be used at BCL. Software is currently being developed to allow file transfer between RSX- and UNIX-based systems over TERRANET channels.

F-5. Inter-System Communication for Data Transfer

Personnel: G. J. Blaine, BCL
J. D. Gorman, BCL
K. H. Haserodt, M.S., Computer Science
R. E. Hermes, BCL
E. W. Kiebler, M.S., Computer Systems Laboratory
M. I. Miller, BCL
D. W. Stein, Jr., BCL

Support: RR 01380
Washington University

A working group was formed to discuss mechanics for data transport between various host computing systems, within our local Resource. Media transfers (9-track magnetic tape, floppy disk, and hard disk) have been primarily used for this purpose.

The following types of information exchanges were identified:

1) binary data files to support acquisition analysis and display of medical images;

2) electronic mail for both campus and national collaborators;

3) remote program execution to allow data submission, application, execution and remote harvesting of results.

The most immediate needs are based on system resources which include, VAX-11/750, 4.2BSD UNIX; VAX-11/750, VMS; PDP 11/34, 4.2BSD UNIX; PDP-11/34, RSX-11; LSI-11/23, RT-11; and MASSCOMP 500, UNIX-masscomp. A concensus suggested a first level solution to be based on the following design:

Physical Layer = serial, 9600 bps, asynchronous, RS-232, full duplex;

Data Link Layer = small packets, error detection and retransmission.

UNIX uucp services provide sufficient flexibility for data transfers between UNIX systems, likewise, DECNET is a proven means for communication between DEC operating systems. However, the local predominance of both

UNIX and RSX-11M necessitates a data transmission link between these systems as well.

The RSX-11M terminal driver was studied to determine the feasibility of implementing data transfers via serial communication lines on a PDP 11/34. The driver was found to have limitations including input character buffers of limited size (36 characters), and the need for system interrupts on a character by character basis. Significant modification of the terminal driver could circumvent these limitations so that efficient block transfers of data could be accomplished. Alternatively, data transfers of small data packets (less than 20 characters) seems practical with no driver changes provided sufficient protocols are provided for data transmission, verification and correction.

Recent acquisition of an inter-system communication software package called KERMIT may also prove helpful. KERMIT has been used elsewhere for communication between dislike systems, including RSX-11M, VMS, and UNIX. This software is known to work for transmission of ASCII character data, but tests are still to be conducted to determine its suitability for binary data transmission.

F-6. A Picture Communication System for Radiology

Personnel: G. J. Blaine, BCL
J. C. Chabut, BCL
J. R. Cox, Jr., BCL and Computer Science
R. L. Hill, BCL and Radiology
R. G. Jost, M.D., Radiology
A. Kumar, B.Tech., Radiology
S. R. Phillips, BCL
A. P. Rueter, B.S., Radiology
C. D. Shum, BCL

Support: RR 01380
RR 01379
Mallinckrodt Institute of Radiology
Washington University

A pilot cable system to transport analog and digital radiology pictures and support terminal-to-computer digital data transmission has been designed and installed (PR 19, F-7, F-8). A dual-cable 400 MHz system utilizes "off-the-shelf" cable television components to provide approximately 50 channels, achieved by frequency multiplexing channels of 6 MHz each. The system provides a workbench environment for the evaluation of commercial digital transmission equipment in addition to supporting experiments related to digital picture networking and archiving studies. The topology is illustrated in Figure 1.

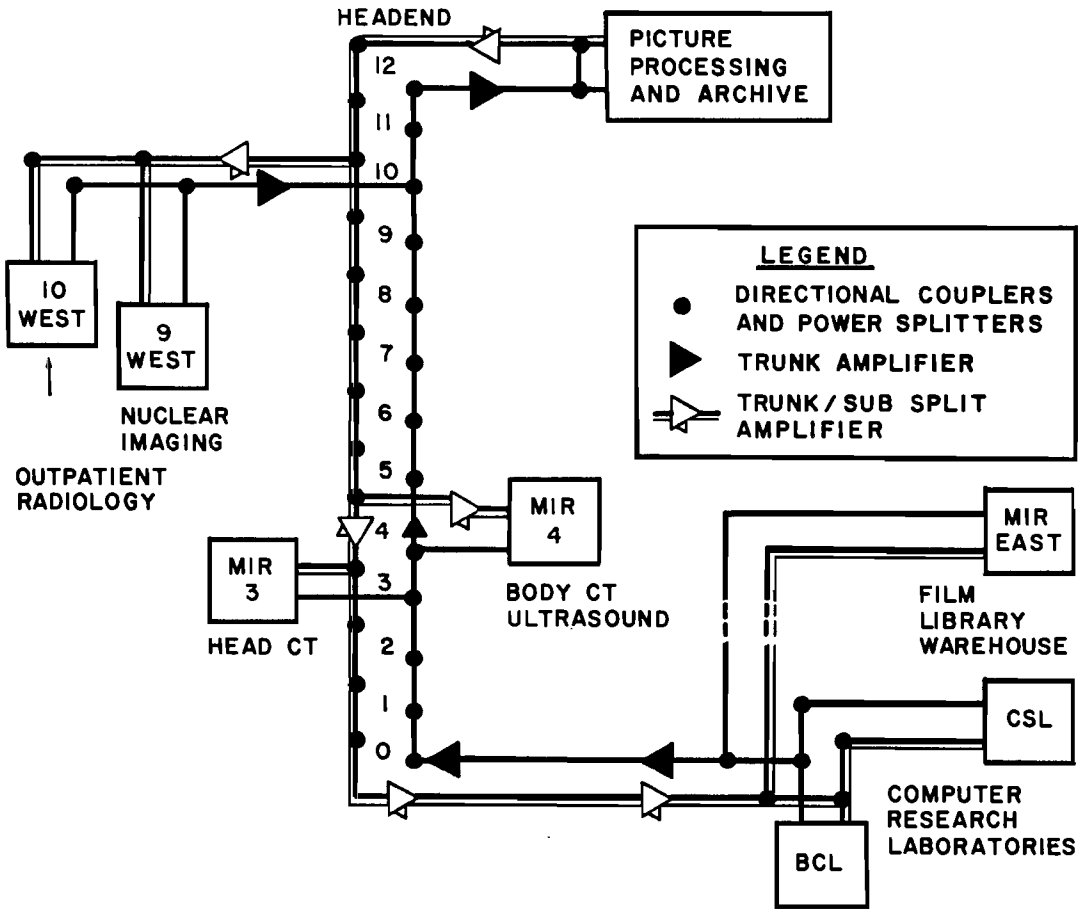

Figure 1. PACS workbench picture network block diagram illustrating topology of the MIR broadband local area picture network.

Over the past year, studies and subsequent designs have been directed at communicating radiological images using channels based on frequency division of the 400 MHz channel. Multiple shared-transmit/receive channels were shown to have favorable cost-delay characteristics.[1] Most of the MIR efforts (F-11) have been directed at accessing and displaying images which are stored in a database, whereas the focus of our activities has been upon the digital and analog transmission and reception of images.

A variety of analog modulators and demodulators for both video transmission and reception were obtained and have been tested to determine their bandwidth limitations.[2] Such bandwidth limitations were demonstrated to have a direct effect upon the transmission and reception of picture detail.

The lack of readily available high-speed modems, at reasonable cost, has fostered exploration of novel approaches to the problem. Two approaches to greater than 1 Mbps rates are currently being explored. The first utilizes commercial TV modulators and demodulators with a specialized integrated circuit chip set developed for baseband digital communication applications. The second is based on the extension of a product by a recently formed data communications company. A pair of the proprietary modems have been provided for one evaluation. In order to test these digital communications schemes, a "bit error tester" has been designed and fabricated and is now under evaluation. Future digital tests will involve consideration of bandwidth, phase, and multiple device effects.

1. C. D. Shum, "Design Analysis of a Wideband Picture Communication System," Master of Science thesis, Department of Computer Science, Washington University, St. Louis, Missouri, December 1983.

2. J. C. Chabut, "Testing Modulator/Demodulator Frequency Response," BCL Working Note No. 57, April 1984.

3. J. R. Cox, G. J. Blaine, R. L. Hill, R. G. Jost, and C. D. Shum, "Some Design Considerations for Picture Archiving and Communication Systems," IEEE Computer, vol. 16, no. 9, p. 41, August 1983.

F-7. Data Compression Studies

Personnel: J. G. Dunham, BCL and Electrical Engineering
S. E. Elnahas, M.S., Electrical Engineering
R. G. Jost, M.D., Radiology

Support: RR 01380
RR 07054
Mallinckrodt Institute of Radiology
Washington University

In radiology, the introduction of new technology has increased the number of images stored in digital form. Most studies are still recorded on film, but digitally generated examinations are becoming more common. Typically, digital exams have a greater number of images per study, so that half the images produced in some departments today are already generated in digital form. This trend toward digital imaging in radiology will continue and should accelerate as conventional examinations find their way into digital form. As radiologists turn their attention to problems associated with storing and transmitting these digitally generated images, the need for data compression will become increasingly important.

A wide spectrum of images is found in a radiology department. The differences among modalities are significant enough to suggest that different data compression techniques may be appropriate for different image classes. In order to study the differences among and within various image modalities, we have developed[1] an extensive database of digital diagnostic images for general compression studies. Thirteen different classes of images are included in the database to represent several imaging modalities including CT, nuclear medicine, ultrasound, and MRI.

In a preliminary investigation (PR-19), the major classes of data compression were reviewed with respect to their suitability for picture archiving and communication systems (PACS) in radiology. In a PACS environment, noisy compression provides high compression ratios (20:1, 30:1). The distortion introduced by noisy compression techniques has yet to be evaluated clinically for different classes of radiological images and diagnostic modalities. On the other hand, noiseless compression provides perfect image reproductions with low compression ratios (2:1, 3:1). We have investigated[1] the possibility of reducing the gap of compression ratios between noisy and noiseless systems. The compression limits of linear predictive coding, when followed by entropy coding, are determined by estimating the noiseless compressibility of the input images. Arithmetic coding as well as Huffman coding are considered for the entropy coding part. Formulation of the problem of designing optimal linear predictors has been studied and solutions discussed. In general, linear least squared-error (LLSE) predictors do not necessarily minimize the entropy of the predictive coder output. However, the performance of most fourth-order predictors is very close to that of optimal predictors. For LLSE prediction, there is no need to consider predictors of order higher than four for all of the image classes in the database. This is an important result when considering the practical implementation of LLSE

predictors. The use of image training sequences for the design of LLSE predictors has been proven experimentally to be successful and the results obtained when predictors are used outside the training sequences are promising. On the average, one can expect compression ratios between 2.0:1 and 6.3:1 from systems employing arithmetic coding while one can expect ratios between 11.7:1 and 3.8:1 from systems employing Huffman coding.

With nonlinear block predictive coding, we have combined[2] noisy and noiseless compression systems in a novel way that may have a potential impact on the PACS environment. The approach does not ignore the investment in noisy compression systems that can provide attractive high compression ratios. It may also provide a technical solution to the suitability issue, from a clinical standpoint, of noisy compression systems by allowing a means for perfect reproduction of the input images. We have investigated the application of adaptive fast discrete cosine transform (AFDCT) coding to compression of MRI and CT images. The subjective quality of image imperfect reproductions from the AFDCT system, at a code rate of one bit/pixel, is very promising and prompts future research on the transform coding of diagnostic images and the clinical evaluation of these systems. The off line storage requirements for archiving MRI and CT images are reasonably reduced by the noiseless block nonlinear predictive coding system. The on line performance, however, seems to be bounded by that of linear predictive coding. We conjecture that, linear systems using predictive coding techniques, determine the noiseless compressibility of diagnostic images in radiology.

1. S. E. Elnahas, R. G. Jost, and J. G. Dunham, "Compression of Digital Diagnostic Images in Radiology," Proceedings of the ACR 8th Conference on Computer Applications in Radiology 1984, St. Louis, Missouri, May 23-25, 1984, in press.

2. S. E. Elnahas, "Data Compression," D.Sc. Dissertation, advisor: J. G. Dunham, in preparation.

F-8. M68K/VERSAbus Hardware Support

Personnel: S. M. Moore, BCL
K. H. Haserodt, M.S., Computer Science

Support: RR 01380
HS 03792

The M68000-based VERSAmodule system was used as the host system for running pattern matcher experiments (F-3). As previously reported (PR 19, F-10), the system is capable of running the UNIX V7 operating system. User

access is gained through two serial ports, one connected to a terminal as the console and the second connected to TERRANET.

Minor modifications were made to the VERSAmodule system to accomodate the pattern matcher. A dual-ported memory was designed and interfaced to the system through the VERSAbus. A PLA on the VERSAmodule computer board was changed to allow the system to recognize the additional memory. The pattern matcher interfaces to the M68K system through a parallel port which already existed on the VERSAmodule computer board. The parallel interface is used only for control information; all data are transferred between the VERSAmodule system and pattern matcher through the dual-ported memory.

When not used for pattern matcher experiments, the dual-ported memory can be used as data space for user programs. The memory is placed outside of the normal UNIX address space and can only be addressed when a user program informs the system of its presence. The memory is not designed to respond to byte references and so can only be used by programs which access the memory on a word (16 bit) basis.

F-9. Systems Support for Programming and Image Processing

Personnel: R. E. Hermes, BCL
S. Husodo, BCL
S. M. Moore,BCL
R. J. Paisley, BCL
S. R. Phillips, BCL
D. W. Stein, Jr., BCL

Support: RR 01380

Hardware and software support of programming and image processing continues to be an important Resource activity (PR 19, F-11). Most of our scientific programming is supported by a PDP 11/34 running RSX11M. The system is configured with disk and tape storage devices which are predominant in the local computing community. This allows for data transfers from other research labs to the BCL via a common magnetic storage media. The system also includes a Lexidata 3400 color display system with a resolution of 640 by 512 pixels. Recent development of easy to use display software on this system has simplified the common problem of image display after the data is processed on the system.

The system, although limited in memory and computational capacity, supports several simultaneous users doing program entry and debugging. Programs which require large amounts of system resources are run as background processes, often overnight. Programs which require extensive machine time can be run on a second PDP 11/34 running RSX11M. This second processor is available to run RSX11M or UNIX depending upon user needs.

Additional computer and display capability is provided by a MASSCOMP MCS-500 system (F-10). Efforts are underway to provide means for data transfer between all systems via serial communication (F-5). Display utilities similar to those used on the Lexidata are being developed so that a comparable user environment exists on both image display systems.

F-10. MASSCOMP Workstation System

Personnel: R. E. Hermes, BCL
G. J. Blaine, BCL
K. H. Haserodt, M.S., Computer Science
S. Husodo, BCL
R. J. Paisley, BCL
F. U. Rosenberger, BCL, and Computer Systems Laboratory

Support: RR 01380

To further develop image processing support, the laboratory has acquired a MASSCOMP MCS-500 system. The MASSCOMP system is based upon a Motorola 68000 processor capable of running UNIX System III. With a benchmark performance comparable to that of a VAX 11/750, the system can support a number of simultaneous users as well as support many of the computational needs of those doing image processing and display.

The system employs two 10 MHz 68000 processors in the CPU and for I/O control. The CPU resides on a proprietary system bus with one megabyte of system memory which may be expanded to six megabytes. The system bus is extended to a industry standard Multibus which can support many different peripheral controllers as well as being suitable for interfacing locally designed subsystems or specialized processors.

The current configuration consists of a chassis housing the system busses and processor, a 27 megabyte Winchester disk, a 1 megabyte floppy disk drive, and four serial communication lines. An additional 52 megabyte Winchester disk will be added soon.,

A vast amount of software is available on the system, including a large graphics and graphing library, a menu system called Quick Choice, and all of the software development aids found in most UNIX systems. Efforts are underway to provide system users with convenient methods for displaying images and for communicating with other systems.

F-11. PACSV: A 512 x 512 x 8 Image Buffer

Personnel: A. Kumar, B.Tech., Radiology
G. J. Blaine, BCL
J. R. Cox, Jr., BCL and Computer Science
R. L. Hill, BCL and Radiology
R. G. Jost, M.D., Radiology
A. P. Rueter, B.S., Radiology

Support: RR 01380
RR 01379
Mallinckrodt Institute of Radiology
Washington University

PACSV (for Picture Archiving and Communication System Viewing-Station) was designed in the first quarter of 1983. During the year reported here, a prototype was built to prove the design. PACSV addresses the need for an inexpensive frame-buffer and viewing-station in the PACS network that is taking shape at the Mallinckrodt Institute of Radiology (MIR). Its performance specifications are as follows:

1. It can store and display a 512 x 512 x 8 image.

2. The image can be read from an input environment at a maximum rate of just over 20 x 10^6 bits/sec. In other words, an image can be read in approximately 100 milliseconds.

3. An image can be transmitted from the PACSV to an output environment at the same rate.

4. Picture display is not interrupted by data reads or writes.

5. PACSV can be configured to accept any input and output environment by replacing the input module, the output module, and a ROM chip. Two input modules have been designed, built, and tested, with PACSV. One accepts a 9600 baud RS232 signal; the other obeys a high-speed, 32-bit-parallel, synchronous transfer protocol over a DR750 bus connected to a VAX11/750.

6. The composite-video output of PACSV, capable of driving a standard TV monitor, respects the EIA standard RS330 with only two minor deviations.

The PACSV chip-count is 92 integrated circuits (not including any input or output modules). Of these, 32 are 64K dynamic RAMS with an access time of 200 nanoseconds. The memory cost is $210 with the remaining chips costing another $190.

At the heart of PACSV lies a ROM-based controller, a very simple microprogrammed machine that runs at 20 MHz and puts out a sequence of 32 control words every 1.5 μsec. The following major functions are performed by this cycle of 32 words:

1. Four 32-bit data words are read from the RAM frame-buffer, and packed into synchronizing-buffer register files. These four words are destined for display.

2. Selected registers are opened in the synchronizing-buffer register files to a digital-to-analog converter in the video-generation circuit.

3. A single 32-bit data word may be read from or written into the RAM frame-buffer, for data I/O.

The ROM-based controller also generates the blanking and sync signals for the video-generation circuit, and exchanges handshake signals with the input and output modules. A Motorola MC68000 microprocessor is used to initialize the system, and to conduct a dialog with the input and output environments.

F-12. Word Processing at BCL

Personnel: R. E. Hermes, BCL
R. M. Arthur, BCL
R. J. Bozesky, BCL
K. W. Clark, BCL
S. A. Gonzalez-Rubio, BCL
G. C. Johns, B.S., Computer Systems Laboratory
J. W. Matthews, D.Sc., Computer Systems Laboratory
P. E. Raith, BCL
L. J. Thomas, Jr., BCL

Support: RR 01380

Approximately two years ago, a word processing committee was formed to determine the word processing needs of the BCL and CSL. The committee cataloged an extensive list of prerequisites for a word processing system to support the technical and non-technical writing needs of the laboratories. The committee reviewed available word processing systems to determine whether any could meet our demanding and specialized needs. Unfortunately, none were found suitable.

Within the past year, several circumstances, including the imminent demise of our current word processing system, caused us to pursue the word processing issue again. The prevalence of the UNIX operating system prompted the search for a word processing system supported by UNIX. The system chosen, called MUSE, has been installed for nearly three months on the Institute VAX-11/750.

The MUSE system is capable of supporting dozens of different terminals and printers. MUSE is a menu driven and function key controlled system which provides what-you-see-is-what-you-get displays on the terminal

screen. It supports superscripting, subscripting, greek/math symbols, and underlining without the need for embedded control sequences found in most other systems. A spelling check system employs the use of a master dictionary, as well as dictionaries which can be user, site, or subject specific. Easy to use mechanisms are provided to control text formats and form generation. File management is part of the MUSE system, meaning that users do not need to know the UNIX system to manage their file directories. Output of documents is easily managed by MUSE, allowing the user to vary fonts, character spacing, and output format at print time.

MUSE is a well documented, easily learned system. MUSE users have found the system very powerful, yet simple to use. This progress report was compiled and edited in our first extensive test of MUSE's capabilities.

VI. INDUSTRIAL COLLABORATION

Industrial collaboration provides a mechanism for the deployment of laboratory developments and benefits the staff by keeping abreast of the practical considerations of reliability, maintainability, and cost.

The TERRANET system, which provides a simple low-cost interconnect to support terminal-to-computer and computer-to-computer communications for modest speeds (up to 9600 bps), is currently being produced and marketed in Japan under a licensing agreement with Computer Services Corporation (CSK), a major facilities management consulting firm headquartered in Tokyo. As part of the initial agreement, CSK supplied two evaluation systems of 10 tap-units each for installation in the Computer Science and Electrical Engineering Departments at Washington University. A follow-on research contract with CSK provided partial support of development activities which integrate voice and data transmission into the TERRANET system.

In conjunction with BCL activities in picture archiving and communications (F-6), Dr. G. James Blaine accepted an opportunity to serve for three months as a member of the Applied Technology Department within Hewlett-Packard Laboratories, Palo Alto, California.

BCL has analyzed several tens of long-term ECG recordings for a Mead-Johnson (Evansville, Indiana) sponsored "Multicenter Placebo-Controlled Study of Trazadone's Effects in Depressed Cardiac Patients." Trazadone, a recently marketed antidepressant drug, is chemically unrelated to the tricyclic antidepressants. Studies in animals showed few cardiac effects, and ECG recordings in humans in initial clinical studies showed few changes. More recent studies in humans examined the cardiac effects of trazadone in patients with pre-existing cardiovascular disease and depression. Many of these patients had good responses to depression with minimal aggravation of their underlying cardiovascular condition, although a small number of patients developed a change in ventricular ectopic activity while on trazadone. However, due to the considerable interpatient and intrapatient daily variability in ventricular ectopic activity and lack of a placebo control group in these studies, it had previously not been possible to conclusively attribute changes in ectopic activity to trazadone. The current study is designed to address the issue of the cardiac safety of trazadone. The study plans to enroll 160 patients among 8 clinical units. Four long-term ECG recordings per patient (over 2 weeks) are sent to BCL for analysis. Results are interpreted by the study's cardiologist, Roger Winkle, M.D., of Stanford University.

BCL personnel have worked closely with Biosensor Corporation (Brooklyn Center, Minnesota) to implement Argus algorithms (A-1) in a "real-time analyzer," a device to analyze the ECG rhythm of a patient who wears the small device and goes about normal activities. The device uses CMOS microprocessor technology powered with 5-day lithium batteries. Counts and waveforms of significant events are stored for subsequent telephone transmission (on demand or at suggested intervals) to a central station which plots a report for the patient's physician. Biosensor

brought a prototype of their device to BCL a year ago for intensive side-by-side debugging; BCL personnel have visited Biosensor to observe first hand their development, manufacturing, and marketing procedures. Throughout the year, BCL has provided Biosensor with a variety of digitized waveforms; Biosensor runs a digital waveform through their implementation and returns to BCL beat-by-beat results; BCL then prints a condensed plot of waveform and labels for proper evaluation.

VII. TRAINING ACTIVITIES AND SEMINARS

Training activities of the Biomedical Computer Laboratory are directed toward the goals of informing the local and national scientific communities about resource projects and facilities and of instructing a broad spectrum of people in the application of advanced computer-techniques to problems in clinical medicine and biological research. Training activities include the teaching of formal courses at the School of Medicine and the School of Engineering as well as supervision of graduate students by Laboratory staff. Both individual and small-group training about resource facilities are made available to the biomedical scientist. National workshops and symposia on topics of interest and importance to the resource and community are supported.

The bringing together of biomedical scientists, engineers, and computer scientists provides important cross-fertilization between disciplines. In these settings, students and staff find the need and opportunity to test the relevance of theory and the usefulness of technology in applications to real problems. Also, the biomedical scientists are aided in learning new techniques for acquiring useful information. To this end, some of the courses offered are addressed to biologists without strong technical backgrounds who want and need a below-the-surface appreciation of biomedical computing. Laboratory personnel also participate in regularly scheduled conferences in the clinical departments where both the biological and technological issues are examined.

Seminars and presentations relating to resource projects and applications are conducted by Laboratory staff as well as scientists and engineers from the national community. During the year the following activities were supported:

Seminars

"Reconstruction Algorithm for Time-of-Flight Assisted Positron Emission Tomographs"

September 19, 1983

David G. Politte
Biomedical Computer Laboratory
Washington University
St. Louis, Missouri

Cosponsor: Department of Electrical Engineering

"A Description of the Laboratory of Neuro Imaging"

November 22, 1983

Arthur Toga
Research Assistant and Professor in Neurology
Washington University
St. Louis, Missouri

"Coding of Speech in the Auditory Nerve"

December 12, 1983

Michael I. Miller
Biomedical Computer Laboratory
Washington University
St. Louis, Missouri
Sponsor: Department of Electrical Engineering

"Toward the Prediction of Protein Function and Structure: Applications to Oncogene and MHC Products"

April 5, 1984

Charles DeLisi
Laboratory of Mathematical Biology
National Cancer Institute
Bethesda, Maryland
Sponsor: Institute for Biomedical Computing

"The Future of Image Processing at Lexidata"

April 19, 1984

Dave Ellenberger
Lexidata Corporation
Waltham, Massachusetts

"A Pattern Matcher for Searching Binary Trees"

May 1, 1984

Steve M. Moore
Biomedical Computer Laboratory
Washington University
St. Louis, Missouri

"Experimental Evaluation of the Maximum-Likelihood Method for Reconstructing Radiotracer Distributions in Positron-Emission Tomography"

May 10, 1984

John Gorman
Biomedical Computer Laboratory
Washington University
St. Louis, Missouri

"A Preliminary Evaluation of the EM Algorithm for Estimating Parameters in Dynamic Tracer Studies"

May 17, 1984

John Ollinger
Biomedical Computer Laboratory
Washington University
St. Louis, Missouri

"Maximum-Likelihood Reconstruction for Electron-Microscopic Autoradiographs"

June 7, 1984

Michael I. Miller
Biomedical Computer Laboratory
Washington University
St. Louis, Missouri

"Maximum-Likelihood Reconstruction for Single-Photon Emission Computed-Tomography"

June 14, 1984

Donald L. Snyder
Biomedical Computer Laboratory
Washington University
St. Louis, Missouri

"Recent Results in Quantitative Ultrasonic Imaging"

June 21, 1984

R. M. Arthur
Biomedical Computer Laboratory
Department of Electrical Engineering
and
J. G. Miller
Biomedical Computer Laboratory
Department of Physics
Washington University
St. Louis, Missouri

"Picture Transmission"

June 28, 1984

John Chabut
Biomedical Computer Laboratory
Washington University
St. Louis, Missouri

"The MASSCOMP Raster Graphics Workstation"

June 28, 1984

Russell E. Hermes
Biomedical Computer Laboratory
Washington University
St. Louis, Missouri

- - - - - - - - - - - - -

Other Activities

"A Workshop for Cardiologists:

Personal Computers in Office Practice"

August 8-12, 1983

faculty included:
J. R. Cox, Jr.,
L. J. Thomas, Jr., and
K. W. Clark
Biomedical Computer Laboratory
Washington University
St. Louis, Missouri
Sponsor: American College of Cardiology
held at: Bethesda, Maryland

"Mockingbird: A Composer's Amanuensis"

November 8, 1983

video film presentation by
J. T. Maxwell III and
S. M. Ornstein
Xerox Corporation

A Lecture Series in support of Biomedical Engineering 3/2 Intensive Course
Sponsored by the Program in Biomedical Engineering
Sever Institute of Technology
Washington University

"Scope of Biomedical Engineering" January 2, 1984	Harold W. Shipton Biomedical Computer Laboratory Washington University St. Louis, Missouri
"Biomedical Instrumentation and Transducers" January 3, 1984	R. Martin Arthur Department of Electrical Engineering Biomedical Computer Laboratory Washington University St. Louis, Missouri
"Computers: Technology and Scale" January 4, 1984	G. James Blaine Biomedical Computer Laboratory Washington University St. Louis, Missouri
"Computers, Cardiologists and Cardiograms" January 5, 1984	Lewis J. Thomas, Jr. Biomedical Computer Laboratory Washington University St. Louis, Missouri
"An Engineer Looks at the Brain" and "New Techniques in EEG"" January 7, 1984	Harold W. Shipton Biomedical Computer Laboratory Washington University St. Louis, Missouri
"Physical Principles of Tracer Kinetics in Biological Applications" January 12, 1984	Kenneth B. Larson Biomedical Computer Laboratory Washington University St. Louis, Missouri
"Biophysical Measurements" January 14, 1984	Harold W. Shipton Biomedical Computer Laboratory Washington University St. Louis, Missouri

VIII. PUBLICATIONS AND ORAL PRESENTATIONS

Arthur, R. M., "Signal Quality of Resting Electrocardiograms," Journal of Electrocardiology, vol. 16, no. 3, pp. 235-244, 1983.

Arthur, R. M., Sieger, M. L., and Stein, Jr., D. W., "Assessing Ultrasonic Arrays for Imaging Tissue Properties," Ultrasonic Imaging, vol. 6, no. 2, p. 209, April 1984 (abstract).

Barzilai, B., Madaras, E. I., Sobel, B. E., Miller, J. G., and Perez, J. E., "Effects of Myocardial Contraction on Ultrasonic Backscatter Before and After Ischemia," American Journal of Physiology, in press.

Beecher, D. E., Cox, Jr., J. R., and Thomas, Jr., L. J., "A New Voxel-Model Approach for 3-Dimensional View Generation," Proceedings of the Eighth Conference on Computer Applications in Radiology, St. Louis, Missouri, May 23-35, 1984, in press.

Bergmann, S. R., Fox, K. A. A., Knabb, R. M., Burnes, M. A., and Sobel, B. E., "Effects of Coronary Thrombolysis on Regional Myocardial Perfusion and Metabolism Assessed with Positron Emission Tomography," Journal of the American College of Cardiology, vol. 3, p. 527, 1984 (abstract).

Bergmann, S. R., Fox, K. A. A., Rand, A. L., Colleen, D., and Sobel, B. E., "Recovery of Metabolism and Perfusion Assessed with PET after Coronary Thrombolysis with Plasminogen Activator," Circulation, vol. 68, p. III-38, 1983 (abstract).

Bergmann, S. R., Fox, K. A. A., Rand, A. L., McElvany, K. D., Welch, M. J., Markham, J., and Sobel, B. E., "Quantification of Regional Myocardial Blood Flow in vivo with $H_2{}^{15}O$ and Positron Emission Tomography," Circulation, in press.

Bergmann, S. R., Ter-Pogossian, M. M., and Sobel, B. E., "Biomedical Applications of Positron Emission Tomography," in Cardiovascular Instrumentation: Applicability of New Technology to Biobehavioral Research, S. M. Weiss and J. A. Herd, eds., in press.

Billadello, J. J., Smith, J. L., Ludbrook, P. A., Tiefenbrunn, A. J., Jaffe, A. S., Sobel, B. E., and Geltman, E. M., "The Implications of "Reciprocal" ST Segment Depression Associated with Acute Myocardial Infarction Identified by Positron Tomography," Journal of the American College of Cardiology, vol. 2, pp. 616-624, October 1983.

Blaine, G. J., "Networks and Distributed Systems: A Primer," invited tutorial, presented at MEDINFO 83, Amsterdam, The Netherlands, August 21-26, 1983.

Cain, M. E., Ambos, H. D., Witkowski, F. X., and Sobel, B. E., "Fast-Fourier Transform Analysis of Signal Averaged Electrocardiograms for Identification of Patients Prone to Sustained Ventricular Tachycardia," Circulation, vol. 69, p. 711, 1984.

Chen, C. W., and Snyder, D. L., "A Lower Bound on the Estimation Performance for Stochastic Control Systems," IEEE Transactions on Automatic Control, vol. AC-29, no. 6, pp. 557-559, June 1984.

Clark, K. W., Hart, W. M., Hagen, R. W., Hartz, R. K., and Zelenka, M., "A Microprocessor-Based System for Color Contrast Perimetry," Proceedings of the Seventh Annual Symposium on Computer Applications in Medical Care, Baltimore, Maryland, pp. 933-935, October 23-26, 1983.

Corr, P. B., Gross, R. W., and Sobel, B. E., "Amphipathic Metabolites and Membrane Dysfunction in Ischemic Myocardium," invited review for Circulation Research, in press.

Corr, P. B., and Sharma, A. D., "Alpha-Adrenergic Mediated Effects on Myocardial Calcium," in Calcium, Antagonists and Cardiovascular Disease - Perspectives in Cardiovascular Research, vol. 9, L. H. Opie, ed., Raven Press, New York, p. 193, 1984.

Corr, P. B., Sharma, A. D., and Sobel, B. E., "Temporal Changes in Lysophosphatides in Ischemic Myocardium and Relation to Severity of Dysrhythmia," Circulation, vol. 68, supplement III, p. III-360, 1983 (abstract).

Corr, P. B., and Witkowski, F. X., "Potential Electrophysiological Mechanisms Responsible for Dysrhythmias Associated with Reperfusion of Ischemic Myocardium," Circulation, vol. 68, supplement I, p. I-16, 1983.

Corr, P. B., and Yamada, K. A., "Pathophysiological Mechanisms of Alpha-Adrenoceptor Stimulation in the Ischemic Heart," in Methods in Clinical Pharmacology, Vieweg Publishers, Wiesbaden, West Germany, vol. 5, in press.

Cox, Jr., J. R., Blaine, G. J., Hill, R. L., Jost, R. G., and Shum, C. D., "Some Design Considerations for Picture Archiving and Communication Systems," IEEE Computer Magazine, Special Issue on Digital Image Archiving in Medicine, vol. 16, no. 8, pp. 39-49, August 1983.

Croft, C. H., Rude, R. E., Lewis, S. E., Parkey, R. W., Poole, W. K., Parker, C., Fox, N., Roberts, R., Strauss, H. W., Thomas, L. J., Raabe, Jr., D. S., Sobel, B. E., Gold, H. K., Stone, P. H., Braunwald, E., Willerson, J. T., and the MILIS Study Group, "Comparison of Left Ventricular Function and Infarct Size in Patients with and without Persistently Positive Technetium-99m Pyrophosphate Myocardial Scintigrams after Myocardial Infarction: Analysis of 357 Patients," American Journal of Cardiology, vol. 53, pp. 421-428, February 1984.

Elnahas, S. E., Jost, R. G., and Dunham, J. G., "Compression of Digital Diagnostic Images in Radiology," Proceedings of the ACR 8th Conference on Computer Applications in Radiology 1984, St. Louis, Missouri, May 23-25, 1984, in press.

Ficke, D. C., Beecher, D. E., Hoffman, G. R., Holmes, T. J., and Ter-Pogossian, M. M., "Recent Developments in Image Reconstruction Using a Time-of-Flight Assisted Positron Emission Tomograph: Super PETT I," IEEE Transactions on Nuclear Science, vol. NS-31, no. 1, pp. 605-608, February 1984.

Fox, K. A. A., Abendschein, D. R., Sobel, B. E., and Bergmann, S. R., "Detection of Persistent Metabolic Impairment Despite Reperfusion after Transient (20 Min) Myocardial Ischemia," Federation Proceedings, vol. 43, p. 902, 1984 (abstract).

Fox, K. A. A., Ambos, H. D., Bergmann, S. R., and Sobel, B. E., "External Measurement of Myocardial Oxygen Utilization with O-15 Labeled Oxygen", Circulation, vol. 68, p. III-82, 1983 (abstract).

Fox, K. A. A., Ambos, H. D., Nomura, H., Bergmann, S. R., and Sobel, B. E., "The Importance of Back-Diffusion on Myocardial Kinetics of ^{11}C-Palmitate," Journal of the American College of Cardiology, vol. 3, p. 574, 1984 (abstract).

Fox, K. A. A., Bergmann, S. R., Mathias, C. J., Hopkins, K. T., Jaffe, A. S., Powers, W. J., Siegel, B. A., Sobel, B. E., and Welch, M. J., "The Detection of Acute Coronary Thrombosis in Patients with the Use of In-111 Labeled Platelets," Journal of Nuclear Medicine, vol. 24, p. P59, 1983 (abstract).

Fox, K. A. A., Nomura, H., Sobel, B. E., and Bergmann, S. R., "Consistent Substrate Utilization Despite Reduced Flow in Hearts with Maintained Work," American Journal of Physiology: Heart and Circulatory Physiology, vol. 244, pp. H799-H806, 1983.

Fox, K. A. A., Bergmann, S. R., Mathias, C. J., Hopkins, K. T., Jaffe, A. S., Powers, W. J., Siegel, B. A., Welch, M. J., and Sobel, B. E., "Non-Invasive Detection of Coronary Artery Thrombosis with 111 Indium Labeled Platelets in Patients with Acute Myocardial Infarction," Journal of the American College of Cardiology, vol. 1, p. 628, 1983 (abstract).

Fox, K. A. A., Bergmann, S. R., and Sobel, B. E., "Coronary Thrombolysis: Pharmacological Considerations with Emphasis on Tissue-Type Plasminogen Activator (t-PA)," Biochemical Pharmacology, in press.

Geltman, E. M., Bergmann, S. R., Eisenberg, J. E., Ter-Pogossian, M. M., and Sobel, B. E., "Quantitative Assessment of Regional Myocardial Perfusion and Metabolism in Patients with Time-of-Flight Positron Emission Tomography," Journal of the American College of Cardiology, vol. 3, p. 573, 1984 (abstract).

Geltman, E. M., Bergmann, S. R., and Sobel, B. E., "Cardiac Positron Emission Tomography," in Positron Emission Tomography, M. Reivich, ed., Alan R. Liss, Inc., New York, in press.

Geltman, E. M., Bergmann, S. R., and Sobel, B. E., "PET Studies of the Heart," in Positron Emission Tomography, M. Reivich, ed., Alan R. Liss, Inc., New York, in press.

Geltman, E. M., Smith, J. L., Beecher, D., Ludbrook, P. A., Ter-Pogossian, M. M., and Sobel, B. E., "Altered Regional Myocardial Metabolism in Congestive Cardiomyopathy Detected by Positron Tomography," American Journal of Medicine, vol. 74, p. 773, 1983.

Geltman, E. M., and Sobel, B. E., "Cardiac Positron Tomography," Chest, vol. 83, p. 553, 1983.

Georghiades, C. N., and Snyder, D. L., "Locating Data Frames in Direct Detection Optical Communication," IEEE Transactions on Communications, vol. COM-32, no. 2, pp. 118-123, February 1984.

Glueck, R. M., Mottley, J. G., Miller, J. G., Sobel, B. E., and Perez, J. E., "Cyclic Variation of Myocardial Backscatter: An Ultrasonic Index of Regional Contractile Function," Circulation, pp. III-330, 1983 (abstract).

Goldring, S., "Epilepsy Surgery," in Clinical Neurosurgery, M. H. Weiss, ed., vol. 31, in press.

Goldring, S., "Presidential Address," presented at the annual meeting of the American Academy of Neurological Surgery, Pebble Beach, California, October 23-26, 1983.

Goldring, S., and Gregorie, E. M., "Surgical Management of Epilepsy Using Epidural Recordings to Localize Seizure Focus," Journal of Neurosurgery, vol. 60, pp. 457-466, 1984.

Gray, A. J., Beecher, D. E., and Olson, M. V., "Computer-Based Image Analysis of One-Dimensional Electrophoretic Gels Used for the Separation of DNA Restriction Fragments," Nucleic Acids Research," vol. 12, no. 1, pp. 473-491, 1984.

Hack, S. N., Bergmann, S. R., Eichling, J. O., and Sobel, B. E., "Quantification of Regional Myocardial Perfusion by Exponential Infusion of ^{11}C-Butanol," IEEE Transactions on Biomedical Engineering, vol. BME-30, pp. 716-722, 1983.

Hart, Jr., W. M., "Three Dimensional Topography of the Central Visual Field," Proceedings of the 24th International Congress of Ophthalmology, P. Henkind, ed., J. B. Lippincott, pp. 184-189, 1983.

Hart, Jr., W. M., and Burde, R. M., "Three Dimensional Topography of the Central Visual Field: Sparing of Foveal Sensitivity in Macular Disease," Ophthalmology, vol. 90, pp. 1028-1038, 1983.

Hart, Jr., W. M., Burde, R. M., Johnston, G. P., and Drews, R. C., "Static Perimetry in Chloroquine Retinopathy: Perifoveal Patterns of Visual Field Depression," Archives of Ophthalmology, vol. 102, pp. 377-380, 1984.

Hart, Jr., W. M., and Gordon, M. O., "Color Perimetry of Glaucomatous Visual Field Defects," Ophthalmology, vol. 91, pp. 338-346, 1984.

Hart, Jr., W. M., Hartz, R. K., Hagen, R. W., and Clark, K. W., "Color Contrast Perimetry," Investigative Ophthalmology and Visual Science, vol. 25, pp. 400-413, 1984.

Hart, Jr., W. M., and Kolker, A. E., "Computer Generated Display for Three-Dimensional Static Perimetry: Correlation of Optic Disc Changes with Glaucomatous Defects," Documente Ophthalmologica, vol. 35, pp. 43-49, 1982.

Hart, Jr., W. M., Kosmorsky, G., and Burde, R. M., "Color Perimetry of Central Scotomas in Diseases of the Macula and Optic Nerve," Documente Ophthalmologica, in press.

Hashimoto, H., Grace, A. M., Billadello, J. J., Gross, R. W. Strauss, A. W., and Sobel, B. E., "Nondenaturing Quantification of Subforms of Canine MM Creatine Kinase Isoenzymes (Isoforms) and Their Interconversion," Journal of Laboratory and Clinical Medicine, vol. 103, p. 470, 1984.

Hauser, C. R., Hendry, S. H. C., Jones, E. G., and Vaughn, J. E., "Morphological Diversity of Immunocytochemically Identified Neurons in Monkey Sensory-Motor Cortex," Journal of Neurocytology, vol. 12, p. 617-638, 1983.

Hermes, R. E., "Image Processing and Computation Requirements for Biomedical Research at Washington University," presented to the Lexidata (Interwork) System Planning Committee, Boston, Massachusetts, April 24, 1984.

Hermes, R. E., "The American Heart Association Database and Performance Evaluation," Proceedings of the 19th Annual AAMI Meeting, Washington, D.C., p. 34, April 14-18, 1984.

Herscovitch, P., Markham, J., and Raichle, M. E., "Brain Blood Flow Measured with Intravenous $H_2{}^{15}O$. I. Theory and Error Analysis," Journal of Nuclear Medicine, vol. 24, pp. 782-789, September 1983.

Hill, R. L., Jost, R. G., Blaine, G. J., Chabut, J. C., and Evens, R. G., "Video Distribution of Radiology Images," Proceedings of the Fourth International Symposium on the Planning of Radiological Departments, Cerromar Beach Hotel, Puerto Rico, pp. 285-290, April 29-May 2, 1984.

Hillman, L. S., "Mineralization and Late Mineral Homeostatis in Infants: Role of Mineral and Vitamin D Sufficiency and Other Factors," in Perinatal Calcium Metabolism, M. Hollid, K. Gray, and C. Anast, eds., Elsevier North Holland Biochemical Press, p. 301, 1983.

Holmes, T. J., Ficke, D. C., and Snyder, D. L., "A Statistical Analysis of Count Normalization Methods Used in Positron-Emission Tomography," IEEE Transactions on Nuclear Science, vol. NS-31, no. 1, pp. 521-526, February 1984.

Holmes, T. J., Ficke, D. C., and Snyder, D. L., "Modeling of Accidental Coincidences in Both Conventional and Time-of-Flight Positron-Emission Tomography," IEEE Transactions on Nuclear Science, vol. NS-31, no. 1, pp. 627-631, February 1984.

Holmes, T. J., Snyder, D. L., and Ficke, D. C., "The Effect of Accidental Coincidences in Time-of-Flight Positron-Emission Tomography," IEEE Transactions on Medical Imaging," in press.

Hughes, B., Bergmann, S. R., Corr, P. B., and Sobel, B. E., "External Detection of Increases in B-Adrenoceptor Density in Isolated Perfused Hearts with I-125 Hydroxybenzylpindolol," Journal of Nuclear Medicine, vol. 24, p. P19, 1983 (abstract).

Hughes, B., Marshall, D. R., Bakke, J. E., Sobel, B. E., and Bergmann, S. R., "In vivo Characterization of B-Adrenoceptors with ^{131}I-Pindolol," Federation Proceedings, vol. 43, p. 1097, 1984 (abstract).

Jaffe, A. S., "Complications of Myocardial Infarction," in Cardiology Clinics - Prognosis after Myocardial Infarction, W. B. Saunders Company, vol. 2, no. 1, pp. 79-94, February 1984.

Jaffe, A. S., Garfinkel, B. T., Ritter, C. S., and Sobel, B. E., "Plasma MB Creatine Kinase after Vigorous Exercise in Professional Athletes," American Journal of Cardiology, vol. 53, pp. 856-858, March 1984.

Jaffe, A. S., Geltman, E. M., Tiefenbrunn, A. J., Ambos, H. D., Strauss, H. D., Sobel, B. E., and Roberts, R., "Reduction of Infarct Size in Patients with Inferior Infarction with Intravenous Nitroglycerin: A Randomized Prospective Study," British Heart Journal, vol. 49, pp. 452-460, 1983.

Jaffe, A. S., Lee, R., Perez, J., Geltman, E. M., Wilner, G., and Sobel, B. E., "Factors Responsible for Elevated Platelet Factor Four in Plasma from Patients with Myocardial Infarction," Journal of the American College of Cardiology, in press.

Jaffe, A. S., Ritter, C., Meltzer, V., Harter, H., and Roberts, R., "Unmasking Artifactural Increases in Creatine Kinase Isoenzymes in Patients with Renal Failure," Journal of Laboratory Clinical Medicine, in press.

Jost, R. G., "Image Management Systems for Radiology - A Current Perspective (chairman's paper)," Proceedings of the 4th World Conference on Medical Informatics, J. H. van Bemmel, M. J. Ball, and O. Wigertz, eds., North Holland, pp. 365-368, 1983.

Kleiger, R. E., Miller, J. P., Bigger, Jr., J. T., Moss, A. J., and the Multicenter Postinfarction Research Group, "Heart Rate Variability: A Variable Predicting Mortality Following Acute Myocardial Infarction," Journal of the American College of Cardiology, vol. 3, no. 2, p. 547, February 1984.

Knabb, R. M., Burnes, M. A., Sobel, B. E., Fox, K. A. A., and Bergmann, S. M., "Myocardial Perfusion Following Coronary Thrombolysis Assessed with Positron Emission Tomography (PET) with $H_2{}^{15}O$," Federation Proceedings, vol. 43, p. 709, 1984 (abstract).

Kramer, J. B., and Corr, P. B., "Mechanisms Contributing to Arrhythmogenesis During Ischemia and Infarction," European Heart Journal, in press.

Krone, R. J., Friedman, E., Thanavaro, S., Miller, J. P., Kleiger, R. E., and Oliver, G. C., "Longterm Prognosis after First Q-Wave (Transmural) and Non Q-Wave (Nontransmural) Myocardial Infarction: Analysis of 593 Patients," American Journal of Cardiology, vol. 52, pp. 234-239, August 1983.

Krone, R. J., Miller, J. P., and Gillespie, J. A., "Stress Testing Soon after Myocardial Infarction in Patients Taking Beat-Blocking Agents - Results of a Multicenter Study on 665 Patients," Journal of the American College of Cardiology, vol. 3, p. 577, February 1984 (abstract).

Larson, K. B., review of "Biological Transport of Radiotracers," CRC Press Inc., Boca Raton, Florida, 1982, L. G. Colombetti, ed., Journal of Nuclear Medicine, vol. 25, pp. 543-544, 1984.

Lee, R. G., Weinstein, I. R., Perez, J. E., Geltman, E. M., Wilner, G. D., Sobel, B. E., and Jaffe, A. S., "Serial Platelet Factor 4 in Evolving Transmural Myocardial Infarction," Circulation (Part II), vol. 68, p. 393, 1983 (abstract).

Ludbrook, P. A., Geltman, E. M., Tiefenbrunn, A. S., Jaffe, A. S., and Sobel, B. E., "Restoration of Regional Myocardial Metabolism by Coronary Thrombolysis in Patients," Circulation (Part II), vol. 68, p. 325, 1983 (abstract).

Madaras, E. I., Barzilai, B., Perez, J. E., Sobel, B. E., and Miller, J. G., "Changes in Myocardial Backscatter Throughout the Cardiac Cycle," Ultrasonic Imaging, vol. 5, pp. 229-239, 1983.

Main, D. M., Main, E. K., and Maurer, Jr., M. M., "Cesarian Section Versus Vaginal Delivery for the Less than 1500 Gram Breach Fetus," American Journal of Obstetrics and Gynecology, vol. 146, no. 5, pp. 580-584, July 1983.

McCluskey, E. R., Saffitz, J. E., Murphree, S., Corr, P. B., Kramer, J. B., and Needleman, P., "Reperfusion of Ischemic Canine Myocardium Accelerates the Histologic and Arachidonic Acid (AA) Metabolic Changes," Pharmacologist, vol. 25, p. 205, 1983 (abstract).

Miller, J. D., "Auditory Processing of the Acoustic Patterns of Speech, "Archives of Otolaryngology, vol. 110, no. 3, pp. 154-159, 1984.

Miller, J. G., "Ultrasonic Characterization of Myocardial Tissue," in Frontiers Cardiology for the 80's, Academic Press, Inc., London, pp. 311-315, 1983.

Miller, J. G., Perez, J. E., Mottley, J. G., Madaras, E. I., Johnston, P. H., Blodgett, E. D., Thomas III, L. J., and Sobel, B. E., "Myocardial Tissue Characterization: An Approach Based on Quantitative Backscatter and Attenuation," IEEE Ultrasonics Symposium, vol. 83, CH 1947-1, pp. 782-793, 1983.

Moore, S. M., "A Pattern Matcher for Searching Binary Trees," Master of Science thesis, Department of Electrical Engineering, Washington University, St. Louis, Missouri, May 1984.

Moss, A. J., Bigger, Jr. J. T., Case, R. B., Gillespie, J., Goldstein, R. E., Greenberg, H. M., Krone, R., Marcus, F. I., Odoroff, C. L., and Oliver, G. C., "Risk Stratification and Survival after Myocardial Infarction," New England Journal of Medicine, vol. 309, no. 6, pp. 331-336, 1983.

Mottley, J. G., Glueck, R. M., Perez, J. E., Sobel, B. E., and Miller, J. G., "Regional Differences in the Cyclic Variation of Myocardial Backscatter that Parallel Differences in Contractile Function," Journal of the Acoustical Society of America, in press.

Mukharji, J., Rude, R. E., Poole, W. K., Gustafson, N., Thomas, L. J., Strauss, H. W., Jaffe, A. S., Muller, J. E., Roberts, R., Raabe, D. S., Croft, C. H., Passamani, E., Braunwald, E., Willerson, J. T., and Cooperating MILIS Investigators, "Ventricular Arrhythmia and Left Ventricular Dysfunction Six Months after Myocardial Infarction as Risk Factors for Sudden Death," Circulation (Part II), vol. 68, p. 106, 1983 (abstract).

Mukharji, J., Rude, R. E., Poole, K. W., Thomas, L. J., Strauss, H. W., Jaffe, A. S., Muller, J. E., Roberts, R., Raabe, D. S., Croft, C. H., Passamani, E., Braunwald, E., Willerson, J. T., and the MILIS Study Group, "Late Sudden Death Following Acute Myocardial Infarction: Multivariate Analysis of Risk Factors," American Journal of Cardiology, in press.

Muller, J., Roberts, R., Stone, P., Rude, R., Raabe, D. Gold, H., Jaffe, A. S., Strauss, W., Turi, Z., Poole, K., Passamani, E., Willerson, J., Sobel, B., Braunwald, E., and the MILIS Study Group, "Failure of Propranolol Administration to Limit Infarct Size in Patients with Acute Myocardial Infarction," Circulation (Part II), vol. 68, p. 294, 1983 (abstract).

Muller, J., Turi, Z., Stone, P., Rude, R., Raabe, D., Jaffe, A., Gold, H., Gustafson, N., Poole, K., Smith, T., Braunwald, E., and the MILIS Study Group, "Does Digoxin Therapy Increase Mortality Following Myocardial Infarction?" Circulation (Part II), vol. 68, p. 368, 1983 (abstract).

Perez, J. E., Barzilai, B., Glueck, R. M., Saffitz, J. E., Madaras, E. I., Johnston, P., Miller, J. G., and Sobel, B. E., "Applicability of Ultrasonic Tissue Characterization for Longitudinal Assessment and Differentiation of Calcification and Fibrosis in Cardiomyopathy," Journal of American College of Cardiology, in press.

Perez, J. E., Madaras, E. I., Sobel, B. E., and Miller, J. G., "Quantitative Myocardial Characterization with Ultrasound," Automedica, in press.

Perez, C. A., and Purdy, J. A., "Computed Tomography in Treatment Planning, Technical and Clinical Considerations," in Computerized Treatment Planning Systems, F. Bagne, ed., U. S. Department of Health and Human Services, Rockville, Maryland, pp. 22-45, January 1984.

Politte, D. G., "Reconstruction Algorithms for Time-of-Flight Assisted Positron-Emission Tomographs," Master of Science thesis, Department of Electrical Engineering, Washington University, St. Louis, Missouri, December 1983.

Politte, D. G., and Snyder, D. L., "Results of a Comparative Study of a Reconstruction Procedure for Producing Improved Estimates of Radioactivity Distributions in Time-of-Flight Emission Tomography," IEEE Transactions on Nuclear Science, vol. NS-31, no. 1, pp. 614-619, February 1984.

Raichle, M. E., Martin, W. R. W., Herscovitch, P., Mintun, M. A., and Markham, J., "Brain Blood Flow Measured with Intravenous $H_2{}^{15}O$. II. Implementation and Validation," Journal of Nuclear Medicine, vol. 24, no. 9, pp. 790-798, September 1983.

Roberts, R., Croft, C., Gold, H. K., Tyler, D. H., Jaffe, A. S., Muller, J. E., Mullin, S. M., Parker, C., Passamani, E. R., Poole, W. K., Raabe, D. S., Rude, R. E., Stone, P. H., Turi, Z. G., Sobel, B. E., Willerson, J. T., Braunwald, E., and the MILIS Study Group," Effect of Propranolol on Myocardial Infarct Size in a Randomized, Blinded Multicenter Trial," New England Journal of Medicine, in press.

Rosenberger, F. U., Krippner, K., Stein, Jr., D. W., and Wong, J. W., "Implementation of the Delta-Wave Dose Calculation Algorithm," Proceedings of the IEEE 8th International Conference on the Use of Computers in Radiation Therapy, Toronto, Canada, July 1984, in press.

Rosenberger, F. U., and Wann, D. F., "A Computer Aided Procedure for Performing Static Loading Validation of Digital Logic Systems," IEEE Transactions on Computers, vol. C-33, no. 4, pp. 301-313, April 1984.

Saffitz, J. E., Corr, P. B., Lee, B. I., Gross, R. W., Williamson, E. K., and Sobel, B. E., "Pathophysiologic Concentrations of Lysophosphoglycerides Quantified by Electron Microscopic Autoradiography," Laboratory Investigation, vol. 50, p. 278, 1984.

Shafer, K. E., Santoro, S. A., Sobel, B. E., and Jaffe, A. S., "Monitoring Activity of Fibrinolytic Therapy: A Therapeutic Challenge," American Journal of Medicine, vol. 76, p. 879, 1984.

Sharma, A. D., Ahumada, G. G., Sobel, B. E., and Corr, P. B., "Lysophosphatide-Induced Increases in Alpha-Adrenergic Receptor Number in Intact Myocytes," Circulation, vol. 68, supplement III, p. III-57, 1983 (abstract).

Sharma, A. D., and Corr, P. B., "Adrenergic Factors in Arrhythmogenesis in Ischemic and Reperfused Myocardium," invited review in European Heart Journal, vol. 4, supplement D, p. 79, 1983.

Sharma, A. D., and Corr, P. B., "Alpha-Adrenergic Mediated Effects of Catecholamines in the Ischemic and Reperfused Heart," in Role of Alpha-Adrenoceptors in Cardiovascular Disease, Churchill Livingstone, in press.

Sharma, A. D., and Corr, P. B., "Modulation by Amiodarone of Cardiac Adrenergic Receptors and Their Electrophysiologic Responsivity to Catecholamines," Circulation, vol. 68, supplement III, p. III-99, 1983 (abstract).

Sharma, A. D., Saffitz, J. E., Lee, B. I., Sobel, B. E., and Corr, P. B., "Alpha-Adrenergic Mediated Accumulation of Calcium in Reperfused Myocardium," Journal of Clinical Investigation, vol. 72, pp. 802-818, 1983.

Sheffield, L. T., Berson, A., Bragg-Remschel, D., Gillette, P. C., Hermes, R. E., Hinkle, L., Kennedy, H., Mirvis, D. M., and Oliver, G. C., "Recommendations for Standards of Instrumentation and Practice in the Use of Ambulatory Electrocardiography," a draft standard from the Ad Hoc Subcommittee on Ambulatory Electrocardiography to the American Heart Association Committee on Electrocardiography, March 16, 1984.

Shum, C. D., "Design Analysis of a Wide-Band Picture Communication System," Master of Science thesis, Department of Computer Science, Washington University, St. Louis, Missouri, December 1983.

Shum, C. D., Cox, J. R., and Blaine, G. J., "Design Analysis of a Wide-Band Picture Communication System," Proceedings of the Medical Picture Archiving and Communications Systems Conference (PACS III), Arlington, Virginia, July 24-27, 1984, in press.

Slessinger, E. D., Rosenberger, F. U., and Wong, J. W., "A Technique for Treatment Plan Verification," Medical Physics, vol. 11, no. 3, p. 391, 1984 (abstract).

Snyder, D. L., "Parameter Estimation for Dynamic Studies in Emission-Tomography Systems Having List-Mode Data," IEEE Transactions on Nuclear Science, vol. NS-31, no. 2, pp. 925-931, April 1984.

Snyder, D. L., "Utilizing Side Information in Emission Tomography," IEEE Transactions on Nuclear Science, vol. NS-31, no. 1, pp. 533-537, February 1984.

Snyder, D. W., and Sobel, B. E., "Treatment of Ischemic Heart Disease: Clinical Therapy of Ischemic Heart Disease," in Medical Management of Ischemic Heart Disease, M. Rosen and B. Hoffman, eds., Martinus Nijhoff Publishers, The Hague, The Netherlands, 1983.

Sobel, B. E., and Bergmann, S. R., "The Impact of Coronary Thrombolysis and Tissue-Type Plasminogen Activator (t-PA) on Acute Myocardial Infarction," in Fibrinolysis, M. Verstraete and D. Collen, eds., in press.

Sobel, B. E., Geltman, E. M., Tiefenbrunn, A. J., Jaffe, A. S., Spadaro, Jr., J. J., Ter-Pogossian, M. M., Collen, D., and Ludbrook, P. A., "Improvement of Regional Myocardial Metabolism after Coronary Thrombolysis with Tissue-Type Plasminogen Activator or Streptokinase," Circulation, vol. 69, pp. 983-989, 1984.

Sobel, B. E., Gross, R. G., and Robison, A. K., "Thrombolysis, Clot Selectivity, and Kinetics," Circulation, in press.

Thomas, Jr., L. J., "Perspectives on Computers in Biomedical Research," invited paper, Proceedings of the AAMSI Congress 83, San Francisco, California, vol. 1, pp. 165-169, May 1-4, 1983.

Thomas, Jr., L. J., and Miller, J. P., "Long-Term Ambulatory ECG Recording in the Determination of Antidysrhythmic Drug Efficacy," NIH Workshop on Pharmacology of Antiarrhythmic Therapy, Bethesda, Maryland, September 1-2, 1982, in Perspectives in Cardiovascular Research, Volume 10: Clinical Pharmacology of Antiarrhythmic Therapy, B. R. Lucchesi, J. V. Dingell, and R. P. Schwartz, Jr., eds., Raven Press, pp. 249-265, 1984.

Tilton, R. G., Larson, K. B., Cole, P. A., and Williamson, J. R., "Diltiazem Prevents Coronary Vascular Resistance and Permeability Changes Following No-Flow Ischemia," Federation Proceedings, vol. 43, no. 3, p. 335, 1984 (abstract).

Toga, A. W., Goo, R. L., Murphy, R., and Collins, R. C., "Neuroscience Application of Interactive Image Analysis," Optical Engineering, in press.

Van de Werf, F., Bergmann, S. R., Fox, K. A. A., De Geest, H., Hoyng, C. F., Sobel, B. E., and Collen, D., "Coronary Thrombolysis with Intravenously Administered Human Tissue-Type Plasminogen Activator Produced by Recombinant DNA Technology," Circulation, vol. 69, pp. 605-610, 1984.

Van de Werf, F., Bergmann, S. R., Fox, K. A. A., De Geest, H., Sobel, B. E., and Collen, D., "Coronary Thrombolysis with Human Tissue-Type Plasminogen Activator Produced by Recombinant DNA Technology," Circulation, vol. 68, p. III-185, 1983 (abstract).

Van de Werf, F., Ludbrook, P. A., Bergmann, S. R., Tiefenbrunn, A. J., Fox, K. A. A., De Geest, H., Verstraete, M., Collen, D., and Sobel, B. E., "Coronary Thrombolysis with Tissue-Type Plasminogen Activator in Patients with Evolving Myocardial Infarction," New England Journal of Medicine, vol. 310, pp. 609-613, 1984.

Witkowski, F. X., Cain, M. E., and Corr, P. B., "A System for True Simultaneous Isochronic and Isovoltaic Mapping of the Myocardium," Circulation, vol. 68, supplement III, p. III-360, 1983 (abstract).

Witkowski, F. X., and Corr, P. B., "Mechanisms Responsible for Arrhythmias Associated with Reperfusion of Ischemic Myocardium," in Clinical Aspects of Life-Threatening Arrhythmias, in press.

Witkowski, F. X., and Corr, P. B., "Simultaneous Multiple Electrode Cardiac Mapping System," American Journal of Physiology: Heart and Circulatory Physiology, in press.

Wong, J. W., and Rosenberger, F. U., "Photon Dose Calculations in Radiotherapy Treatment Planning," Proceedings of the Symposium on Computation in Radiation Therapy, Canadian College of Physicists in Medicine, Quebec, Canada, pp. 1-27, June 23, 1983.

Wong, J. W., Slessinger, E. D., Rosenberger, F. U., Krippner, K., and Purdy, J. A., "The Delta-Volume Method for 3-Dimensional Photon Dose Calculations," Proceedings of the IEEE 8th International Conference on the Use of Computers in Radiation Therapy, Toronto, Canada, July 1984, in press.

Wong, J., Slessinger, E. D., Stein, D., Rosenberger, F. U., and Purdy, J. A., "Implementation and Verification of a New CT Based 3-Dimensional Photon Dose Calculation Algorithm," Medical Physics, vol. 10, no. 4, p. 543, 1983.

Yamada, K. A., Lange, L. G., Sobel, B. E., and Corr, P. B., "Alpha-Adrenergic Blockage Ameliorates Mitochondrial Dysfunction Associated with Reperfusion of Ischemia Myocardium," Federation Proceedings, vol. 43, p. 812, 1984 (abstract).

IX. MONOGRAPHS AND WORKING NOTES

The Biomedical Computer Laboratory's Monograph Series was established to systematize the many reports, reprints, program descriptions and other documents written at BCL or supported in part by the Laboratory's facilities or staff.

A forum, much less formal than our monograph series, has been instituted to serve as a repository for materials such as: research notes, system and component documentation, technical survey notes and prepublication drafts. A Working Note File is maintained for access by anyone associated with the Washington University Computer Labs. Distribution for outside use can be made available with the consent of the contributor.

Monographs

Following is a list of the monographs published by BCL during the past year. Copies of the complete index to the Monograph Series are available on request.

Monograph Number	Author(s)	Title	Date
435	Snyder, D. L.	Parameter Estimation for Dynamic Studies in Emission-Tomography Systems Having List-Mode Data	7/83 Rev. 11/83
436	Clark, K. W. Geltman, E. M. Miller, J. P. Moore, P. Madden, K. A. Thomas, Jr., L. J. Hartwell, T. D. Jaffe, A. S. Raabe, D. S. Stone, P. H. Gold, H. K. Rude, R. E. MILIS Study Group	Reproducibility of Dysrhythmia Findings by a Centralized Laboratory Within a Major Multicenter Trial	8/83
437	Tzou, Kou-Hu Dunham, J. G.	A Physiological-Based Human Visual System Model for Image Processing	8/83
438	Shum, Chung-Dak	Design Analysis of a Wide-Band Picture Communication System	12/83
439	Snyder, D. L.	Utilizing Side Information in Emission Tomography	9/83

Monograph Number	Author(s)	Title	Date
440	Politte, D. G.	Reconstruction Algorithms for Time-of-Flight Assisted Positron-Emission Tomographs	12/83
441	Politte, D. G. Snyder, D. L.	Results of a Comparative Study of a Reconstruction Procedure for Producing Improved Estimates of Radio-Activity Distributions in Time-of-Flight Emission Tomography	11/83
442	Gray, A. J. Beecher, D. E. Olson, M. V.	Computer-Based Image Analysis of One-Dimensional Electrophoretic Gels Used for the Separation of DNA Restriction Fragments	11/83
443	Cox, Jr., J. R. Blaine, G. J. Hill, R. L. Jost, R. G. Shum, Chung-Dak	Some Design Considerations for Picture Archiving and Communication Systems	12/83
444	Blaine, G. J. Hill, R. L. Cox, Jr., J. R. Jost, R. G.	PACS Workbench at Mallinckrodt Institute of Radiology (MIR)	12/83
445	Mead, C. N. Pull, H. R. Clark, K. W. Thomas, Jr., L. J.	Expanded Frequency-Domain ECG Waveform Processing: Integration into a New Version of Argus/2H	12/83
446	Herscovitch, P. Markham, J. Raichle, M. E.	Brain Blood Flow Measured with Intravenous $H_2{}^{15}O$. I. Theory and Error Analysis	12/83
447	Raichle, M. E. Martin, W. R. W. Herscovitch, P. Mintun, M. A. Markham, J.	Brain Blood Flow Measured with Intravenous $H_2{}^{15}O$. II. Implementation and Validation	12/83
448	Holmes, T. J. Ficke, D. C. Snyder, D. L.	Modeling of Accidental Coincidences in Both Conventional and Time-of-Flight Positron-Emission Tomography	2/84

Monograph Number	Author(s)	Title	Date
449	Holmes, T. J. Snyder, D. L. Ficke, D. C.	A Statistical Analysis of Count Normalization Methods Used in Positron-Emission Tomography	2/84
450	Miller, M. I.	Algorithms for Removing Recovery Related Distortion	4/84
451	Beecher, D. E. Cox, Jr., J. R. Thomas, Jr., L. J.	A New Voxel-Model Approach for 3-Dimensional View Generation	6/84
452	Blaine, G. J. Ficke, D. C. Hitchens, R. E. Holmes, T. J.	Data Acquisition Aspects of SUPER-PETT	2/84
453	Ficke, D. C. Beecher, D. E. Blaine, G. J. Hitchens, R. E. Holmes, T. J. Ter-Pogossian, M. M. Yamamoto, M.	TOF Acquisition: System Design and Experimental Results	5/83
454	Shum, Chung-Dak Cox, Jr., J. R. Blaine, G. J.	Design Analysis of a Wide-Band Picture Communication System	6/84
455	Moore, S. M.	A Pattern Matcher for Searching Binary Trees	5/84

Working Notes

Following is an index of notes submitted during the current reporting period.

Working Note Number	Author(s)	Title	Date
49	Snyder, D. L.	Single-Photon Emission Computed Tomography	8/83
50	Miller, M. I.	Electron-Microscopic Autoradiography	8/83
51	Miller, M. I.	'EM' Applied to 'EM'	11/83
52	Blaine, G. J.	Data Communications	11/83

Working Note Number	Author(s)	Title	Date
53	Blaine, G. J.	A Review of Bus Standards	11/83
54	Phillips, S. R.	Design Modification: Terminal "Break" Recognition	12/83
55	Blaine, G. J. Moore, S. M. Phillips, S. R.	TERRANET-V: Packet Specification and Experimental Implementation	12/83
56	Moore, S. M.	TERRANET; Flow Control	2/84
57	Chabut, J. C.	Testing Modulator/Demodulator Frequency Response	4/84
58	Moore, S. M. Phillips, S. R. Blaine, G. J. Cox, Jr., J. R.	TERRANET-V Voice Experiments	6/84